AD-A181 329 MODELS FOR THE OXIDATION OF SILICON(U) NORTH CAROLINA 1/2
UNIV AT CHAPEL HILL DEPT OF CHEMISTRY E A IRENE
03 JUN 87 TR-16 N00014-86-K-0305

UNCLASSIFIED F/G 20/12 NL

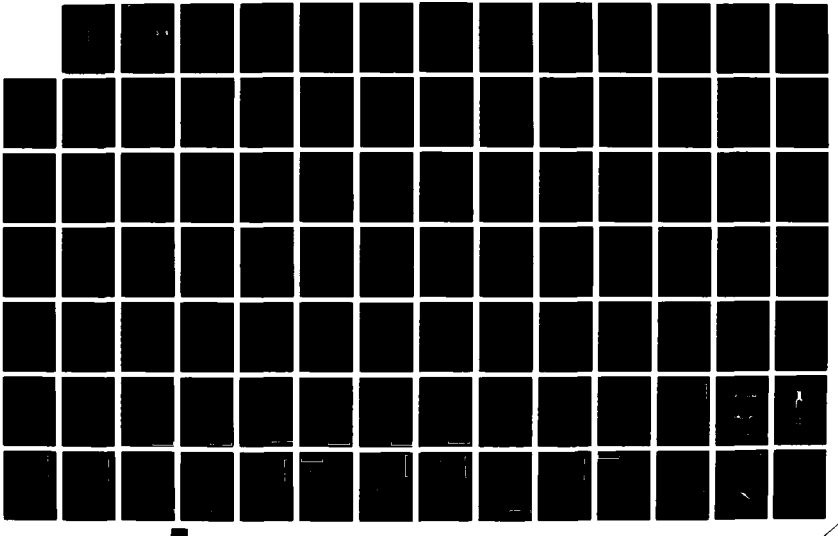

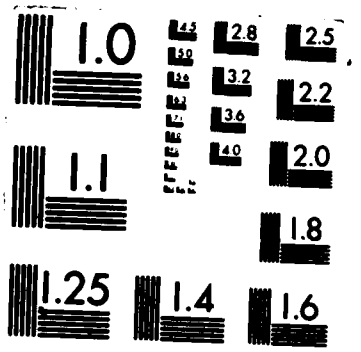
1.0
2.8
2.5
3.2
2.2
3.6
4.0
2.0
1.1
1.8
1.25
1.4
1.6

(12)

OFFICE OF NAVAL RESEARCH

CONTRACT NO. N00014-86-K-0305

TECHNICAL REPORT NO. 16

Models for the Oxidation of Silicon

E.A. Irene
Department of Chemistry
University of North Carolina
Chapel Hill, NC 27514

in

CRC Critical Reviews in Solid State and Materials Science

SECURITY CLASSIFICATION OF THIS PAGE

REPORT DOCUMENTATION PAGE

1a. REPORT SECURITY CLASSIFICATION Unclassified	1b. RESTRICTIVE MARKINGS AD-A181 329
2a. SECURITY CLASSIFICATION AUTHORITY	3. DISTRIBUTION/AVAILABILITY OF REPORT Approved for public release; distribution unlimited.
2b. DECLASSIFICATION/DOWNGRADING SCHEDULE	
4. PERFORMING ORGANIZATION REPORT NUMBER(S) Technical Report #16	5. MONITORING ORGANIZATION REPORT NUMBER(S)
6a. NAME OF PERFORMING ORGANIZATION 11-3 Venable Hall 045A Chapel Hill, NC 27514 6b. OFFICE SYMBOL (If applicable)	7a. NAME OF MONITORING ORGANIZATION Office of Naval Research (Code 413)
6c. ADDRESS (City, State and ZIP Code) 11-3 Venable Hall 045A Chapel Hill, NC 27514	7b. ADDRESS (City, State and ZIP Code) Chemistry Program 800 N. Quincy Street Arlington, Virginia 22217
8a. NAME OF FUNDING/SPONSORING ORGANIZATION Office of Naval Research 8b. OFFICE SYMBOL (If applicable)	9. PROCUREMENT INSTRUMENT IDENTIFICATION NUMBER Contract #N00014-86-K-0305
8c. ADDRESS (City, State and ZIP Code) Chemistry Program 800 N. Quincy, Arlington, VA 22217	10. SOURCE OF FUNDING NOS PROGRAM ELEMENT NO / PROJECT NO / TASK NO / WORK UNIT NO
11. TITLE (Include Security Classification) MODELS FOR THE OXIDATION OF SILICON	
12. PERSONAL AUTHOR(S) Eugene A. Irene	
13a. TYPE OF REPORT Interim Technical 13b. TIME COVERED FROM _____ TO _____	14. DATE OF REPORT (Yr., Mo., Day) June 3, 1987 15. PAGE COUNT 111
16. SUPPLEMENTARY NOTATION Prepared for publication in CRC Critical Reviews in Solid State and Materials Science.	
17. COSATI CODES FIELD / GROUP / SUB. GR.	18. SUBJECT TERMS (Continue on reverse if necessary and identify by block number)

19. ABSTRACT (Continue on reverse if necessary and identify by block number)

This review includes first, a technological overview to define the silicon oxidation problem and the electronic implications; and then a historical perspective which includes a review of the current status of the experimental studies on Si oxidation; and lastly a critical treatment of the latest oxidation models. It is this authors intent to utilize the Technological Overview and Historical Perspective sections of this review to provide the reader with sufficient information and background to be able to fully appreciate the basis for the currently proposed Si oxidation models. The origins and reasoning for many of the newest models lie with facts uncovered fifteen years ago. A brief development of some of these facts is given with references. It should be mentioned that all the models chosen for discussion have some merit based either on a specific experiment finding or by analogy with other oxidation systems.

20. DISTRIBUTION/AVAILABILITY OF ABSTRACT UNCLASSIFIED/UNLIMITED ☒ SAME AS RPT. ☒ DTIC USERS ☐	21. ABSTRACT SECURITY CLASSIFICATION Unclassified
22a. NAME OF RESPONSIBLE INDIVIDUAL Dr. David L. Nelson	22b. TELEPHONE NUMBER (Include Area Code) (202) 696-4410 22c. OFFICE SYMBOL

DD FORM 1473, 83 APR EDITION OF 1 JAN 73 IS OBSOLETE.

SECURITY CLASSIFICATION OF THIS PAGE

Models For The Oxidation Of Silicon

by

Eugene A. Irene

I. Introduction

There exists a variety of books and reviews on the subject of thermal oxidation (for example see references 1-5). A large fraction of the published work deals with the oxidation of metals with the obvious applications to the very important subjects of corrosion and metallurgical property alterations. Recently, two reviews on oxidation appeared in the literature(5,6) which contain separate treatments of the oxidation of silicon and one very recent review of silicon oxidation(7). It will be unavoidable to overlap with some of the issues raised in these past reviews as they are both extensive and learned. It is, however, the intention of the present review to stay wholly within the confines of the area of silicon oxidation and to remain in view of only the electronics applications and implications of the $Si-SiO_2$ system, where SiO_2 is in thin film form and the Si substrate is the high quality single crystal material that is used for the production of Si based devices for microelectronics. These restrictions elevate the priority of special issues to be treated in more detail in the present review. For example, we will need to deal with the following phenomena: chemical reaction on a Si surface rather than bulk reactions; the transport of an oxidant through an amorphous thin film rather than through bulk crystalline matter; the mechanical properties of thin films on substrates; the prevailing electronic situation at the $Si-SiO_2$ and SiO_2-O_2 interfaces, in terms of interfacial and bulk charges; and impurities,

both unwanted impurities and others that are necessary to the technology (so-called dopants), with both kinds often greatly affecting the mechanism of the oxidation of Si. These issues provide the focus for the present review and indeed many of the experimental studies of the oxidation of Si support the importance of these unique aspects of the Si oxidation problem. These studies will be discussed and the results will be used to provide a reference data set from which to judge the veracity of the various proposed Si oxidation models.

With respect to the organization of this review, the following sequence will be used: first, a technological overview to define the silicon oxidation problem and the electronic implications; and then a historical perspective which includes a review of the current status of the experimental studies on Si oxidation; and lastly a critical treatment of the latest oxidation models. It is this authors intent to utilize the Technological Overview and Historical Perspective sections of this review to provide the reader with sufficient information and background to be able to fully appreciate the bases for the currently proposed Si oxidation models. The origins and reasoning for many of the newest models lie with facts uncovered fifteen years ago. A brief development of some of these facts is given with references. It should be mentioned that all the models chosen for discussion have some merit based either on a specific experimental finding or by analogy with other oxidation systems.

II. Technological Overview

A. The Semiconductor Surface Problem

Contained within several recent publications(7-11) are answers to three questions that provide the historical back drop for the present review by providing goals, guidelines and the type of information that is being sought about Si oxidation. The questions are the following: why Si, why SiO_2 and why thermal oxidation?

Why Si and Why SiO_2?

The first question, why Si, is the most difficult to answer without some further knowledge about the answers to the other two following questions. At this point it is tempting to conjecture that the answer simply lies with a comparison of the fundamental semiconductor properties of Si with other important semiconductor materials. A perusal of Table 1 reveals that Si has about the same band gap as the other popular semiconductors in the Table. Si has a smaller carrier mobility compared to Ge, GaAs and InP; and the gap for Si is of the indirect type. The comparison of relative mobilities shows that Si is inferior to the other listed semiconductors, since carrier mobility in large part determines the maximum speed of the device(12). The issue of the gap being direct or indirect is more subtle. Some optical devices (LED's for example) require direct gaps where the transitions are not altered by phonon assisted processes. Since Si displays an indirect type gap, its use as an optical device is limited. While this comparison of properties is narrow and selective, it does point to the fact that the basic semiconducting properties of Si are not superior to other competitive materials, and thus there must be other reasons for the preeminence of Si. It is sometimes argued that Si is simply less expensive as a raw material than most other competitive semiconductor materials, and since it is elemental it is easier to obtain in high quality single crystal form than are compound semiconductors, where at the very minimum there exists the non trivial problem of maintaining stoichiometry. While these latter arguments cannot be totally ignored, it is this author's belief that these are only of secondary importance and the truly relevant reason lies with the chemical reaction at the Si surface to form an oxide film. It is also this author's belief that the reason for the preeminence of Si is intimately related to the kind of technological evolution that has taken place and this technology is now briefly discussed as it sets the general requirements for the SiO_2 film on Si.

In the 1960's semiconductor technology shifted in emphasis from discrete devices to integrated circuits, IC's. IC's are composed of many similar devices fabricated adjacent to

one another on the same substrate and linked together for a particular purpose, such as providing functions such as memory, logic, or signal processing, etc. The IC's soon adopted a planar technology, namely where the finished device array is flat or planar, rather than mesa-like as with the technologies which preceeded the planar trend. The method used to define regions in the semiconductor substrate that were to receive the necessary dopant, was via the growth of an oxide film of SiO_2 on the Si surface and this was followed by a photolithographic step which requires flatness. Since this film grows in air on the Si surface, it provided for Si a straightforward solution that was compatible and complimentary to the planarization technology. For the purpose of the present discussion, the most exciting event of this era was the discovery that the SiO_2 film effected a seemingly magical improvement in the electrical characteristics of the Si surface(13). This feature of the Si surface will be treated below in some detail. Essentially, it would have been decidedly advantageous to be able to use only the surface or near the surface of the semiconductor for electrical conduction. In this manner the advantages of the planar technology is fully utilized.

The problem with the Si surface to be addressed, or for that matter with any surface, is that the termination of the regular crystalline lattice at the surface provides a large number of unsatisfied chemical bonds. The number of these bonds is about $10^{15}/cm^2$ which is of the order of the number of surface atoms. This simple idea is illustrated in Figure 1. The existence of the dangling bonds was predicted(14) and the fact that the bonds are to give rise to states within the forbidden gap of the semiconductor was also treated(15) in the 1930's. From this analysis it is deduced that the unsatisfied orbitals could be filled from electrons on the semiconductor surface, thus the states act as acceptor states which when filled leave the surface in short supply of electrons and hence p-type. The early experimental work aimed at confirming these ideas was done on Ge surfaces(16,17) and indeed confirmed these results and later work on Si surfaces also supported these results(13).

Extensive measurements show that both donor and acceptor states are found on the Si surface(18-20 and reviewed extensively in ref. 37).

Because of the existence of these surface states, the electronic properties of devices are profo undly affected. We first consider the implications for bipolar devices with the simple case of a pn junction bounded by a surface upon which there are surface states as shown in Fig. 2a. Any applied electrical bias between the sides of the pn, B to E, will be felt across the junction depletion zone in the absence of surface effects. Hence the bias will appropriately affect the operation of the junction by altering the current from E to C. With surface states, however, the altered type of the surface due to the charge exchange with the states could facilitate the creation of a low resistance path on the surface thereby short circuiting the current around the junction. The result is that the B to E bias does not control the E to C current, hence the junction useless due to the loss of current control. Also, one often observes anomously high currents from the electrical surface leakage path. Next we consider the case of a field effect device as depicted in Fig. 2b, in which the application of an external voltage to G creates an internal electric field across the gate dielectric located below G. This electric field modifies the semiconductor surface potential. It is possible by the application of a surface potential to actually invert the semiconductor type in a thin skin at the surface, viz. change the carrier type by bringing minority carriers to the surface of the semiconductor. Notice that the inversion layer from p to n connects the two similarly doped parts of the device with a similar type conducting channel. With surface states present, however, part of the charge resulting from an externally applied bias voltage, which creates an electric field that operates the device, will be compensated by the charges in the surface states. The resulting change in the semiconductor surface potential will be smaller than if no states were present. The actual measurement of this surface charge using the Si surface itself as the detector will be discussed later and comprises the very important capacitance - voltage measurements. If

sufficient surface state charge is present, this charge may actually prevent inversion of the surface and thus prevent the turn on of the field effect device. This calamitous situation is termed Fermi level pinning, since as a result of charge exchange with the surface states, the Fermi level of the semiconductor cannot be altered sufficiently relative to the conduction or valence band edges at the surface, to change the dominant carrier type at the surface and thereby enable field effect device operation. The result is that surface states disrupt and even prevent device operation both for bipolar and field effect devices. The major issue becomes how to reduce or eliminate surface states from semiconductor surfaces and thereby be able to construct a high device density chip. The answer to this problem exists for the case of the Si surface. It has been found(13) that while the above discussion indeed demonstrates that the Si surface intrinsically displays a large number of surface states as do most bare surfaces, when Si is exposed to an oxidation ambient the number of states decreases by orders of magnitude. Chemically, a film of amorphous SiO_2 forms on the surface. The SiO_2 film apparently ties up the dangling bonds that gave rise to the surface states. Thus the question posed as to why is Si the semiconductor of choice lies with the fact that SiO_2 forms on the surface quite naturally in an oxygen containing ambient. The SiO_2 film not only reduces the number of the interfering surface states to well below the typical number of current carriers utilized for electronics devices, but also provides a list of bonus properties, discussed in the following section. The former property often termed electronic surface passivation, has not been obtained to the same extent with any other semiconductor and film combination at the present time. This then provides the answer to the first two questions: why Si and why SiO_2. These two materials are intimately combined into a chemically favored transformation of one into another upon the surface of the Si. The free energy for this transformation is approximately - 200 kcal/mole which attests to the reactions favored status and to the stability of the interface.

Why Thermal Oxidation?

It is now useful to consider additional benefits that specifically render the process of the thermal oxidation of Si so technologically important. The electronic passivation of the semiconductor surface seems only to require fully satisfied surface bonds. Therefore, one may deduce that virtually any method that results in an adherent film on the semiconductor surface would result in a satisfactorily passivated surface. Unfortunately, however, this is not the case even for the successful combination of SiO_2 on Si. Table 2 shows a comparison of the different ways to prepare SiO_2 on a Si surface in terms of the resulting surface states. It is seen that thermal oxidation results in the lowest number of surface states, although based on chemical analyses the films have the same composition within error limits. The surface state numbers used for the processes other than thermal oxidation are averages used here for illustrative purposes and in practise can be found to vary considerably with the specific process employed, but are always found to be higher than for thermal oxidation. It is interesting to contemplate why the other methods are inferior to thermal oxidation, or similarly why thermal oxidation reliably yields the best results. In fact there is no complete answer to this question and indeed not even a satisfactory description. The following sections on the presently practised Si oxidation process and on specific thermal oxidation mechanisms will reveal some of the important characteristics of the oxidation process that seem to answer this question, but no complete answer is available and this issue and the attainment of successful semiconductor surface passivation is the focus of current research. Before the experimental and theoretical details of what is known about thermal oxidation is presented in the following sections of this review, it is useful to first present three major practical issues that will lend perspective and background to the more weighty issues addressed later. The first issue is to consider uses for SiO_2 on Si other than as a means to electrically passivate the semiconductor surface by the reduction of surface electronic states. The second is to consider how the oxidation of Si is actually carried out and the final practical issue is how the resulting interfacial electronic

properties are measured and compared. An understanding of the measurement of the minute amounts of charge that can disrupt the operation of microelectronics devices is a vital part of the science and the factor upon which many oxidation models are based.

B. Practical Considerations

Other Uses For SiO_2

Figure 3 shows a cross section of a metal-oxide-semiconductor field effect transistor, a so-called MOSFET. In this structure several regions are shown that have SiO_2 films, but each film is grown for a different purpose. The oxide labelled "gate oxide" is subject to the most stringent quality requirements. This dielectric must support the electric field that inverts the Si surface, and thus enables conduction from source to drain. The requirements for this gate SiO_2 film are as outlined above, viz. that the surface states are to be reduced to the 10^{10} cm^{-2} level. The thicker oxide between adjacent devices is called the field or isolation oxide. This oxide has the function of electrically isolating one device from another. The $Si-SiO_2$ interfacial electronic properties in this device region are far less critical than for the gate oxides. Several orders of magnitude more surface states are tolerable in the isolation regions of the device. Therefore, according to Table 2, preparation methods other than thermal oxidation can and oftentimes are used. There are cost and process advantages with the use of the other methods as well as the possibility of less exposure of devices to the high temperatures and long process times that are required for thermal oxidation to form thick field oxide films. These engineering advantages will be discussed in more detail later as more is revealed about the oxidation mechanism. advantages. Not seen in Figure 3 are oxide films used to delineate the variously doped Si regions or to delineate electrical contacts to the various device regions. These so-called "masking" films are usually removed by etching procedures after they have served their masking purposes. While we choose not to discuss here the photolithographic processes used

for these purposes, suffice for the present discussion that the oxide electrical quality is usually not of great concern so long as the film adequately covers the desired regions of the surface to be masked. The SiO_2 films need only support optically active resist materials, and the oxides are usually entirely removed and are also quite remote from active device regions. Thus, virtually any process compatible method can be employed for the preparation of masking oxide films. Indeed for some isolation requirements and most masking functions it is not even necessary that the films be SiO_2. Si_3N_4, Al_2O_3 and various organic and other ceramic films have been used over the years within specific technologies. Thus while thermal oxidation produces the highest quality SiO_2 films for critical device areas such as gate areas, for the other device areas and for masking and isolation other film formation methods can yield acceptable films and even result in substantial benefits in cost and time. These other film preparation methods along with some pros and cons are discussed elsewhere(21).

The Method of Thermal Oxidation of Silicon

In this section we consider the technological process steps that are utilized to prepare SiO_2 films via thermal oxidation of single crystal slices of Si. The first process of this sequence is Si single crystal growth. However, to treat this broad area justly would require great length, hence only a brief outline is given herein. After that we discuss the directly relevant area of the preparation of Si wafers for oxidation followed by the oxidation apparatus, the oxidation process itself, the required post oxidation treatments, and finally the measurement of SiO_2 film electronics parameters. These parameters include such properties as film thickness and refractive index, interface fixed and mobile charges and the number of dangling bonds or interface states remaining after oxide growth.

The method for thermal oxidation is dictated by the needs of the semiconductor industry. Firstly, it is well to realize that in order to achieve both competitive electronic device performance and density at a reasonable cost, the Si devices must be fabricated on the surface of a nearly perfect single crystal of Si. Nearly perfect single crystal boules of Si can be grown by the Czochralski or Float Zone techniques(22-24). Since both Bipolar and MOS devices are constructed on or very near the surface of the single crystal, a Si slice from a boule would be ideal for this purpose. With thin flat slices of Si, both sufficient area for many devices is obtained and the costly defect free Si single crystal material is conserved. Such slices are sawn from the grown boules and then chemically etched to remove saw damage. The wafers then receive a final chem-mechanical polishing, in order to obtain a high quality surface that is flat to better than several microns and nearly perfectly smooth and specular. High quality Si wafers are presently commercially available up to about eight inches in diameter with larger sizes becoming available as needed and with a thickness from several thousandths to several tens of thousandths of an inch. These high quality Si substrates are available with various crystal orientations with the (100) and (111) being the most common, and with various levels of dopants of either n or p type. Later it will be pointed out that

the oxidation kinetics is related to both the doping level and the crystal orientation.

Cleanliness of the Si wafer itself and of the oxidation environment is of utmost importance both from the point of view of device performance and oxidation kinetics, and this latter aspect will be addressed later in this review. The attainment and maintenance of cleanliness had been recognized as important since the 1960's(13,25). From this kind of work it was made clear that the achievement of stable insulator-semiconductor interfaces was tantamount to removing unwanted impurities in the $Si-SiO_2$ system, since the formation of the oxide itself on the Si surface was found to be adequate to reduce the surface states to tolerable levels. During this era, the so-called Capacitance Voltage, C-V, measurement was invented(26) which enabled the measurement of minute amounts of charge at the $Si-SiO_2$ interface, viz of the order of 10^9 cm^{-2}. If this amount of charge were distributed in a 10nm thick layer it would represent a volume concentration of 10^{15} cm^{-3}. This incredibly small concentration of electrically active impurity is readily measured, and the principles of the measurement which include the use of the Si surface as a detector will be discussed below. The creation, measurement and avoidance of surface charge is crucial to the oxidation process.

In order to prepare a polished single crystal Si wafer for oxidation, a wet chemical cleaning process is typically employed. A number of recipes appear in the literature. With one notable exception(27) very little justification has been given for the use of one recipe over another, thus the present discussion will be limited to this relatively well justified method which has now become somewhat of an industrial standard, although usually modified to fit specific processing needs. The so-called RCA cleaning process(27) is based on hydrogen peroxide, H_2O_2 which is known to remove organic materials via oxidation and dissolution of the oxide products. Essentially, it was reported that high pH H_2O_2 solutions are particularly effective for removing organic contaminants from the Si surface while low pH solutions are effective for removing metal contaminants through complexation reactions. Thus the RCA

cleaning process is two sequential steps. The first step is made up of H_2O-H_2O_2-NH_4OH and this is followed by H_2O-H_2O_2-HCl. Quite often modifications are made such as to include: an initial organic solvent degreasing step, a thorough deionozed H_2O, D.I., rinse in between each step, a slightly elevated temperature of around 65°C, ultrasonic agitation, an HF or buffered HF (HF plus NH_4F) solution dip, in order to remove an oxide grown during the previous steps(see for example ref. 28).

Once having cleaned the as-received Si wafers, they are loaded in the vertical position onto a fused silica boat which is then inserted into a lined tube furnace for oxidation. Figure 4 shows the main features of an oxidation system. Of course many of the steps of boat loading into and out of the furnace and furnace heat cycles have been automated, but the main features of the apparatus remain the same. Virtually all of the wafer handling apparatus that contacts the high temperature oxidation ambient is made from high purity fused silica. The desired properties of fused silica are high temperature and oxidation inertness, strength at high temperatures, availability in high purity, ability to be cleaned and used repeatability, and compatability with Si and virtually all the necessary chemicals that are required to process Si. Prior to use all fused silica parts are cleaned, usually in a solution called "white etch". This is a rather concentrated solution of HNO_3 and HF (while not strictly defined it is oftentimes about 10/1 stock HNO_3/HF). This solution will slowly attack the surface of the fused silica (depending on the relative amount of HF). Thus the uppermost layer of the fused silica part, the most contaminated layer, will be removed. White etch vigorously attacks Si itself, hence any Si dust particles will be removed. This solution attacks most other common metals and inorganic materials. Oftentimes the white-etch step is preceeded by degreasing steps in organic solvents and rinses in 18 mega-ohm water. The white etch step is always followed by the D.I. water rinse. The cleaning of the large furnace tubes can be quite a feat considering the volumes of dangerous acids and the sizes of the tubes (6 feet long by 6 inches or more in diameter as minimum industrial dimensions). Thus there are

commercially available closet like automatic furnace tube cleaning apparatus' that can do this job safely and efficiently. The other small parts are cleaned individually in appropriate hoods. It should be mentioned that the cleaning chemicals and solutions are all commercially available in proper quality ratings for the microelectronics industry.

With the Si wafers vertically loaded on the boat, the boat is placed in a furnace endcap, sometimes called a "white elephant". The end cap provides a chamber in which to commence the gas purging prior to heating to the oxidation temperature, and after oxidation provides a place for the wafers to come to room temperature in a controlled ambient before exposure to the atmosphere. From the end cap the wafers are pushed into the oxidation zone of the furnace. The push and pull cycles are carefully controlled when batches of large diameter Si wafers are used. The reason is that the large wafers cool with substantive temperature gradients which produce appreciable strains resulting in dislocations in the Si and distortations to the planarity of the wafers. To reduce the steepness of the thermal gradients slow push and pull rate are employed.

Notice that Figure 4 shows a furnace that has resistance coils. Thermal oxidation systems require constant temperatures over a rather large volume for long process times, hence resistance heating is universally employed. The oxidation furnace shown is equipped with a double wall fused silica tube in which the oxidation is carried out. The purpose of the double wall arrangement is to preclude impurities from diffusing through the fused silica and contaminating the oxidation environment. Typical offending impurities are H_2 and Na. Both of these are found (as H_2O and NaCl) in normal ambient; and they can readily migrate through fused silica at the higher oxidation temperatures(29); and both of these species can alter the oxidation kinetics and/or the electrical quality of the Si-SiO_2 interface. These specific issues will be discussed later in this review. The remaining issue with the oxidation apparatus to be treated here is the quality of the gases that are directed into the oxidation apparatus. O_2 is fed into the oxidation tube inner chamber where the wafer load resides. The

O_2 is obtained from the boil off of clean liquid O_2. This practice will insure that most of the impurities such as H_2O and Na are absent in the boil off, but such non condensibles as hydrocarbons will still be present(28) in small concentrations. However, even ppb and certainly ppm of these impurities will affect the oxidation process. Hydrocarbons in amounts of about 20ppm have been found to oxidize in the oxidation furnace at the high temperatures to form H_2O which decidedly affects the oxidation kinetics(28-30) and the electrical characteristics of the oxide, this mainly being effects on the carrier trapping characteristics of the oxide(31-33). The hydrocarbon impurities can be simply removed by passing the otherwise clean boil off O_2 through a furnace to first combust the hydrocarbons to H_2O and then into a cold trap at solid CO_2 temperature (-80°C) to reduce the H_2O to less than 1 ppm, and then finally into the oxidation furnace. Between the outer and inner walls of the furnace tube, and as a flush or warm up gas in the main oxidation chamber, an inert clean gas is used. Typically N_2 or Ar is used with a preference for Ar, since under some conditions N_2 has been found to react with the Si surface(34,35) with damaging results. After oxidation, a post oxidation anneal at the oxidation temperature but in an inert ambient (preferably Ar) is performed. This anneal has been found necessary to reduce the fixed oxide charge, discussed in the next section, to acceptable levels. Ten to twenty minutes is usually adequate at temperatures above 900°C. After this treatment, the wafers are withdrawn to the end cap to cool.

Electronics Of The Si-SiO_2 Interface

In this section the physical principles and some applications of the most important Si-SiO_2 electronic diagnostic measurements are presented. A more complete and precise discussion of the Si-SiO_2 interfacial electronics properties is given elsewhere(12,36,37) with one entire book devoted to this topic(37). The intention of this section of the review is to relate enough information for a reader to be able to understand both the goals of the thermal oxidation of Si and the basis for several of the proposed models that utilize the specific

electrical nature of the $Si-SiO_2$ interface.

The first measurement we discuss is the Capacitance-Voltage, C-V, measurement. It will be shown that this technique is used to measure the important dielectric and passivating properties of the $Si-SiO_2$ interface through the use of a Metal-Oxide Semiconductor, MOS, structure depicted in Figure 5a. Essentially, this structure represents a network of capacitors of which one capacitor corresponds to the surface of the C_{Si}, can be varied through the application of an external voltage, V_g applied to the metal contact as seen in Figure 5b. Figure 6 shows the energy band structure for the ideal MOS capacitor in Figure 5 at the condition when $V_g = 0$. An ideal MOS capacitor is herein defined as one in which the metal work function ϕ_m is equal to the semiconductor work function, $\chi + E_g/2q$. For this condition for the p-type semiconductor and with no extraneous charges in the system, the potential barrier for electrons from the metal to the semiconductor, ϕ_{ms} is given as:

$$\phi_{ms} = \phi_m - (\chi + E_g/2q + \psi_B) \qquad (1)$$

where ϕ_m is the barrier between metal and insulator, and χ is the electron affinity for the semiconductor, E_g is the Si band gap, and ψ_B is the energy difference between the intrinsic Fermi level, E_i, ie. the highest energy for electrons for the undoped Si, and the Fermi level for the doped Si, E_F, which is near highest electron energy level for the specific sample. It is seen in this Figure for the ideal MOS capacitor that the Fermi levels for the different materials are aligned, and that all the electron energy bands are flat up to the interfaces. This important situation is termed the "Flat Band" condition. For the situation just described the Flat Band condition was achieved with $V_g = 0$ and no charge within the MOS structure. It is now instructive to examine the situation when V_g is changed to a value other than zero. Essentially, this is the case in which an externally applied voltage places charges on the metal surface and charge is induced in the semiconductor. Depicted in Figure 7 are the three possible situations for p-type Si. We observe that the bands in all three situations are bent at the $Si-SiO_2$ interface. The band bending is called ψ_S which denotes the

Si surface potential as compared with the bulk electron potential denoted by Ψ_B. The band bending or Ψ_S is understood by considering that the bands in the energy band picture represents the potential for electrons to move from one position to another, since the differences in energy will determine the probability for such motion. If as in Figure 7a the metal is made negative, ie. $V_g < 0$, and with a perfect dielectric through which no current flows, a positive compensatory charge is induced on the Si. This positive charge creates an energy barrier for electrons to cross the Si-SiO_2 interface, hence the electron energy bands bend towards higher energies, i.e., upwards, to represent this situation. In effect holes, the majority carriers in p-type Si, are pushed or pulled to the surface. The abundance of majority carriers at the surface of a semiconductor is called "accumulation". For an n-type Si with $V_g < 0$ the bands also bend upwards, since again we are attempting to represent the overall effect of V_g on the electron potential energy. However, with electrons as the majority carrier, the positive potential on the Si draws electrons away from the surface resulting in the condition of "depletion" of majority carriers at the Si surface. The extreme of this condition is that not only are the majority electrons depleted but simultaneously the minority carrier holes could outnumber the depleted electrons. Such a situation is called "inversion" as the majority carrier type at the Si surface has been inverted (as in Fig. 7c). Returning to the p-type sample in Figure 7b and c we see that as V_g grows more positive, a larger negative charge is induced in the Si thus drawing more holes, the majority carriers, away from the Si surface. In this way the conditions of depletion and then inversion are produced at the Si surface. The result is that V_g can control the Si surface potential, Ψ_S, which in turn controls the carrier type and abundance at the Si surface. As mentioned previously, it is this alteration of the surface conductivity which is used to operate MOS devices. It is now shown how to measure these conditions at the Si-SiO_2 interface using the Si surface as the detector. To accomplish this, we need first derive a relationship between charge, Q, and surface potential, Ψ, with the use of the Poisson equation which in one

dimension, x, has the form:

$$d^2\Psi/dx^2 = \rho(x)/\epsilon_o \qquad (2)$$

where $\rho(x)$ is the charge density and ϵ_o is the permitivity of free space. Rembering that:

$$\Psi = -\int E dx \qquad (3)$$

then

$$E = -d\Psi/dx \qquad (4)$$

and from Maxwell's relations:

$$\nabla\epsilon_o E = \rho(x) \qquad (5)$$

Thus the first integration of Poisson' equation yields the electric field, E, and the second integration yields the potential, Ψ, related to the charge density, $\rho(x)$. For the case of charge resulting from ionized donors, N_D^+, and acceptors, N_A^-, and holes, p, and electrons, n, the charge density is given as:

$$\rho(x) = q(N_D^+ - N_A^- + p_p - n_p) \qquad (6)$$

Later we consider that other sources of charge exist in the MOS system, but for now we seek only the ideal case and the resultant analytical relationships resulting therefrom. Remembering that the charge, Q, potential Ψ or for an externally applied potential we can use the voltage, V, and the capacitance are related by:

$$CV = Q \qquad (7)$$

and

$$\partial Q_s/\partial \Psi_s = C_D \qquad (8)$$

where the s subscript refers to the surface of the Si and D refers to the depletion layer. What is shown here is that the change in charge in the Si surface by means of the external voltage applied to the metal contact alters the capacitance of the depletion layer. The result is a capacitor whose capacitance is altered by the external voltage. This variable capacitance, C_D or C_{Si}, is in series with the oxide capacitance, C_{ox}, as shown in Figure 5b. The solution to the Poisson equation for the electric field, E, at the surface yields E_S at Ψ

$= \psi_S$ and the form for this equation is(12) :

$$E_S = \pm\left[(2^{\frac{1}{2}}kT/qL_D)F(\beta\psi_S, n_{po}/p_{po}) \right] \qquad (9)$$

where

$$L_D = (kT\epsilon_S/p_{po}q^2) \qquad (10)$$

and

$$F(\beta\psi_S, n_{po}/p_{po}) = \left[(e^{-\beta\psi}+\beta\psi-1) + (e^{\beta\psi}-\beta\psi-1)n_{po}/p_{po} \right]^{\frac{1}{2}} \qquad (11)$$

From Gauss' law where charge is related to the electric field:

$$Q_S = -\epsilon_S E_S \quad (12)$$

and the above relationship for E plus equation (8) we obtain the relationship:

$$C_{Si} = \epsilon_S\left[1-e^{-\beta\psi}S+(n_{po}/p_{po})(e^{\beta\psi}S-1) \right]/2^{\frac{1}{2}}L_D F(\beta\psi_S,n_{po}/p_{po}) \qquad (13)$$

which under flat band conditions, viz. $\psi_S = 0$, and with the series expansion of the exponentials we obtain for C_{Si}:

$$C_{Si}(\psi_S=0) = \epsilon_S/L_D \qquad (14)$$

For the MOS structure depicted in Figure 5, an applied voltage, V_g, will appear partly across the oxide, V_{ox}, and partly across the Si as the Si surface potential, ψ_S. The resulting electric field and potential are obtained from the integration of Poisson's equation. The total capacitance of the system is a series combination of the oxide capacitance, C_{ox}, and the capacitance of the Si, C_{Si}, which results from the depletion layer. Thus from Figure 5b we obtain:

$$C = C_{ox}C_{Si}/C_{ox}+C_{Si} \quad (15)$$

For the condition of accumulation (Figure 7), we see that there is no depletion layer, hence $C=C_{ox}$. This represents the maximum C to be measured. As V_g is changed towards depletion C_{Si} grows and the measured C decreases. This is shown in Figure 8. At inversion we again find that $C_{Si}=0$ and C should rise. For the case labeled low frequency, we observe that C approaches C_{ox}. The difference between low and high frequency measurements refers to the ability of the inversion layer minority carrier response to follow the test signal. For very

high frequencies (1 MHz) the inversion layer charge does not follow the measurement signal, hence the capacitance remains low, i.e. the specific conditions of the measurement does not sense the charge. For a very slow measurement (using a slow ramp of V_g on the order of 0.1V/s) C returns to C_{ox}. The specific experimental details of the measurement will not be treated here, but as shown in Figure 8, the ideal high frequency C-V characteristic is derived, ie. without charges except those induced by V_g. Now we need to consider the real situation, viz. that other charge may be present and consider the observed alterations to the ideal C-V characteristic.

Firstly, we consider the four kinds of charges that occur and these are summarized in Figure 9. The interface trapped charge, Q_{it}, resulting from the surface electronic states and the charges arising from mobile impurities, Q_m, were discussed above. These and the other charges such as fixed oxide charge, Q_f, located at the $Si-SiO_2$ interface and oxide trapped charge, Q_{ot}, which is distributed in the bulk of the oxide will be referred to later. Next we consider the problem of how these charges affect the ideal C-V characteristic curve developed above. Figure 10 shows that with fixed charge, Q_f, near the $Si-SiO_2$ interface some of the electric field lines arising from the applied V_g terminate on the charges rather than in the Si depletion layer. This means that some of the applied field is prevented from affecting the depletion width. Hence with charge present, a larger V_g is necessary to achieve the same value of total capacitance. The result is a parallel shift of the C-V characteristic as shown in Figure 11b. Interface trapped charge, if present in large quantities causes an assymetry in the characteristic C-V curve. This is called stretch-out and is illustrated in Figure 11a. It arises from the fact that the surface states, both donors and acceptors, are not uniformly distributed across the band gap and their frequency response is complex. Since the filled traps are sensed, the different energy regions of the gap contain differing amounts of charge and result in an assymetrical shift. Usually this high frequency C-V technique is not used to obtain Q_{it}, because it is neither quantitative nor sensitive. Use is often made of the test

signal frequency sensitivity of the charge in interface traps. It is observed that most of the interface trapped charge is not sensed at the high test frequencies. Hence a comparison of high and low frequency C-V curves with the ideal curve will yield fixed and interface trapped charge(37). Mobile charges are sensed by applying a positive V_g and mild heating (about 150°C) then cooling with positive V_g applied and remeasuring the C-V curve. Then apply a negative V_g and repeat the heating and measuring sequence. Mobile charge will be moved close to the $Si-SiO_2$ interface where it will be sensed and then the negative gate bias will serve to move it away. Again a comparison of the two measurements, yielding a parallel shift in the C-V characteristic as in Fig. 11 b, will yield Q_m and this type of measurement is called a bias temperature stress measurement.

While the Capacitance based measurements comprise the so-called MOS measurements and are used extensively to evaluate the electronic quality of the $Si-SiO_2$ interface, there are other important measurements used to assess the quality of devices. Two such measurements are dielectric or oxide breakdown measurements and trapped oxide charge measurements. Both of these kinds of measurements are required to evaluate the quality of MOS and Bipolar devices. There exists an extensive literature on the results obtained using these measurements and a repeat of this information here would detract from the main issue of Si oxidation models.

It remains now to appreciate that the capacitor-like nature of the $Si-SiO_2$ system provides insights into the oxidation problem. Some notion of this is obtained when we consider that many of the oxidation parameters such as temperature and Si orientation which have profound effects on oxidation kinetics, also similarly affect the charge at the $Si-SiO_2$ interface. It is not yet clear whether these charges affect the kinetics or vice versa, yet some relationship exists. The electronic barrier at the $Si-SiO_2$ interface is now being considered in various models, and for some time the electrical and ionic conductivity of the SiO_2 was considered. These aspects will be discussed below in light of the measured charges as described above.

III. Silicon Oxidation: A Historical Perspective

In order to be able to follow the course that Si oxidation modeling has taken and thereby appreciate the newer models, it is useful to recount older experimental studies and modeling efforts. While this literature is extensive and many of the issues are treated in detail in the presently available reviews(6-11,38,39), herein we focus on only certain specific issues that are necessary for an understanding of the survey of new models to follow. For a complete coverage of the issues presented, the reader will require recourse to the other reviews and the original literature. The issues to be covered here are: the shape of the thickness, L, versus oxidation time, t, data; the nature of the oxidant species; the oxidation temperature; the oxidation ambient; impurity effects; the nature of the SiO_2 film that is formed; and the effect of electric fields on thermal oxidation. Following a brief section on the shape of the data and the main migrating species the linear-parabolic, L-P, oxidation model will be introduced. This model has traditionally served as a basis from which to interpret many of the more recent studies, some of which identfy deviations to the L-P model.

The Oxidation Data

The shape of the oxide growth data, ie. the L versus t curve, an example of which is shown in Figure 12, can reveal much about the nature of the oxidation mechanism, and perhaps equally importantly, about what the mechanism cannot be. It was recognized that for Si oxidation, the oxidation rate both in O_2 and steam decreased with increasing oxidation time as is evidenced in Figure 12. The earliest studies (13,40) have used a parabolic rate law to describe the oxidation kinetics as:

$$L^2 \propto t \qquad (16)$$

which displays a decrease in the rate, dL/dt, as the oxidation proceeds (as L increases). This indicates that the oxidation kinetics are limited by transport which is deduced from the phenomenological diffusion equation, Fick's first law, in which the mass flux, F(D), is dependent on the reciprocal path length as:

$$F(D) \propto 1/L \qquad (17)$$

For the case of simple chemical diffusion, so called Fickian diffusion, the constant of proportionality is the diffusivity, D, and the flux is dependent on the concentration gradient across the film. The integration of equation(17) leads to the parabolic dependence on L as in relation(16). Such a rate law is directly applied to the case of the uniform motion of material across a growing film where the motion of the interface is slow relative to the relaxation of the concentration gradients(3). From plots of the logarithms of thickness versus time, the early workers(29,41,42) deduced that a parabolic law only obtained for very thick oxide films. The exponent of L was found to be closer to unity for very thin films. Hence, as to be discussed below, a linear-parabolic law was derived with the parabolic law as one limit and a linear law which represents an interface reaction as the other limit.

Considering that the shape of the data shows a decrease of rate with time a power law fit has also been attempted(43,44). However, it has been shown that a power law is not satisfactory for a large range of data (see ref. 42, Fig 12.). Of greater importance is the fact that even if the power law or any other purely mathematical function should fit the oxidation data very well, very little understanding of the oxidation phenomena is obtained through the use of arbitrary data fitting functions.

The early workers were searching for a physically reasonable oxidation model that not only gave a good fit to the oxidation data, but also conformed to what was known about the mechanism for the oxidation reaction. It is clear that whatever physical oxidation model one derives, the final thickness-time predictions must conform to the shape of the data within experimental uncertainty; but the fit of the data to a physical model does not alone prove the correctness of the model.

The Migrating Species

Since the shape of the data indicates a transport limitation, the next item of importance in the development of a physically based oxidation model is to identify the species that

move. Figure 13 shows that as the oxide film grows, the oxidant gas is separated from the Si surface, ie. the reactants are separated. Thus, for oxidation to proceed beyond the very initial monolayer formation, either oxidant or Si or both must migrate through the growing oxide film since the transport in the gas phase is fast relative to transport in the solid. The parabolicity of the L versus t data as discussed above is likely due to this transport limitation and possibly governed by Fickian diffusion. A number of early experiments were performed which concordantly showed that oxidant migrates(45,46), and a more modern experiment has confirmed this result(47). One definitive experiment(45) utilized the oxygen isotope, $^{18}0$. First an oxide was grown in $^{16}0$ containing 0_2 then in an $^{18}0$ enriched 0_2. The $^{18}0$ was found at the interface. This experiment showed that the new oxide was formed oy the long range migration of oxygen. Another experiment(46) used a layer of phosphosilicate glass formed on the Si surface. The oxidation of the glass film covered Si resulted in the phosphosilicate glass remaining as the top layer with the newly formed SiO_2 film growing under the glass film and adjacent to the Si surface, again confirming that the oxidant species migrates during oxidation. The latest experiment(47) utilized a nuclear resonance technique to depth analyze for the oxygen isotope. Not only was it confirmed that the oxidant migrated, but further experiments(48,49) also demonstrated that for ultra dry oxidation of Si by 0_2 there was no detectable exchange of O with the SiO_2 network after about 2mm of oxide is formed(50).

The issue of whether the migrating species during Si oxidation is atomic or molecular oxygen is decidedly in favor of the molecular species. Firstly, from a kinetics point of view, the parabolic oxidation rate constant to be discussed later as eqn.(25) which is directly related to the transport of oxidant is dependent on the oxidant concentration in the SiO_2, C_1. C_1 should be proportional to the oxygen pressure, $P(O_2)^n$. It is found(42,166) that n is one which is indicatative of molecular 0_2. The 0_2 molecule does not appreciably interact with the SiO_2 network unless H is present(48,49), thus a straight forward mechanism

to produce atomic O is apparently not available in SiO_2. The size of O_2 is about the same as Ar, namely about 1.8 Å (167). If the permeation of molecular O_2 occurs, then it should cause about the same perturbation to the SiO_2 network as Ar. The activation energies associated with this process, indeed are nearly the same value of about 31.2 kcal/mole for O_2 and 32.1 kcal/mole for Ar or about 1.4eV(168). Furthermore, this energy is also quite close to the reported activation energies for the parabolic rate constant of 1.2 - 1.3eV(42,56) for high temperature thick film oxidation. Thus a rather consistent argument is made based on molecular O_2 transport. It should be mentioned that this issue is not yet closed. There is some data at high presures which is not in accord with this argument(169,170). However, questions also remain as to the mechanism of high pressure oxidation.

The Effect of Electric Fields

Many metal oxidation systems are known to exhibit electric field effects during oxidation. If the oxidation proceeded by the motion of charged species, then the imposition of an external electric field (both magnitude and field direction) would alter the oxidation kinetics. Based on an early study by Jorgenson(51) in which an externally applied electric field was reported to enhance, retard and indeed stop the formation of SiO_2, depending on the magnitude and direction of the electric field, a number of field and charged species dependent oxidation models have been published. The notion of applying an electric field in the manner of the Jorgenson experiment was contested(52). It was argued that such an experiment included an external circuit that enabled a counter flow of the charge that was transported to the interface by the diffusing charged species outside of the natural path through the oxide. Without this counter flow the accumulation of charge would prevent further charged species motion. Experiments at our laboratory(53) showed that the Jorgenson experiment likely fails because the Pt that was used for electrical contact reacts with the Si rendering the experiment uninterpretable. More recent experiments have confirmed that the Jorgensen experiment was likely not correct(54) and that the results were explainable based

on silicide formation. Thus there exists no clear evidence that charged species affect the thermal oxidation of Si and we therefore eliminate such models from serious consideration at this time.

The Linear-Parabolic Model

Based on the shape of the data which indicates that transport alone cannot explain the oxidation data and that the oxidant species, primarily uncharged O_2, are actually migrating, a very successful oxidation model was derived in the 1960's called the linear-parabolic, L-P, model(29,41,42). Figure 14 shows that essentially two fluxes are considered. As a departure from the original derivation(42), the flux of oxidant from the gas to the SiO_2 surface is ignored here. This gaseous flux is generally fast relative to the other fluxes in the solid phases and therefore not kinetically significant in a series process. The flux of oxidant across the growing oxide film, F_1, is given by Fick's first law:

$$F_1 = DdC/dX \qquad (18)$$

where D is the oxidant species diffusivity, and dC/dX is the concentration gradient. For a steady state situation the gradient can be approximated as:

$$dC/dX \propto (C_1-C_2)/L$$

where C_1 is the solubility of oxidant in SiO_2, C_2 is the smaller oxidant concentration at the Si-SiO_2 interface, and L is the SiO_2 film thickness as above. The other flux, F_2, is the number of oxide molecules forming per cm^2s and is expressed kinetically by a first order chemical dependence on the oxidant concentration at the Si-SiO_2 interface, C_2:

$$F_2 = k_s C_2 \qquad (19)$$

where k_s is the surface reaction rate constant. By imposing the condition of steady state we obtain:

$$F = F_1 = F_2 \qquad (20)$$

which means that the series fluxes are self regulatory. A rate equation is then formulated in terms of the rate of formation of the oxide film:

$$dL/dt = F/\Omega \qquad (21)$$

where Ω is the conversion constant for SiO_2 film thickness to oxygen flux. C_2 can be eliminated and the rate equation rewritten as:

$$\Omega\, dL/dt = (k_s D C_1)/(k_s L + D) \qquad (22)$$

This equation is readily integrated to yield:

$$AL^2 + BL = t + const \qquad (23)$$

where A and B are the reciprocals of the parabolic, k_p, and linear, k_1, rate constants, respectively. The integration constant is evaluated at $t=t_o$, $L=L_o$ so as to be able to shift the coordinate axes to any position in L,t space. With this boundary condition, we obtain the following:

$$t-t_o = (L^2-L_o^2)/k_p + (L-L_o)/k_1 \qquad (24)$$

The use of the region L_o,t_o in L,t space is twofold: at $t_o=0$, L_o represents an initial oxide thickness either as a native oxide or from some previous processing; and L_o,t_o can be used to define a region of oxidation that does not conform to linear-parabolic kinetics. For oxidation in dry O_2 such a region has been identified extending to several tens of nm(42,55). Later this important initial oxidation regime will be discussed further as it has been the subject of a number of recent oxidation models.

Experimentally obtained oxidation data is often interpreted using the L-P oxidation model. The linear, k_1, and parabolic, k_p, rate constants are obtained from curve fitting routines and the variation of the parameters with process variables are explained using the ideas contained within the L-P model. As will be discussed later, there are instances where the L-P model does not explain the experimental results, and thus revisions and entirely new models are sought.

Temperature Dependence of the Kinetics

In strict accordance with the L-P model, a single activation energy should be associated with each rate constant for each elementary step. The transport process should yield the

activation energy for diffusion of O_2 in SiO_2 since k_p is given as:

$$k_p = 2DC_1/\Omega \qquad (25)$$

and is combined with the probably good assumption that the solubility is only a weak function of temperature. The interface reaction with the associated rate constant k_1, should also display a single activation energy associated with k_s, the surface reaction constant (see equation (19)).

For some of the data above(56,57), an analysis is made of the L,t data according to an Arrhenius equation of the form:

$$k = k_o e^{-Ea/RT} \qquad (26)$$

Figure 15 shows the Arrhenius plots for both k_1 and k_p for the temperature range of 780° to 1150°C(56,57). It is clear that there is curvature in the plots. This curvature can arise from two sources. One is that the Arrhenius notion that the process represents Boltzmann like phenomena is not accurate for Si oxidation; and the other is that the process is not an elementary kinetic step. Since there is no evidence to suspect the former, it is concluded that the phenomenological L-P model as derived above does not adequately account for the complexity of the actual Si oxidation process.

From the direction of the curvature, ie. concave up or down, the kind of rate process that is responsible can be deduced (58). The concave upward shape for k_1 indicates that parallel rate processes are ocurring while for k_p a series process is indicated by the concave downward shape. We return to this discussion later as the shape of the Arrhenius plots can be useful to eliminate some proposed oxidation models.

The Oxidation Ambient

Typically, Si oxidation is carried out in a pure O_2, pure H_2O, H_2O in O_2 or any of these ambients with HCl or some other Cl containing chemical. The reasons for these variations are now discussed and are mainly technological, however, with the use of these additional chemicals considerable complexity results for the Si oxidation mechanism.

The process advantage of H_2O over dry O_2 is the accelerated rate of oxidation with H_2O, hence a process time advantage is gained where a thick SiO_2 film is desired. However, a price is to be paid with the degraded electrical performance of the SiO_2 film. The H_2O reacts with the SiO_2 network forming two Si-OH groups. These network defects have been associated with an experimentally observed SiO_2 bulk charge trapping phenomena(31-33). This internally trapped charge gives rise to internal electric fields which affect device performance. Dry ambient annealing reduces the trapping somewhat, but never quite to reproduce dry O_2 grown SiO_2 films(33). Therefore, for active device areas such as under the gate contact for an MOS device, ie. for the gate oxide, a dry O_2 grown film is usually required. However, for masking and isolation oxides, one can often use the more rapid and economical wet O_2 or steam oxidation process. The specific kinetic role of H_2O in the oxidation ambient has been given considerable attention. It was discovered that even traces of H_2O in O_2 of about 25ppm altered the oxidation rate by an unexpectedly high 20%(28). A series of careful kinetics measurements using in-situ ellipsometry(30) have shown that both the linear and parabolic rate constants are affected. Figure 16 shows the thickness versus time data for various amounts of H_2O (30). Figure 17 shows the rate constants obtained from the L-P model plotted versus H_2O concentration. For the interface reaction there is a smooth increase in k_1 with H_2O addition, but the effect on transport is more pronounced initially with a levelling of the effect with more H_2O. According to the L-P model this has been interpreted to be a loosening of the SiO_2 network due to the reaction with H_2O, the result of which is more rapid diffusion of oxidant. If this interpretation is correct then the loosening should not only enhance the transport of H_2O but also of O_2. To test this, an analysis was performed that considered the independent transport and reaction of two oxidant species: one related to O_2 and the other related to H_2O. The resulting expression for L and t contains only the individual k_1 and k_p values obtained from pure O_2 and pure H_2O oxidations which are available from independent experiments(30). The prediction of this model is compared with experimental

data for oxidation in a controlled ambient in Figure 18 which shows an additional enhancement, that is interpreted by the L-P model to be a loosening effect of the SiO_2 network. It is interesting to observe that the effect is reversible. If the ambient is switched from dry to wet and again to dry, the oxidation rate responds. The rate increases upon introduction of H_2O to the O_2 and then slows down when the H_2O is turned off. The result of this experiment is shown in Figure 19(30).

The use of a Cl in an oxygen ambient is aimed at achieving ultra clean oxidations. The appearance of mobile charges, Q_m, is usually attributed to Na contamination from the ambient process environment. It was found that the effects of the mobile charges due to Na could be substantially reduced through the use of a Cl containing oxidation ambient(59-67). In terms of oxidation kinetics many of the chlorine containing additives contain hydrogen which reacts with oxygen to form H_2O. Once H_2O is formed then an oxidation rate enhancement is anticipated as discussed above. A detailed thermodynamic analysis of the oxidation environment has been made with the formation of H_2O and other components(64).

The issue of impurities and their effect on Si oxidation is rather complex and by no means complete. In one of the earliest (1959) and seminal papers on the subject of Si oxidation(13) the effect of impurities that can enter the oxidation process as a result of improperly cleaned Si on resultant SiO_2 and $Si-SiO_2$ interfacial electronic properties was clearly realized. Interestingly, these early workers found that impurities left on the Si surface preceeding oxidation affected the reverse current characteristics of fabricated diodes by about seven orders of magnitude. The effect of electrically active but unwanted impurities on oxidation kinetics was also studied(29) in connection with the oxidation apparatus. At very high oxidation temperatures the furnace tube was found to transpire impurities such as H_2 and Na into the oxidation zone. Both of these were found to enhance the oxidation rate. While it was generally appreciated that metallic impurities caused electrical problems in the Si substrate that are primarily related to the lifetime of minority carriers,

this author is not aware of any definitive studies on oxidation kinetics effects of metals. Also, very little effort has been expended about the efficacy of the various cleaning procedures that are practised in the Si industry. One notable exception is work on the so-called RCA cleaning process(27) as discussed under "The Method of Thermal Oxidation of Silicon." These studies concluded that H_2O_2 solutions are effective for cleaning Si surfaces. High pH solutions were found effective for the removal of organics and low pH for the removal of metallic impurities. After this time there was the addition of a brief HF dip to remove the residual oxide. Usually this HF dip is accomplished after the two H_2O_2 treatments but it has been suggested(68) that the HF dip should come prior to the acidic H_2O_2 step so as to bare the Si surface for better organic removal. Other studies(69,70) using SIMS, Auger and TEM analyses have also shown that H_2O_2 based cleaning solutions are effective at removing contaminants. Very little has been published concerning the specific effects of cleaning or the lack of it on both oxidation kinetics or electrical properties. However one brief report(71) has shown that Si cleaned using an acidic peroxide solution yielded higher Si oxidation rates than for Si cleaned using basic peroxide solutions. Higher quantities of both mobile ions and fixed oxide charge were observed on the basic peroxide cleaned Si. Very recently(72,174) this work was substantially confirmed. While it is now clear that impurity effects are readily measurable, the specific kinetic roles for specific impurities, with the exception of H_2O, are largely unknown. Based on the known role of H,H_2O, Na, and some of the dopants, it is clear that more research on the role of impurities is needed.

Quite often it is necessary to oxidize heavily doped Si substrates (dopant concentration about $10^{20}cm^{-3}$). Usual Si dopants fall into two categories: n-type dopants such as P and As; and p-type dopants such as B. Extensive experimental oxidation results are shown in Figure 20(56). It is observed that at the lower oxidation temperatures P doping accelerates the oxidation rate, but at temperatures above 1000°C, B provides the faster oxidizing Si. In order to understand these results, an understanding of the redistribution of the dopants

during oxidation is required. From this literature(73-77) it is shown that the donor impurities (As, P, Sb) accumulate at the Si-SiO_2 interface and this comprises the so-called snow plow effect, while acceptor impurities (Al, B, Ga, In) deplete. These effects are understood by comparing the relative solubilities of the dopants in SiO_2 and Si and the diffusivity of the dopant in SiO_2 and Si. The analysis of this oxidation data in terms of the linear and parabolic rate constants enabled some interpretation. There was found both a change in k_l and k_p values. The k_l values were enhanced whenever there was maximal amount of that species at the Si-SiO_2 interface, ie. at the low temperatures for P and the higher temperatures for B. The large effects found for k_p were attributed to structural changes in the oxide due to the presence of P and B. Later work on the oxidation of heavily P, As and B doped Si(78) indicates that the change in k_l may be related to the enhanced concentrations of point defects (vacancies) at the Si surface and reasonable fits to the data was obtained. Given the stress related models to be discussed later which arise from a consideration of the volume requirements for the oxidation reaction, the production of vacancies by dopants may also have relevance for other modeling efforts. The effect on the parabolic rate constants are not explained very well, but this may be an artifact due to the fitting of the data to the L-P model. This point will be discussed further later.

The Nature of Thermally Formed SiO_2 Films

It is useful to discuss here what is presently accepted to be the nature of both the thermally formed SiO_2 films and the interfacial region which is thought to be different than the bulk film. Considerable attention has been paid to the details of the SiO_2 structure (6,79,80 and references therein). Using any of the presently practised thermal oxidation schemes, the resulting SiO_2 film is non-crystalline, ie. there exists no long range order. However, the tetrahedral arrangement of O's around each Si is about the same as for the crystalline SiO_2, ie. the stoichiometry and local geometry is preserved. It should be recognized that this short range ordering is decidedly different from the situation for some

non-crystalline materials in which there is neither long nor short range order. For this reason the term vitreous is sometimes used to describe materials that have short but no long range order. Whatever is the semantics, it remains that all the studies indicate that there is chemical stoichiometry in thermally prepared SiO_2 films (see for example ref 81), but the situation is quite different for the interfacial region at the Si-SiO_2 interface. In fact most of the experimental findings concur that the Si-SiO_2 interface is comprised of a thin layer of up to 1nm of a suboxide of Si (81-84). That this is the situation is somewhat intuitive. The reaction at the interface between Si and oxidant is thermodynamically favored with about -200 kcal/mole for the change in free energy. Hence this chemical energy along with the available thermal energy, since the thermal oxidation is usually performed above 700°C, makes it reasonable that the interface is diffuse at least to several bond lengths. Later we report possible implications of this along with some new experiments and oxidation models.

IV. SILICON OXIDATION: NEW RESULTS AND MODELS

In this section several areas of new research on Si oxidation are covered: the initial oxidation regime with extensive new experimental data under a variety of conditions; film defects that could affect oxidation; charged species oxidation; photon enhanced oxidation; electron beam enhanced oxidation; mechanical film stress effects; and oxidation of metallic silicides resulting in SiO_2 films. Recently, several reviews on new oxidation models have appeared(85-87). Unavoidably, some of this material is presented here with a sometimes different perspective.

The Initial Oxidation Regime

This oxidation regime comprises the region of SiO_2 film thickness, oxidation time space that does not comform to L-P kinetics, ie. up to L_o,t_o, which is about several tens of nm. In order to better comprehend the relevance of the various experimental studies to be discussed, we dichotomize the initial regime into two parts. The first part includes the very initial regime, that is from a bare Si surface up to about 1nm; and this is followed by the regime of about 1nm to several tens of nm. The former regime is very important from the fundamental point of view, since it emphasizes the reaction at the Si surface without SiO_2 being present. The latter regime is of particular practical importance because most Si oxidation experiments begin with Si samples that already have a native oxide of up to 2nm. In a previous review of thin SiO_2 films, and followed in this review, the symbol, L_o was used to denote the upper limit of the initial regime of several tens of nm, and L_n to denote the upper limit of the native oxide thickness(11).

The study of the ultra thin film regime from 0 to L_n is fraught with experimental difficulties such as the cleanliness of the Si surface, and the vacuum conditions during the experiments. One study of surface energy measurements(88) using contact angle techniques was made in room ambient. A steep change in surface energy was reported for oxide thickness changes from 0 to 3nm. It was suggested that only a change in composition would explain the

large observed changes in surface energy. Later Rutherford backscattering measurements on thin oxides appear in agreement(81), however an ambiguity exists as to whether the etch solution (HF in H_2O) used to etch SiO_2 for the contact angle experiments is altering the surface energy. Recently, an alternative interpretation(89,90) was proposed which is based on image charges. If it is assumed that fixed oxide charge, Q_f, exists near or at the outer (ambient-oxide) interface then the interfacial energy is altered as one replaces the atmosphere (θ=1) with H_2O which has a high dielectric constant (θ=80). A good agreement to the contact angle data is obtained using charges located .3 to .6 nm from the surface and charge densities of the order of 10^{13} cm^{-2} are calculated. Whether these image charges exist and are related to the fixed oxide charge measured at the $Si-SiO_2$ interface has not yet been established. Measurements of both charge and contact angle on the same samples are required.

The usual studies of this regime, 0 to L_n are made using ultra high vacuum, UHV, and in which particular attention is paid to the cleanliness of the Si surface. One in-situ UHV study(91) utilizing Auger (AES) and electron energy loss (EELS) spectroscopies, and surface cleaning using high temperatures, reported the disappearance of surface states upon exposure to oxygen as well as the formation of oxide. Initially the oxide appears to be a suboxide in agreement with previous studies(81-84). Another similarly careful UHV study utilizing EELS(92) reported three different stages of Si oxidation. The earliest stage after oxygen exposure at low temperatures (100°K) involves molecular oxygen species which at higher temperatures converts to atomic species as stage two. The final stage for higher exposures indicates the formation of SiO_2. Optical absorption of an UHV cleaved Si crystal(93) also shows that surface electronic states within the Si band gap disappear upon oxygen exposure; these states are associated with dangling bonds at the Si surface. The valence band states are observed to be unaffected. Therefore, these studies indicate that the intuitive notion that the $Si-SiO_2$ interface has some transition region is true and that the formation of a stoichiometric SiO_2 film occurs beyond a few atomic layers and at temperatures above room

temperature.

The next growth regime from L_n to L_o which extends to several tens of nm is presently technologically important, whereas ten years ago it was merely an interesting curiosity. The reason that technology is now demanding thinner high quality SiO_2 films is a direct result of the economics which demands greater device densities for manufactured chips (for more on this issue see refs. 8 and 9). In order to achieve greater device densities, it is obvious that smaller device areas are required, and along with this but less obvious is that thinner dielectric films are also required. This latter and presently most germane requirement is best understood by considering MOS devices that are designed to operate at certain applied electric fields. The operating fields in the gate region are determined in part by the capacitance of the oxide in the MOS structure which is given as:

$$C = KA/L \qquad (27)$$

where K is the dielectric constant, A is the gate area and L is the dielectric thickness or in our case SiO_2 thickness. Thus it is easily seen that in order to down scale a device with a designed operational C to smaller area, A, in order to achieve greater densities, the SiO_2 film thickness, L, must also decrease. Present advanced technologies find L at about 20nm or less, and hence below L_o. For the highest quality SiO_2 grown in dry O_2, this thickness is within the offset region of the L-P model, ie. below L_o,t_o and hence without description.

In terms of the oxidation data representing this regime, the best data is obtained from in-situ ellipsometric experiments of which there are several published studies (55-57,94-96,162,163). The data of Hopper et al(94) shows that the shape of the initial regime up to L_o is basically linear-parabolic, as is the thicker film regime but with different L-P rate constants to describe the two thickness regimes. Later, similarly precise work revealed that the shape of the L versus t data is more parabolic when the ambient contains more H_2O (55,97). This was established based on the fit of the initial regime data to a simple linear equation of the form:

$$t = k_1 L + k_2 \qquad (28)$$

where k_1 and k_2 are simply the slope and intercept, respectively, and have no other physical significance(97). The quality of the fit is given in Table 3 and it is seen that from 780° to 980°C the dry O_2 data fits best. The parabolic term in the L-P model is derived from the consideration that the formed SiO_2 film actually protects the Si surface from further oxidation, ie. the grown film provides a barrier to further oxidant penetration. Thus with this idea, the parabolic shape of the oxidation data is interpreted as the films ability to protect the underlying substrate from further oxidation, and one deduces that the wet grown oxides are more protective. This interesting point will be discussed further in the next section on oxide film defects. The extensive new data of Massoud et al.(57,162,163) generally agrees with the other data on the appearance of the initially fast oxidation regime. Massoud et al used exponentials with appropriate damping lengths to precisely fit the data in the initial regime. One of the most interesting feature of the Massoud et al data is the observed Si substrate orientation dependence for the L,t data. The earliest reports of this orientation dependence(98) showed that for high pressure oxidation the (111) Si was the fastest with the (110) next. According to the L-P model this might be interpreted in terms of the number of available Si atoms at the various surfaces. However, as is seen in Table 4 the (110) has the greatest areal density of Si atoms, so a more convoluted model was constructed that depended on the number of available bonds at the Si surface(98). The original L-P model(42) contains the orientation dependence implicitly in the linear rate constant, k_1, since the substrate surface ought to dominate the surface reaction. The Massoud et al data clearly shows that for the thinnest films on the three major low index planes of Si, the order for the oxidation rate, R, is:

$$R(110) > R(111) > R(100)$$

and this order parallels the areal density of Si atoms without convoluted arguments. Sample data is shown in Figure 21. It is both interesting and comforting to note that there is a

crossover in the order of the (110) and (111) Si for the thicker films, such that agreement with the literature(98) is achieved for the thicker films.

An explanation for this crossover effect was based on the interface reaction and the effects of stress on Si oxidation(99). As above, the early rate should and does scale with the areal density of Si atoms. Beyond the crossover, however, another dominant physical mechanisn is required. A model based on mechanical stress was invoked(100,101). With the observation that Young's modulus, E, for Si varies with orientation as:

$$E(111) > E(110) > E(100)$$

and with the observation that an intrinsic stress develops during thermal oxidation this stress model proceeds. The observed tensile stresses in the Si surface are considered to accelerate the surface reaction rate by increasing the reactivity of the stretched Si bonds. The order for the magnitude of the observed stress should be the same as the order for E above considering a constant strain. The actual force is obtained from the product of the stress and film thickness, hence the force increases with the oxide film growth. Thus, the dominance of this stress modification to the initial rate does not occur until the forces become sufficient which seems in accord with the crosssover effects. The origin of the stress, the measurement and further implications are to be reviewed further in the section entitled "Mechanical Stress Effects". In short this stress model seems to predict the qualitative aspects of the crossover observations and is even relatively quantitative with the (111) and (110) orientations(99).

In order to prove or disprove this model the Massoud et al data has recently been extended down to 600°C oxidation temperature where the stresses are larger and to include the (311) and (511) Si orientations(95,96). The crossover has been seen in the oxidation data from below 1100°C down to 750°C; for lower temperatures the films were too thin to exhibit the crossover. The (311) and (511) orientations were chosen because they would have higher Si atom densities if the planes are flat. However, this is fictitious because these planes are

actually vicinal planes of the low index major planes, the (111) and (100) planes(102). These vicinal planes are composed of (111) risers and (100) terraces and therefore the actual areal densities of Si atoms is between the (111) and (100) as is shown in Table 4. Figure 21 shows that the oxidation rate order is:

$$R(110) > R(111) > R(311) > R(511) > R(100)$$

which confirms that the areal densities for these vicinal planes scales with the initial oxidation rate. It was also found(96) with the aid of new data that neither the stress alone nor the stress multiplied by the thickness could explain the crossover as was previously proposed(103). Thus if stress really does control the crossover in oxidation rate, the effect was incorrectly incorporated into the model(103). The latest results(96) strongly suggest that the crossover is related to the film stress where the concentration of oxidant is reduced by a compressive oxide stress. The appearance and disappearance of this stress was found to modulate the oxidation rate(161). It is clear that further work on this issue is necessary.

It is also instructive to consider the oxidation of Si in the initial regime at pressures less than 1 atm. The most extensive recent work has been the work of Rochet et al.(147) using O_2 pressures about 10 torr and the temperature range of 600 - 1100°C. They used nuclear resonance techniques and the isotope $^{18}O_2$ to measure transport effects, XPS and TEM to observe structural effects, and they paid careful attention to H_2O content of the ambient maintaining it at less than a fraction of a ppm. Their results for the thin oxide regime are almost completely different from 1 atm. oxidation results. They see no Si orientation dependence , and a reversed dependence on doping, viz. heavy P doping, retards the rate at low oxidation temperatures. The very initial rate of oxidation is slower than the regime that follows, and the oxide has some crystalline quality. The distribution of ^{18}O in the SiO_2 indicates that O atoms are transported via network hopping.

Other work using low O_2 pressures have also been reported which show unusual results

compared with 1 atm. oxidation. On one study(171) a different Si orientation dependence was reported, viz. the (100) became faster oxidizing than (111). In another study done at pressures near the critical pressure, viz. near the equilibrium betweem SiO and SiO_2, clear evidence for crystalline SiO_2 was found(172).

The Rochet et al.(147) work has taken extraordinary measures to keep H_2O from entering the gas stream. They could not measure H_2O content less than a fraction of a ppm, the results scaled with different levels of care in removing the H_2O. While it is true that more in-situ analytical studies will be required to fully substantiate the levels of H_2O that they claim to monitor other impurities, the results strongly suggest that the O_2 pressure decidedly alters the Si oxidation mechanism.

Oxide Defects

The SiO_2 films prepared by Si oxidation are usually amorphous but with a definite stoichiometry. Structurally, this means that the films are composed of SiO_4 tetrahedra with rather fixed tetrahedral angles and Si-O bond lengths, but that there is a random arrangement of these tetrahedra and hence a distribution of Si-O-Si bridge bond angles. Thus, the O-Si-O bond angles are near tetrahedral while the Si-O-Si inter-tetrahedron angles can display a wide variation, so as to provide a random arrangement of the well defined tetrahedra. In short, the SiO_2 films possess short range but no long range order. Without extended planes of atoms or molecules the definition of line and planar defects, one and two dimensional defects, respectively, which require long range periodicity, becomes virtually impossible. However, point defects such as vacancies, interstitials, impurities, and three dimensional defects such as pores, channels, cracks, etc, are similar to those found in crystalline materials. As discussed in the previous section entitled "The Migrating Species-O_2" it was shown that for pure dry O_2 oxidation, the dominant mobile species are O_2 molecules which migrate without substantial interaction with the SiO_2 network, hence via long range

interstitial motion. Therefore, unless one is considering the oxidation of Si in the presence of H_2O or other ambient impurities, the oxidation via oxide point defects need not be considered. An interesting aspect of interstial point defects which is relevant to the oxidation of Si in pure O_2 is the issue of Si interstitials(104-106). It has been proposed that the reaction between oxidant and Si is incomplete thereby resulting in excess Si atoms which can migrate as interstitials back into the Si possibly causing extrinsic oxidation induced stacking faults and/or migrate into the SiO_2 where the Si interstitial is subsequently oxidized. This latter idea(106) will be returned to when stress effects are discussed in the section entitled "Mechanical Stress Effects".

Based on the possible arrangements of the SiO_4 tetrahedra(107,108), the formation of higher density channels in the SiO_2 films was proposed. Such regions were called "microchannels" and could provide novel transport properties such as the rapid lattice diffusion of oxygen atoms during oxidation. No direct evidence has yet been provided for the existence of these structures. Alternatively, the existence of negative density regions, or "micropores," was also proposed(97). This proposal was based on several experimental observations, namely, dielectric breakdown histograms, rapid initial oxidation kinetics and transmission electron microscopy, TEM, observations of chemically etched SiO_2 films. The dielectric breakdown histograms are plots of the number of SiO_2 capacitors that breakdown versus the electric field at which the breakdown occurs. The capacitors were made using very thin SiO_2 films of about 15nm thick. Theoretically, such a histogram should be a delta function at the maximum electric field that the particular material can withstand. In fact, however, a distribution with a low electric field tail is usually observed. The magnitude of the low field tail is usually interpreted in terms of oxide defects(109). The main observation as shown in Figure 22, is that few low field breakdowns were observed for oxides grown with H_2O present. Electron trapping which is known to be present in thicker wet grown oxides(31-33), and which could result in apparently improved breakdown results due to bulk

charge trapping, was shown not to be causative for these thin oxides(97). As was previously discussed, the dry 0_2 grown SiO_2 films were found to display more linear kinetics (in terms of L versus t) in the initial regime than for wet grown films. In concordance with the L-P model, this linearity is an indication that the oxide is less protective than wet grown oxides which display relatively parabolic kinetics. In order to try to observe oxide defects, the thin dry grown SiO_2 films were prepared for TEM analysis by chemical removal of the Si substrate. The Si etchant was a mixture of HF in HNO_3 which vigorously attacks Si but only relatively mildly attacks SiO_2. Hence by monitoring the light transmitted through the Si wafer, the etching process can be terminated when the Si is just removed, and oftentimes before the oxide is totally removed, thus yielding a partially etched SiO_2 film for TEM examination. If the SiO_2 films were totally homogenous, then one would expect layer by layer removal of the oxide leaving thinned but uniform oxide without holes. However, TEM revealed holes in the oxide films. Following this work, careful high resolution TEM observations also uncovered inhomogenieties in the dry gown SiO_2 films which could be interpreted as micropores (110,111). The size and density of the inhomogenieties were about 1 nm in diameter and 10^{12} cm^{-2}, respectively. These three experimental results indicated that micropores existed in the oxide films. Micropores explain the linear like kinetics by providing short circuit paths through the oxide directly to the interface. The breakdown results are rationalized based on locally enhanced electric fields in the oxide film in the vicinity of the pores; and the appearance of pores even using conventional TEM suggests that the pores are readily etched to a larger diameter by the chemical etchants.

Using this direct evidence for the existence of micropores, an oxidation model based on micropores was proposed(103). Essentially, the flow in micropores was considered to be Knudsen-Poiseuille flow where the flux of flowing particles, dn/dt, in small cylindrical pores with diameters, d, and length, L, is directly proportional to the pressure drop across the pores and inversely to the length as:

$$dn/dt \propto P/L \qquad (29)$$

With the pressure drop converted to concentration this formula resembles Fick's first law as used in the L-P model. Hence one would expect a similar shape for the resulting integrated rate expression. If it is assumed that the number of pores is greatest for thin films, then an initially fast regime is obtained which is concordant with observation. Recent calculations have supported the notion that Fickian diffusion is not limiting the oxidation mechanism up to at least several tens if not hundreds of nm of SiO_2(96,112). This may indicate that one of the basic assumptions of the L-P model is flawed. Table 5 excerpts some of the results(96,112) which shows the ratio of the maximum O_2 Fickian flux to the O_2 flux calculated from the observed SiO_2 growth rate. With this ratio greater than one, the Fickian flux cannot be rate limiting as it is larger than the observed flux. Also from published values for the O_2 diffusivity(113), random walk calculations show that O_2 travels about 10^5 nm in seconds which supports the above calculations that show for $L < 100$nm diffusion is faster than the observed oxidation rate(39,112,173).

These results seem contrary to many of the ideas about Si oxidation, and give rise to a new oxidation model to be presented below in the section entitled "A New Initial Regime Oxidation Model." It is possible that either the literature D values are in error or Fickian transport is not the correct form for O_2 transport, or both. Confirmatory measurements of the chemical diffusivity of O_2 are sorely needed in order to definitely prove the role of Fickian diffusion on the oxidation mechanism.

Electrically active point defects in SiO_2 are also important from the point of view of the electrical properties of the oxide. In SiO_2 films the E' center which is a trivalent Si bound to three O atoms has been identified by electron spin resonance techniques(114,115). This E' center has also been implicated in charge trapping effects in the SiO_2 films. However, no correlation of this bulk SiO_2 defect with Si oxidation has yet been made, and from what we know about dry O_2 oxidation, viz. the small amount of exchange of O with the

SiO_2 network during oxidation, the invoking of point defect models in the oxide appears non-productive.

Charged Oxidant Species

As discussed previously, for many metal oxidation systems, charged oxidant species play a major role and a number of detailed oxidation models have been formulated (see for example refs 1-5). For the case of Si oxidation, however, there exists no experimental evidence that charged species are important. Also, as mentioned above there is significant evidence that for dry O_2 oxidation, molecular O_2 migrates interstially through the SiO_2 thus eliminating charged defects from consideration. While we could now dispense with further discussion of charged species and electric field assisted oxidation it is useful to review some recent models in the light of the literature on this issue, in order to point out the apparent inconsistencies with presently available experimental observations.

In the section entitled, "The Migrating Species", the possibility of considering the long range motion of charged species during Si oxidation was found to be unwarranted. However, for films thinner than several tens of nm, the importance of charged species and electric fields cannot be entirely ruled out especially for the very initial oxidation regime.

With the early recognition of an initially fast oxidation regime, the Cabrerra-Mott model(116) was invoked(42). This model predicts the effect of the space charge due to ionic species on the oxidation rate. The flow of both ions and electrons is important with the latter by tunneling or thermionic emission. The Cabrerra-Mott ideas have had wide application for many metal oxidation systems where the oxide is electrically conductive, thus providing a path for electrons, and where ionic transport via lattice exchange is dominant. For the case of SiO_2 grown on Si, neither of these conditions are met for films thicker than 5nm, hence this model is thought not to be applicable(117). Recent explanations have attempted to utilize the general observation of positive Q_f at the $Si-SiO_2$ interface, as a starting point for charged species models. One such model(118) considers that the positive Q_f at the

interface attracts negative oxidant species within several tens of nm where the electric field resulting from the Q_f is strongest. Through the inclusion of electric field dependent transport terms into the L-P model, a good fit to the experimental L,t data was obtained via the extra fitting parameters in the final rate expression. Two other recent models(119,120) similarly argue that the field effects due to Q_f are important but in a direction opposite to the model above. The reasons for the chosen directionality are not clear to this author. Another field dependent oxidation model(121) considers broken bonds at the Si surface to give rise to the Q_f which in turn gives rise to field driven changes in the oxidation kinetics. Again, a good fit to the experimental data is obtained. While the physical reasoning for each of these models is different, good fits to the experimental data is obtained with all of them. This is, of course attributable to the similarity in form for the integrated rate expressions and to the number of fitting parameters. None of these models has been critically tested either through experimental verification of the tenets of the models or against the wide variety of published oxidation experiments. Thus this author concludes that these models are presently unfounded.

Photon Effects

Early experiments aimed at discovering possible photon effects on Si oxidation utilized photons emanating from both a mercury arc lamp and iodine vapor lamp and sometimes in combination(122) that were focused onto the cleaned and heated Si surface. An enhancement of the oxidation rate was seen for all temperatures from 955°C to 1215°C with the greatest enhancement at the lower temperatures. Using a L-P analysis it was concluded that the initial regime is most affected. With a UV filter in place, normal oxidation rates were observed as was the case when the Si was masked from the light but the gas was not, and IR analysis of the grown SiO_2 films always indicated no change of structure for the uv grown SiO_2 films. The conclusion was that the uv light elevates electrons over the $Si-SiO_2$ barrier. No further mechanism was offered. Also, high freqency C-V curves were obtained which compared the Q_f for

the irradiated samples. The Q_f measurements revealed that uv irradiation during growth decreased the positive Q_f as does a normal inert post oxidation anneal. No large effect was seen for Q_{it} as measured from the (lack of) stretch-out in the high frequency C-V curves. Several more recent investigations have been reported in which laser light has been used as the source of photons(123-128). In one study(123) the uv light from an Ar laser was shown to enhance the oxidation rate even after the calclated temperature rise was accounted for, thus both a thermal and photonic effect was reported. Si bond breaking was proposed to account for the effect. In a following study by the same authors(124), a wavelength dependence was reported which indicated that for light with energies greater than about 3 eV an additional enhancement was observed. In another study(125) a scanning Ar laser was used to heat a large area of the Si surface and thereby increase the oxidation rate. Again both thermal and photonic enhancements were reported. In another study in which the laser beam power density was carefully considered, an even greater photonic effect was reported(127). More recently an extensive wavelength study(128) shows a much greater enhancement of the oxidation rate with light above 3 eV and greater effects with p-type Si. The wavelength studies(124,128) strongly suggest that electrons and electron related effects are important for Si oxidation as was originally suggested(122). Electron effects were postulated as causitive possibly through the destabilization of the O_2 molecule and this point will be returned to below. It thus appears that all the light stimulated Si oxidation studies are in agreement on the issue that there does exist a purely photonic oxidation enhancement effect for photon energies greater than 3 eV, and these thoughts have recently been summarized into a photonic oxidation model(128).

A New Initial Regime Oxidation Model

The photon effects seem to point to the importance of the electron barriers to Si oxidation kinetics and a new model for oxidation(129). Thus, a consideration of the appropriate energies may also be important for normal thermal oxidation, especially in the

very initial regime where oxidant transport, by whatever mechanism, is not affecting the oxidation rate. It is necessary to test whether any of the barrier energies, shown in the energy band diagram for the Si-SiO_2 system in Fig. 6, could control the thermal oxidation rate, and also explore whether any of the barrier energies could alter the thermal oxidation rate.

From Fig. 6 it is seen that several routes having different energies are available to promote electrons from Si to the SiO_2 conduction band. From the Si valence band an energy of about 4.15 eV is required, while for the Si conduction band, about 3 eV is necessary. Intermediate in energy are the defect levels (for n and p Si) and the intrinsic Fermi level at which there are no electron states, only a probability. To determine which, if any, of these barriers may be oxidation rate limiting, we calculate the electron flux, F_{et}, from the Richardson-Dushman thermionic emission equation and compare that with the flux of O_2 which is derived from the experimental oxidation rates(55-57,95,96),(F(exp). This assumes that one electron per O_2 molecule is required for oxidation, which is justified later when the specific mechanism is proposed. Since we are mainly dealing with orders of magnitude approximations here, factors up to ten are of little consequence. Table 6 shows the calculated barrier heights, χ_o, such that the F_{et} equals F(exp) at various oxidation temperatures. It is seen that barriers of the order of 3 eV are appropriate. This is the energy barrier value for the Si conduction band electrons. A simple calculation confirms that there are sufficient conduction band electrons for oxidation, by a factor of ten or more, at any temperature above room temperature at which the numbers are marginal.

Now we propose a mechanism in which there exists a rapid flux of O_2 to the Si surface relative to the consumption of O_2 on the SiO_2 side of the Si-SiO_2 interface, and also a rapid flux of electrons on the Si side, with the flux of electrons over the barrier to be rate limiting and an activation energy of χ_o. Once an electron goes over the barrier it attaches by a favorable reaction(130) to O_2 forming O_2^- which decomposes to O atoms more readily than

O_2 (by 25% or more). Oxidation then proceeds readily by reaction of Si with O atoms. In a parallel way, oxidation can also occur, but much more slowly by reaction with O_2. Such a parallel reaction scheme was already suggested(131) for the initial regime and more recently, further data was found in support of the idea(94). Also, the curvature found for Arrhenius plots for linear rate constants could be explained based on a parallel path reaction scheme(58).

Finally, this electron limited mechanism yields insight into the formation of the 1 nm native oxide which forms virtually instantly on a fresh Si surface even at room temperature, yet virtually ceases to grow after 2 nm unless the temperature is raised. If we consider the approximately 10^{15} Si surface electronic states per eV, most of which have eventually captured an electron from the bulk Si, then there are about 10^{15} electrons available for Si oxidation. These electrons exist in closely spaced levels and require only little energy promotion. Thus these electrons are available in addition to the thermionically produced electrons. The 10^{15} electrons could yield about 1 nm SiO_2 at the rate of one electron per O_2 molecule. The native oxide thickness is 1-2 nm. Once the states are removed via oxidation, however, this native oxide can no longer form and the thermionic and/or photonic excited electrons are required for further oxidation.

Mechanical Stress Effects

Early studies on SiO_2 film stress(132,133) were performed on films grown using high oxidation temperatures greater than 1000°C which was appropriate to the technology at that time. These studies concordantly reported that the measured residual room temperature stress could be completely explained based on the thermal expansion stress, σ_{th}, which develops upon cooling from the oxidation temperature, and as a result of the difference in thermal expansion coefficients, $\underline{\Delta}\alpha$, between SiO_2 and Si. Since σ_{th} is proportional to both $\underline{\Delta}\alpha$ and $\underline{\Delta}T$ as:

$$\sigma_{th} \propto \underline{\Delta}\alpha\underline{\Delta}T \quad (30).$$

Since at the oxidation temperature $\underline{\Delta}T=0$, σ_{th} cannot be implicated in any oxidation models. In the late 1970's a study (100) indicated that for oxidation temperatures below 1000°C an intrinsic stress, σ_i, is observed which increased for lower oxidation temperatures. The existence and temperature variation of this intrinsic stress, σ_i, was confirmed (101,134,135), and a model was proposed(101) which not only explained the appearance of the stress, but also the simultaneous appearance of an increased SiO_2 film density as the oxidation temperature decreased (101,136). The model called the "viscous flow model" (101) was based on earlier proposed ideas(100,137) and is explained with the use of Figure 23. A 120% increase in molar volume occurs in converting Si to SiO_2 which establishes the volume requirement in order for the reaction to proceed. With the SiO_2 formation on the Si surface there is a free direction into which the SiO_2 can expand as it is formed, viz., the direction normal to the Si surface. If the oxide can find this direction then the expansion of the newly formed SiO_2 film will occur unimpeded. The viscous flow model assumes that this free direction is "found" by viscous flow. At the high oxidation temperatures, above 1000°C, where the oxide viscosity is sufficiently low, the oxide is constrained by adhesion in the plane of

the Si surface, and flows readily into the normal direction. However, at lower oxidation temperatures, the higher oxide viscosity precludes easy flow within the time frame for oxidation, and an intrinsic stress develops. Since the oxide viscosity increases as the temperature decreases, it then follows that the intrinsic stress which develops should also increase with decreasing oxidation temperature, as is observed. Along with the observation of the intrinsic stress and its temperature dependence, is the parallel observation of an increase of the SiO_2 film density(101,136,138,139) with decreasing oxidation temperature. With the viscous flow model, the densification is understood as the accomodation of the SiO_2 film growth system to the accumulation of stress, viz. the system attains as small a volume as possible so as to minimize the stress. Although the SiO_2 network is quite open, only a small density increase is permitted before large repulsive forces are encountered. Between the oxidation temperatures of 1100°C and 700°C about a 3% density increase is observed. The experimental measurement of the density, ρ, for these thin films is worthy of further comment. The first report of a density increase with lower oxidation temperatures was by Taft(136), and was based entirely on the precise measurement of the refractive index, n, values as a function of oxidation temperature and the application of the Lorentz-Lorenz relation to convert n to density. Later Irene et al.(139) found nearly identical refractive indices, but went further and obtained the density directly from measurements of the film volume and mass. While this latter measurement of density is not as precise as the measurement of n, the direct measurement yielded the same temperature dependence as the n derived values and approximately the same absolute value, so as to give more confidence to the ellipsometrically obtained ρ values. Figure 24 shows both the measured film stress, σ_i, and density, ρ, as obtained from n measurements, as a function of oxidation temperature. Recently, the same density change as a function of oxidation temperature was found using infrared spectroscopy techniques(138). Figure 25 shows the IR spectra for three oxidation temperatures; and a shift towards lower frequency, v, for the 1075 cm^{-1} band is observed.

This band is associated with the Si-O-Si bond angle, θ, which is the angle between adjacent SiO_4 tetrahedra and is a measure of the Si-Si distance which relates directly to parting of tetrahedra, hence SiO_2 density. The lower v the smaller is θ, and hence the smaller is the Si-Si distance and the higher is the film density. From the IR, a 2-3% increase in density is obtained in substantial agreement with the other measurements. Also, in Fig. 24, an orientation dependence of the intrinsic stress is shown, and the implications of this orientation dependence on the oxidation kinetics orientation dependence was discussed above in the section entitled "The Initial Oxidation Regime."

New Low Temperature Oxidation Data

Several new thermal oxidation studies have appeared(57,95,96,162,163) that have employed in-situ ellipsometry techniques. The two main advantages of this technique are that dense data sets which are amenable to significant data analysis are obtained and that the oxidized samples are not subject to damage or impurity contamination through exposure to the laboratory ambient during an experiment, ie. all the data in a given oxidation experiment are obtained from one sample. Massoud et. al. have found that exponentials are quite useful to fit the very initial regime and that two rapidly decaying exponentials seem to fit best. Greater film thicknesses are well represented using the L-P model from which linear and parabolic rate constants were obtained. Similar to the results in Figure 15(56), the dense and complete data of Massoud et al.(57,162,163) confirm the break seen in the Arrhenius plots of the linear and parabolic rate constants at about 950°C. This work reviewed a number of mechanisms that are relevant to the oxidation mechanism. Of particular importance to the oxidation problem was the establishment of the Si substrate orientation dependence of the kinetics (57,162,163) and which was recently extended to include lower temperature oxidation data (95,96).

The viscous flow ideas(101) described above were recast in terms of possible effects on oxidation kinetics in two ways. One way is to permit the stress to affect the interface

reaction(103) and the other is to alter transport(140-142).

For the initial regime, the rate of oxidation is considered to be proportional to the rate at which newly formed SiO_2 can flow into the free direction. The specific formulation was based on the linear rate constant, k_1, as given by equation(19) above rewritten as:

$$R = k_1 C_2$$

where the rate, R, is proportional to the oxidant concentration at the interface, C_2 and k_1, contains information about the Si surface. In order to include stress, the expression for R is modified. First we make explicit the Si surface atom per area concentration, C_{Si}, but as an effective Si concentration, C^*_{Si}. C^*_{Si} is given as the product of C_{Si} multiplied by the rate at which the oxide flows away from the Si surface, $\dot{\theta}$:

$$R = k' C_2 C_{Si}$$

and

$$R = k' C_2 C_{Si} \dot{\theta}$$

But $\dot{\theta}$, the strain rate is given as the stress in the Si surface, σ, divided by the SiO_2 viscosity, η, according to the Maxwell viscoelastic model for a solid. Hence the final result for the initial rate is:

$$R = k' C_2 C_{Si} \sigma/\eta$$

As discussed above in "The Initial Oxidation Regime," the initial rate should then scale with the product $C_{Si}\sigma$ for a given C_2, with different Si orientations, but, this was not always found to be the situation.

For the models of transport, all the workers(140-142) indicate that the oxide stress, being compressive, decreases the diffusivity, D. Some workers(140,141) consider a SiO_2 thickness, L, dependence of the strain field, hence D(L). Another group considers a time dependence through the relaxation formulas, hence D(t). All these workers attempt to describe both the initially fast oxidation regime and the thick film growth kinetics based on

the stress (or strain) dependence of D. It has not yet been made clear how a smaller D, due to compressive oxide strain, can cause an initially fast oxidation regime. Yet the authors get good fits of their models to the experimental data.

On the issue of data fitting to one model, or another, it is useful to reconsider this question. With the advent of dense L,t oxidation data via in-situ ellipsometry experiments (55-57,94-96,162,163), it is tempting to try to distinguish among models based on the quality of the fit to the data. However, caution must be exercised in that different forms of similar equations will give identical fits to the data(65,143) though the forms are based on different physics. Also errors in the data or the formulation of the correct physics may yield worse fits than an incorrect but mathematically more flexible model. The reader is cautioned that many incorrect oxidation models that fit the L,t data rather well are reported in the literature.

Si-SiO_2 Interfacial Layer Models

The references summarized above in the section entitled " The Initial Oxidation Regime" concordantly suggest that the Si-SiO_2 interface is different than either Si or SiO_2. A recent extensive review of the interfacial regime(144) strongly supports the notion that the interfacial region is structurally distinct. It is therefore useful to consider possible implications of the interfacial region on the Si oxidation kinetics.

From several published studies(106,145,146), it was suggested that there is likely an epitaxial relationship between the first several layers of oxide grown on the Si surface. This is derived from structural compatibility arguments and the minimization of the molar volume difference between the two phases. In terms of an oxidation model a two step process was envisioned(106) in which the first step produced the epitaxial layer of oxide but with a concentration of interstitial Si atoms. The interstitials resulted from the imperfect match across the phase boundary. The second step was the oxidation of the interstitial Si atoms with the concomitant amorphization of the oxide due to the lattice expansion.

Recent studies on the transport of oxidant through a growing oxide(50,147) yielded some evidence that the very initial oxide forms as a result of the motion of O atoms as opposed to the findings for thicker oxides in which O_2 was found to be the transported species as was discussed in the previous section entitled "The Migrating Species". This new mode of transport for the very thin films suggested the possibility for an ionic transport mechanism(147).

Theoretical studies(148) have considered the existence of an array of disclinations in the oxide near to the Si-SiO_2 interface which arise from oxidation at the various surface sites such as kink sites. Prior to this work was the report(149) of the existence of a blocking layer near the Si surface. This blocking layer was modeled in terms of the oxidation kinetics effects and essentially gave a satisfactory growth law. Essentially the transport through two series layers was considered and agreement with the linear-parabolic model was obtained with two layers but one oxidant species in each layer. As discussed above, the mere consistency cannot be taken as proof for the model, but these ideas are certainly worthy of further consideration.

From x-ray photoelectron spectroscopy studies(150,151) as well as a consideration of a wide variety of complementary studies (as reviewed in ref 144), an argument was made for the existence of a strained layer near the Si-SiO_2 interface. This layer was characterized by having a higher density and different ring statistics than the other SiO_2. The implications for oxidation kinetics were not made clear in this work except by reference to other studies which considered the effects of stress on Si oxidation kinetics (see the section entitled "Mechanical Stress Effects").

While none of these intriguing studies are conclusive, many possible effects have been investigated and some experimental evidence has been given. It remains to be established if the existence of the strange interfacial layer actually determines the oxidation kinetics via an altered transport and/or reaction term, or are these novel structures simply the by-

product of the oxidation mechanism.

Silicide Oxidation

Recently considerable attention has been paid to research on the oxidation of technologically important metal silicides(152-155). For many of the silicide films on a Si substrate, the oxidation conditions can be adjusted so that exclusively SiO_2 forms on the silicide surface. Thus the silicide is preserved. Since the silicide films are used for interconnects, it is imperative that the cross section be preserved, in order to insure low resistivity. For the present purposes, we do not choose to review the details of this research (the interested reader is directed to refs. 152-155 and refs. therein), but rather briefly describe the work that yields information relative to our understanding of Si oxidation to form SiO_2, the subject of the present review.

Under carefully chosen oxidation conditions that yield only SiO_2, it has been observed that a large number of the silicides oxidize at a faster rate than pure Si itself(152,156-158). Also, evidence is presented that shows that groups of silicides oxidize similarly, viz. the transition metal silicides oxidize fastest, with refractory metal silicides next, and with Ir,Re and Ru silicides at about the same rate as for Si. Fig. 26 summarizes these findings with our recent data that illustrates the grouped oxidation behavior(158). For the oxidation to proceed to produce only SiO_2 and preserve the silicide, there must be a net flux of Si from the Si substrate to the SiO_2-silicide interface to fuel the oxidation reaction. The thermodynamic criteria for this situation has been discussed(152-154). A kinetic model has been suggested(159) that is analogous to the L-P model but includes this new Si flux. Of course this net flux is not necessarily the actual flux. For the transition metal silicides, the silicide decomposes during oxidation with the metal moving towards the Si substrate where it reforms silicide. For the refractory silicides, indeed Si moves from the substrate to the oxidizing surface as is also the case for many of the noble metal silicides. Thus the net flux of Si necessary to the oxidation reaction may arise from different Si supply mechanisms.

However, whatever is the nature of the net Si flux, this flux cannot of itself be the cause for the increased rate observed for some of the silicides. The addition of a series flux in a series process cannot enhance the rate. Thus, the oxidation rate enhancement must arise from other causes. Assuming that the SiO_2 films formed are nearly the same on all of the silicides oxidized to produce SiO_2, then the transport mechanism of oxidant through the SiO_2 can also be eliminated from consideration as the rate enhancing step. The interface reaction is then implicated as the likely step that is different on the fast versus slow oxidizing surfaces. A model was proposed that included the net Si flux but concluded with the suggestion that the bonding of Si at the silicide surface must be different to explain the faster observed oxidation rates(159).

Some very recent work(158) has suggested that the rate enhancement is due to the availability of electrons at the oxidizing surface. The background for this idea lies with work that demonstrated that the Si surface oxidizes more rapidly with a disordered sub-monolayer of metal as compared with an ordered sub-monolayer(160). Surface analysis showed that the ordered surface possessed a smaller density of electron states. The recent work on silicide oxidation(158) has also shown from optical absorbtion studies that the faster oxidizing silicides possess a higher density of surface carriers. Thus it was concluded that the electronic nature of the oxidizing is crucially important for silicides and as discussed above with the thermionic oxidation model for Si itself. The information obtained from oxidation studies on silicides, has yielded further insight on Si oxidation.

V. Summary

The purpose of this review was to critically summarize the most recent Si oxidation models. In order to develop the perspective necessary to appreciate both the newest models and the older models, the silicon oxidation technology, and key experimental facts were also briefly and selectively reviewed. It is the authors belief that much of the evolution of the Si oxidation experiments and models is driven by technological requirements. It is, therefore, essential that the reader be aware of the cleanliness requirements and the electrical criteria for charge and interface states at the semiconductor surface, in addition to a more straightforward treatment of the film formation kinetics.

The chemical reaction between Si and oxidant is complex. It involves the tranformation of one crystalline phase, Si, into another usually amorphous phase, SiO_2, in thin film form. It is, therefore, easy to appreciate why our understanding of the apparently simple reaction between Si and oxidant is not well understood when one considers that even the pure gas phase reaction chemistry of other equally simple molecules is not well understood. The inclusion of such complexities as condensed phases, both crystalline and amorphous, mass transport restrictions, constrained molar volume changes plus the reaction chemistry renders the Si oxidation problem a general model system for broad materials science research.

The Si oxidation system provides a unique and almost perfect interface, the $Si-SiO_2$ interface, whose electrical properties have been intensely investigated. The inclusion of the electronic dimension to the study of the film formation adds to the scientific breadth of the problem. The simple C-V measurements enable the direct assessment of the electrical quality of the film-substrate interface with a sensitivity unequaled by any other analytical procedure. These measurements have been performed on SiO_2 grown under a variety of conditions and attempts have been made to correlate the electrical and kinetics results. The fact that SiO_2, as an insulator, is optically transparent in a large portion of the optical spectrum and the near perfection of the Si surface, enables the employment of reflection in-

situ ellipsometry to follow the course of the SiO_2 film formation kinetics as it occurs. With all this electronic and kinetic data, plus the employment of an arsenal of other spectroscopies to both SiO_2 and Si, the questions of what is yet to be done, and why is there still controversy arise and remain.

The controversial aspects of Si oxidation stem from several sources. One is that the numerous experimental studies have not all employed the best tools, and thus the control and reliability of the data is questionable. Another source of controversy is that many of the proposed models are based on premises that far exceed the experimental data. It appears that the pressures to publish first in a fast paced technology have spurred the publication of ill thought out models that usually fall by the wayside equally quickly as new experiments are done. Another major source of controversy is simply the lack of experimental information. There is considerable argument about the mechanism of oxidant transport, its dominance or lack thereof and the numerical parameters such as the chemical diffusivity for oxidant. Whether Fickian transport diffusion occurs has never been substantiated, yet most workers assume its correctness. The major kinetic effects of minute amounts of impurities, of stress, of Si orientation, of interfacial electronic parameters still require careful correlation with the oxidation rates. The experiments required are very difficult, time consuming and costly. Only one or two industrial laboratories support this kind of research and in a minor way. The U.S. government, which crucially depends upon Si, has with a few exceptions deemed the Si area not fundable and has focused on more esoteric materials systems that represent a miniscule fraction of useable devices. The erroneous presumption made is that industry is supporting the research. A few universities have been active and are addressing some of the above mentioned issues.

The $Si-SiO_2$ system represents a model semiconductor system from which a clear understanding of the requirements for surface passivation can proceed. Studies aimed at passivating III-V and other electronic materials have attempted to imitate the $Si-SiO_2$ system

but without much success. It is clear that understanding is lacking. The essential criteria to obtain surface passivation, viz. the unpinning of the Fermi level, are not understood. It would seem that further research starting from the one eminently successful system, $Si-SiO_2$, is required so as to proceed from the known to the unknown.

Acknowledgements

This research was sponsored in part by the Office of Naval Research. The author is particularly indebted to the following for critical comments and helpful discussions: S. Clay-Vitkavage, A. Cros, F.M. d'Heurle, R.D. Frampton, R. Ghez, G. Gould, E. Kobeda and E.A. Lewis.

References

1. A.T. Fromhold, "Theory of Metal Oxidation - Volume 1, Fundamentals," Defects in Crystalline Solids, Vol. 9, North Holland, Amsterdam (1976).
2. A.T. Fromhold, "Theory of Metal Oxidation - Vol. 2, Space Charge," Defects in Crystalline Solids, Vol. 12, North Holland, Amsterdam (1980).
3. U.R. Evans, "The Corrosion and Oxidation of Metals," Edward Arnold Ltd., London (1960).
4. K.R. Lawless, "The Oxidation of Metals," Rep. Prog. Phys., 37, 231 (1974).
5. A. Atkinson, Rev. Mod. Phys., 57, 437 (1985).
6. F.P. Fehlner, "Low Temperature Oxidation: The Role of Vitreous Oxides," John Wiley and Sons, New York (1986).
7. S. Rigo, "Instabilities in Silicon Devices: Silicon Passivation and Related Instabilities," Chapter 1, "Silica Films on Silicon," Eds. G. Barbottin and A. Vapaille, Elsevier, North Holland (1986).
8. E.A. Irene, Semiconductor International, April 1983, p. 99.
9. E.A. Irene, Semiconductor International, June 1985, p. 92.
10. E.A. Irene, "Silicon Oxidation: A Process Step for the Manufacture of Integrated Circuits," Ed. P. Stroeve, in "Integrated Circuits," American Chem. Soc., p. 31 (1985).
11. E.A. Irene, in "Passivity of Metals," Ed. M. Froment, Elsevier, p. 11, May 30 - June 3, 1983, Bombannes, France.
12. S.M. Sze., "Physics of Semiconductor Devices," John Wiley and Sons, 2nd edition, New York (1981).
13. M.M. Atalla, E. Tannenbaum and E.J. Scheiber, Bell Syst. Tech. J., 38, 749 (1959).
14. I. Tamm, Physik Z. Sowjetunion, 1, 733 (1932).
15. W. Schockley, Phys. Rev., 56, 317 (1939).
16. J.T. Law and C.G.B. Garrett, J. Appl. Phys., 27, 656 (1956).
17. D.R. Palmer and C.E. Davenbough, Bull. Amer. Phys. Soc., 3, 138 (1958).

18. C.N. Berglund, IEEE Trans. Electron Dev., ED-1B, 701 (1966).

19. R. Castagne and A. Vapaille, Surface Sci., 28, 557 (1971).

20. P.V. Gray and D.M. Brown, Appl. Phys. Lett., 8, 31 (1966).

21. J.M. Aitken and E.A. Irene, "Treatise on Materials Science and Technology," Eds. M. Tomazawa and R.H. Doremus, Academic, New York (1985), Vol. 26, p. 1.

22. "VLSI Technology," Ed. S.M. Sze, McGraw Hill, New York (1983).

23. R.A. Colclaser, "Microelectronics Processing and Device Design," John Wiley (1980).

24. S. Wolf and R.N. Tauber, "Silicon Processing for the VLSI Era, Volume 1 - Process Technology," Lattice press, California (1986).

25. E.H. Snow, A.S. Grove, B.E. Deal, and C.T. Sah, J. Appl. Phys., 36, 1664 (1965).

26. L.M. Terman, Solid State Electron., 5, 285 (1962).

27. W. Kern and D.A. Poutinen, RCA Review, 31, 187 (1970).

28. E.A. Irene, J. Electrochem. Soc., 121, 1613 (1974).

29. A.G. Revesz and R.J. Evans, J. Phys. Chem. Solids, 30, 551 (1969).

30. E.A. Irene and R. Ghez, J. Electrochem. Soc., 124, 1757 (1977).

31. E.H. Nicollian, A. Goetzberger, and C.N. Berglund, Appl. Phys. Lett., 15, 174 (1969).

32. E.H. Nicollian, C.N. Berglund, P.F. Schmidt and J.M. Andrews, J. Appl. Phys. 42, 5654 (1971).

33. D.R. Young, E.A. Irene, D.J. DiMaria, R.F. DeKeersmaecher amd H.Z. Massoud, J. Appl. Phys., 50, 6366 (1980).

34. S.I. Raider, R.A. Gdula and J.R. Petrak, Appl. Phys. Lett., 27, 150 (1975).

35. B.H. Vromen, Appl. Phys. Lett., 27, 152 (1975).

36. A.S. Grove, "Physics and Technology of Semiconductor Devices," Wiley, New York (1967).

37. E.H. Nicollian and J. Brews, "MOS (Metal Oxide Semiconductor) Physics and Technology," John Wiley and Sons (1982).

38. W.A. Pliskin and R.A. Gdula, "Passivation and Insulation" in Materials Properties and Preparation—Vol. 3, Ed. S.P. Keller, North Holland (1980).

39. E.A. Lewis and E.A. Irene, J. Vac. Sci. Technol. A, 4, 916 (1986).

40. M.M. Attala, "Semiconductor Surfaces and Films; The Silicon-Silicon Dioxide System" in "Properties of Elemental and Compound Semiconductors, Ed. H. Gatos, Vol. 5, Interscience (1960).

41. W.A. Pliskin, IBM J. Res. Dev., 10, 198(1966).

42. B.E. Deal and A.S. Grove, J. Appl. Phys., 36, 3770 (1965).

43. C.R. Fuller and F.T. Strieter, Proc. of Electrochem. Soc. Meeting, Toronto, Canada, May 3-7 (1964).

44. H.C. Evitts, H.W. Cooper and S.S. Flaschen, J. Electrochem. Soc., 111, 688 (1964).

45. J.R. Ligenza and W.G. Spitzer, J. Phys. Chem. Solids, 14, 131 (1960).

46. W.A. Pliskin and R.P. Gnall, J. Electrochem. Soc., 111, 872 (1964).

47. E. Rosencher, A. Straboni, S. Rigo and G. Amsel, Appl. Phys. Lett., 34, 254 (1979).

48. S. Rigo, F. Rochet, B. Agius and A. Straboni, J. Electrochem. Soc., 129, 867 (1982).

49. R. Pfeffer and M. Ohring, J. Appl. Phys., 52, 777 (1981).

50. F. Rochet, B. Agius and S. Rigo, J. Electrochem. Soc., 131, 914 (1984).

51. P.J. Jorgenson, J. Chem. Phys., 37, 874 (1962).

52. D.O. Raleigh, J. Electrochem. Soc., 113, 782 (1966).

53. E.A. Irene and R. Barton, unpublished results.

54. D.N. Modlin and W.A. Tiller, J. Electrochem. Soc., 132, 1659 (1985).

55. E.A. Irene and Y.J. van der Meulen, J. Electrochem. Soc., 123, 1380 (1976).

56. E.A. Irene and D. Dong, J. Electrochem. Soc., 125, 1146 (1978).

57. H.Z. Massoud, J. Plummer and E.A. Irene, J. Electrochem. Soc., 132, 1745 (1985).

58. E.A. Irene, Appl. Phys. Lett., 40, 74 (1982).

59. P.H. Robinson and F.P. Heiman, J. Electrochem. Soc., 118, 141 (1971).

60. R.S. Ronen and P.H. Robinson, J. Electrochem. Soc., 119, 747 (1972).

61. R.J. Kriegler, Y.C. Cheng and D.R. Colton, J. Electrochem. Soc., 119, 388 (1972).

62. K. Hirabayshi and J. Iwamura, J. Electrochem. Soc., 120, 1595 (1973).

63. Y.J. van der Meulen and J.G. Cahill, J. Electronic Materials, 3, 371 (1974).

64. R.E. Tressler, J. Stach and D.M. Metz, J. Electrochem. Soc., 124, 607 (1977).

65. D.W. Hess and B.E. Deal, J. Electrochem. Soc., 122, 579 (1975).

66. A. Rohatgi, S.R. Butler, F.J. Feigl, H.W. Kramer and K.W. Jones, Appl. Phys. Lett., 30, 104 (1977).

67. G.J. Declerck, T. Hattori, G.A. May, J. Beaudouin and J.D. Meindl, J. Electrochem. Soc., 122, 436 (1975).

68. W. Kern, Semiconductor International, p. 94, April 1984.

69. B.F. Phillips, D.C. Burkman, W.R. Schmidt and C.A. Petersen, J. Vac. Sci. Technol. A, 1, 646 (1983).

70. R.C. Henderson, J. Electrochemical Soc., 119, 772 (1972).

71. F.N. Schwettmann, K.L. Chiang and W.A. Brown, 153rd Electrochem. Soc. Meeting, Abs. #276, May 1978.

72. G. Gould and E.A. Irene, J. Electrochem. Soc., 134, 1031 (1987).

73. M.M. Atalla and E. Tannebaum, Bell Syst. Tech. J., 39, 933 (1960).

74. F. Leuenberger, J. Appl. Phys., 33, 2911 (1962).

75. A.S. Grove, O. Leitstiko and C.T. Sah, J. Appl. Phys., 35, 2695 (1964).

76. B.E. Deal, A.S. Grove, E.H. Snow and C.T. Sah, J. Electrochem. Soc., 112, 308 (1965).

77. B.E. Deal and M. Sklar, J. Electrochem. Soc., 112, 430 (1965).

78. C.S. Ho and J. Plummer, J. Electrochem. Soc., 126, 1516 and 1523 (1979).

79. "The Physics of SiO_2 and Its Interfaces," Ed. S.T. Pantelides, Pergamon 1978.

80. "The Physics of MOS Insulators," Eds. G. Lucovsky, S.T. Pantelides and F.L. Galeener, Pergamon 1980.

81. T.W. Sigmon, W.K. Chu, E. Lugujjo and J.W. Mayer, Appl. Phys. Lett. 24, 105 (1974).

82. S.I. Raider and R. Flitsch, J. Vac. Sci. Technol., 13, 58 (1976).

83. C.R. Helms, J. Vac. Sci. Technol., 16, 608 (1979).

84. F.J. Grunthaner, P.J. Grunthaner, R.P. Vasquez, B.F. Lewis, J. Maserjian and A.

Madhukar, J. Vac. Sci. Technol., 16, 1443 (1979).

85. E.A. Lewis and E.A. Irene, J. Vac. Sci. Technol., A4, 916 (1986).

86. E.A. Irene, "The Effects of Temperature, Stress and Orientation on the Initial Si Oxidation Regime," Abs. #364, presented at Electrochem. Soc. Meeting, Oct. 1986.

87. E.A. Irene, "Thermal Oxidation of Silicon: New Results and Models," International Conference on Insulating Films on Semiconductors, Belgium, April 1987.

88. R. Williams and A.M. Goodman, Appl. Phys. Lett., 25, 531 (1974).

89. A.M. Stoneham and P.W. Tasker, J. Phys. C: Solid State Phys., 18, L 543 (1985).

90. A.M. Stoneham and P.W. Tasker, Semicond. Sci. Technol., 1, 93 (1986).

91. J. Derrien and Commandre, Surface Science, 118, 32 (1982).

92. H. Ibach, H.D. Bruchmann and H. Wagner, Appl. Phys. A, 29, 113 (1982).

93. P. Chiaradia and S. Nannarone, Surface Science, 54, 547 (1976).

94. M.A. Hopper, R.A. Clarke and L. Young, J. Electrochem. Soc., 122, 1216 (1975).

95. E.A. Lewis, E. Kobeda and E.A. Irene, "Proceedings of Fifth International Symposium on Silicon Materials Science and Processing," Ed. H.R. Huff, Boston, Mass., May 1986.

96. E.A. Lewis and E.A. Irene, J. Electrochem. Soc., accepted for publication 1987.

97. E.A. Irene, J. Electrochem. Soc., 125, 1708 (1978).

98. J.R. Ligenza, J. Phys. Chem., 65, 2011 (1961).

99. E.A. Irene, H.Z. Massoud and E. Tierney, J. Electrochem. Soc., 133, 1253 (1986).

100. E.P. EerNisse, Appl. Phys. Lett., 30, 290 (1977); 35, 8 (1979).

101. E.A. Irene, E. Tierney and J. Angillelo, J. Electrochem. Soc. 129, 2594 (1982).

102. K. Ueda and M. Inoue, Surf. Sci., 161, L578 (1985).

103. E.A. Irene, J. Appl. Phys., 54, 5416 (1983).

104. S.M. Hu, J. Appl. Phys., 45, 1567 (1974).

105. T.Y. Tan and U. Goesele, Appl. Phys. Lett., 39, 86 (1981); 40, 616 (1982).

106. W.A. Tiller, J. Electrochem. Soc., 128, 689 (1981).

107. A.G. Revesz and H.L. Schaeffer, J. Electrochem. Soc., 129, 137 (1982).

108. A.G. Revesz and V. Gibbs, "Proceedings of Conference on Physics of MOS Insulators," Eds. G. Lucovsky, S.T. Pantelides and F.L. Galeener, p. 92 Pergamon (1980).

109. N.J. Chou and J.M. Eldridge, J. Electrochem. Soc., 117, 1287 (1970).

110. J.M. Gibson and D.W. Dong, J. Electrochem. Soc., 127, 2722 (1980).

111. J.K. Srivastava and J.B. Wagner Jr., Proceedings of Electrochem. Soc. Meeting, Cincinnati, Ohio, May 7-11 (1984).

112. E.A. Irene, Phil. Mag. B, 55, 131 (1987).

113. F.J. Norton, Nature, 191, 701 (1961).

114. Y. Nishi, Jap. J. Appl. Phys., 10, 51 (1971).

115. E.H. Poindexter, E.R. Ahlstrom and P.J. Caplan, in "The Physics of SiO_2 and Its Interfaces," Ed. S.T. Pantelides, P227, Pergamon, 1978.

116. N. Cabrerra and N.F. Mott, Rep. Prog. Phys., 12, 163 (1948/49).

117. N.F. Mott, in "Passivity of Metals," Ed. M. Froment, Elsevier, p. 1, May 30 - Jun. 3, 1983, Bombannes, France.

118. Y.Z. Lu and Y.C. Cheng, J. Appl. Phys., 56, 1608 (1984).

119. M. Hamasaki, Solid State Electron., 25, 479 (1982).

120. M. Naito, H. Homma, N. Momma and Y. Sawahata, Proc. Electrochem. Soc. Meet., Cincinnati, Ohio, May 7-11, 1984.

121. S.A. Schafer and S.A. Lyon, Appl. Phys. Lett., 47, 154 (1985).

122. R. Oren and S.K. Ghandi, J. Appl. Phys., 42, 752 (1971).

123. S.A. Schafer and S.A. Lyon, J. Vac. Sci. Technol., 19, 494 (1981).

124. S.A. Schafer and S.A. Lyon, J. Vac. Sci. Technol., 21, 422 (1982).

125. Ion W. Boyd, Appl. Phys. Lett., 42, 728 (1983).

126. Ion W. Boyd, "Surface Studies with Lasers," Eds. F.R. Aussenberg, A. Leitner and M.E. Lippitech, Springer-Verlog 1983, p. 193.

127. E.M. Young and W.A. Tiller, Appl. Phys. Lett., 42, 63 (1983).

129. E.A. Irene and E.A. Lewis, Appl. Phys. Lett., submitted for publication 1987.

130. L.M. Chanin, A.V. Phelps and M.A. Biondi, Phys. Rev., 128, 219 (1962).

131. R. Ghez and Y.J. van der Meulen, J. Electrochem. Soc., 119, 1100 (1972).

132. R.J. Jaccodine and W.A. Schlegel, J. Appl. Phys., 37, 2429 (1966).

133. M.V. Whelan, A.H. Gormans and L.M. Goossens, Appl. Phys. Lett., 10, 262 (1967).

134. E. Kobeda and E.A. Irene, J. Vac. Sci. Technol. B, 4, 720 (1986).

135. E. Kobeda and E.A. Irene, J. Vac. Sci. Technol. B, 5, 15 (1987).

136. E.A. Taft, J. Electrochem. Soc., 125, 968 (1978).

137. W.A. Tiller, J. Electrochem. Soc., 127, 619, 625 (1980).

138. G. Lucovsky, M. Mantini, J.K. Srivastava and E.A. Irene, J. Vac. Sci. Technol. B, 5, 530 (1987).

139. E.A. Irene, D. Dong and R.J. Zeto, J. Electrochem. Soc., 127, 396 (1980).

140. A. Fargeix, G. Ghibaudo and G. Kamarinas, J. Appl. Phys., 54, 2878 (1983); 54, 7153 (1983); 56, 589 (1984).

141. G. Camera Roda, F. Santarelli and G.C. Sarti, J. Electrochem. Soc., 132, 1909 (1985).

142. R.H. Doremus, Thin Solid Films, 122, 191 (1984).

143. J. Blanc, J. Electrochem. Soc., 133, 1981 (1986).

144. F.J. Grunthaner and P.J. Grunthaner, "Chemical and Electronic Structure of the SiO_2/Si Interface," Materials Science Reports 1987.

145. F. Herman, I.P. Batra and R.V. Kasowski, in "The Physics of SiO_2 and Its Interfaces," Ed. S.T. Pantelides, p. 333, Pergamon, N.Y. 1979.

146. B. Agius, S. Rigo, F. Rocket, M. Froment, C. Maillot, H. Roulet and G. Dufour, Appl. Phys. Lett., 44, 48 (1984).

147. F. Rochet, S. Rigo, M. Froment, C. d'Anterroches, C. Maillot, H. Roulet and G. Dufour, "Advances In Physics," 35, 237 (1986).

148. J.P. Hirth and W.A. Tiller, J. Appl. Phys., 56, 947 (1984).

149. W.A. Tiller, J. Electrochem. Soc., 130 501 (1983).

150. F.S. Grunthaner and J. Maserjian, in "Physics of SiO_2 and Its Interfaces," Ed. S.T. Pantelides, Pergamon, p. 389 (1978).

151. F.S. Grunthaner, P.J. Grunthaner, R.P. Vasquez, B.F. Lewis, J. Maserjian and A. Madhukar, J. Vac. Sci. Technol., 16, 1443 (1979).

152. F.M. d'Heurle, A. Cros, R.D. Frampton and E.A. Irene, Phil. Mag..

153. F.M. d'Heurle, in "Solid State Devices 1985," ed. P. Balk and O.G. Folberth, Elsevier, Amsterdam, p. 213 (1986).

154. H. Jiang, C.S. Petersson and M.A. Nicolet, Thin Solid Films, 140, 115 (1986).

155. S.P. Murarka, "Silicides for VLSI Applications," Academic Press, New York (1983).

156. M. Bartur and M.A. Nicolet, Appl. Phys. Lett., 40, 175 (1982).

157. F.M. d'Heurle, R.D. Frampton, E.A. Irene, H. Jiang and C.S. Petersson, Appl. Phys. Lett., 47, 1170 (1985).

158. R.D. Frampton, E.A. Irene and F.M. d'Heurle, J. Appl. Phys., in press (1987).

159. L.N. Lie, W.A. Tiller and K.C. Saraswat, J. Appl. Phys., 56, 2127 (1980).

160. A. Cros, J. de. Phys. 44, 707 (1983).

161. J.K. Srivastava and E.A. Irene, J. Electrochem. Soc., 132, 2815 (1985).

162. H.Z. Massoud, J.D. Plummer and E.A. Irene, 132, 2686 (1985).

163. H.Z. Massoud, J.D. Plummer and E.A. Irene, 132, 2693 (1985).

164. B.E. Deal, J. Electrochem. Soc., 127, 979 (1980).

165. E.H. Nicollian and A. Goetzberger, Bell Syst. Tech. J. 46, 1055 (1967).

166. L.N. Lie, R.R. Razouk and B.E. Deal, J,. Electrochem. Soc., 129, 2828 (1982).

167. J. Jeans, "An Introduction to Kinetic Theory of Gases," Cambridge University Press, London, p. 183 (1967).

168. R.M. Barrer, J. Chem. Soc., 378 (1934).

169. R.J. Zeto, C.G. Thorton, E. Hryckowian and C.D. Bosco, J. Electrochem. Soc., 122, 1419 (1975).

170. J.K. Srivastava and E. Irene, Abs. No. A-4, presented at Electronics Materials Conference, Amherst, Mass., June 25-27 (1986).

171. S.I. Raider and L.E. Forget, J. Electrochem. Soc., 127, 1783 (1980).

172. F.W. Smith and G. Ghidini, J. Electrochem. Soc., 129, 1300 (1982).

173. E.A. Irene and R. Ghez, Appl. Surf. Sci., in press 1987.

174. J.M. deLarios, C.R. Helms, D.B. Kao and B.E. Deal, Appl. Surf. Sci., in press 1987.

List of Tables

Selected Properties of Common Semiconductors

Property	Si	Ge	GaAs	InP
Energy Gap (eV)	1.1	0.7	1.4	1.4
Density of States (cm^{-3})				
Conduction Band	3×10^{19}	1×10^{19}	5×10^{17}	—
Valence Band	1×10^{19}	6×10^{18}	7×10^{18}	—
Intrinsic Carrier Mobility at 300°K (cm^2/Vs)				
electrons	1500	3800	8500	4000
holes	450	1800	400	150

Table 1 Trans

Comparison of Surface States Resulting from Different SiO_2 Preparation Methods

SiO_2 Preparation Technique	Approximate Number of Surface Electronic States (per area)
Thermal Oxidation	10^{10}
Chemical Vapor Deposition (CVD)	10^{11}-10^{12}
Physical Vapor Deposition (PVD)	10^{11}-10^{13}
No SiO_2 on Si	10^{15}

Table 2 Irene

Temperature (C)	Ambient	Std Dev of Fit	$1/k_l$ (Å/min)	k_{LIN}* (Å/min)
780	D	0.86	0.56	0.57
	W	4.0	0.1	0.10
893	D	0.40	2.8	2.2
	W	1.0	0.78	0.60
980	D	0.37	8.9	7.7
	W	1.1	3.3	4.6

*k_{LIN} from the linear - parabolic model

Table 3 Irene

Silicon Surface Atom Densities

Silicon Orientation	Si Atom Density ($cm^{-2}.10^{-14}$)
(110)	9.59
(111)	7.83
(311)	7.21*
(511)	7.05*
(100)	6.78

(from ref. 96, Table 3, where * refers to vicinal surfaces)

Table 4 Irene

Ratio of Diffusive Flux, F(D), to the

Experimental Flux, F(exp) at Several Thickness Regimes

	Film Thickness (nm)	F(D)/F(exp)
(111) Si at 700°C	5	14.2
	10	9.1
	20	5.2
(111) Si at 1000°C	100	3.3
	200	3.0
(111) Si at 1100°C	100	1.5
	500	1.1
	700	1.1

Table 5 Irene

Electron Barrier Heights Calculated

from Experimental Oxidation Rates on Si (100) Surfaces

Oxidation Tempertature (°C)	X (eV)
600	2.87
700	2.92
750	3.02

Table 6 Irene

List of Figures

Figure 12. Typical SiO_2 film thickness, L, versus oxidation time, t, data for Si oxidation (after ref. 55, with permission of the Electrochemical Soc., Inc.).

Figure 13. Pictoral representation of SiO_2 film separating reactants: oxidant and silicon.

Figure 14. Pictoral representation of the important fluxes for the Linear - Parabolic model (after ref. 21, Figure 4, with permission of Academic Press, Inc.).

Figure 15. Arrhenius activation energy plots for the linear, k_1 and parabolic, k_p, rate constants (after ref. 9, with permission of Semiconductor International).

Figure 16. The effect of controlled H_2O additions to O_2 on the Thermal Oxidation of Si (after ref. 30, with permission of The Electrochemical Soc., Inc.).

Figure 17. The variation of the linear and parabolic rate constants with H_2O additions to O_2 on Si oxidation (after ref. 10, Figure 5, with permission of the American Chemical Soc.).

Figure 18. A comparison of a model for parallel diffusion and reaction for two oxidant species for the oxidation of silicon with experimental data for two species (H_2O, O_2) and one species (O_2) (after ref. 30, with permission of the Electrochemical Soc.).

Figure 19. The effect of switching oxidation ambients from dry to wet O_2 then back to dry O_2 (after ref. 30, with permission of the Electrochemical Soc.).

Figure 20. The effect of heavy P and B doping (nominally 0.001 /cm) on Si oxidation kinetics for the following temperatures: (a) 780°C. (b) 893°C, (c) 980°C, (d) 1000°C, (e) 1040°C, (f) 1150°C (after ref. 56, with permission of the Electrochemical Soc., Inc.).

Figure 21. Si orientation Crossover in oxidation rates between (110) and (111) orientations (after ref. 96, with permission of the Electrochemical Soc., Inc.).

Figure 22. Dielectric breakdown histograms for (a) dry grown SiO_2 and (b) wet grown SiO_2 (after ref. 97, with permission of the Electrochemical Soc., Inc.).

Figure 23. Pictorial representation of the viscous flow model for Si oxidation (after ref. 101, with permission of the Electrochemical Soc., Inc.).

Figure 24. (a) Intrinsic SiO_2 film stress as a function of oxidation temperature; (b) SiO_2 film density from refractive index values, as a function of oxidation temperature ((a) after ref. 135 with permission of the American Vacuum Soc. and (b) after ref. 112, with permission of Phil. Mag.).

Figure 25. Normalized IR adsorption spectrum for SiO_2 films grown in dry O_2 at three oxidation temperatures. The atomic displacements of the three main features are indicated (after ref. 138, with permission of the American Vacuum Soc.).

Figure 26. SiO_2 film thickness versus oxidation times for oxidation of various metal silicides (after ref. 158).

Silicon (100) Surface

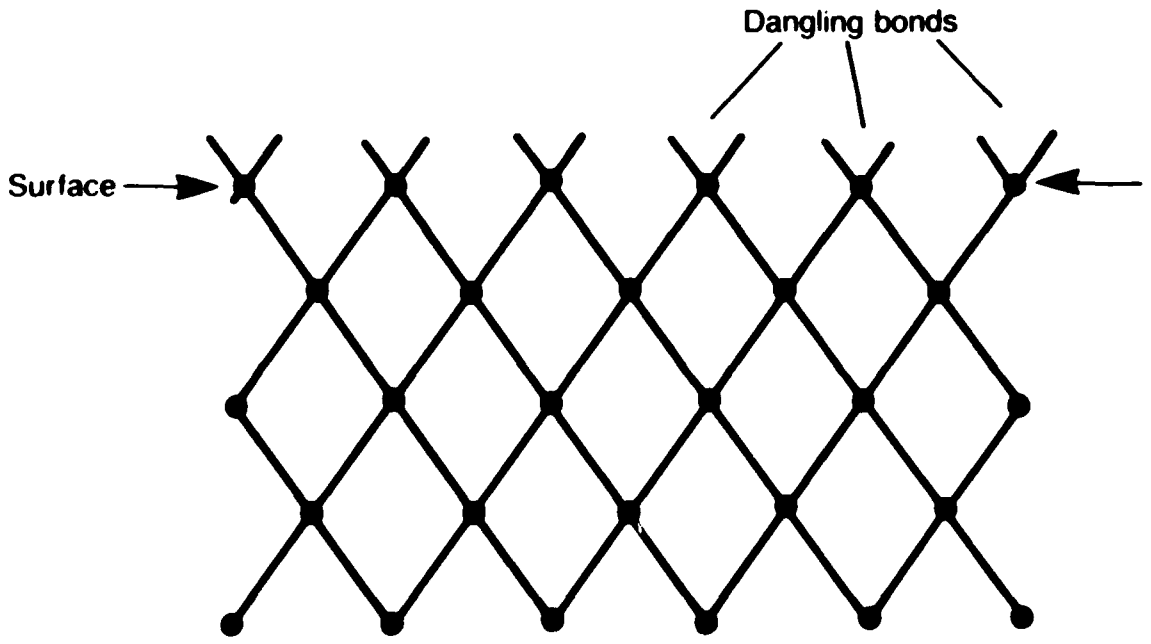

Fig 1 Irene

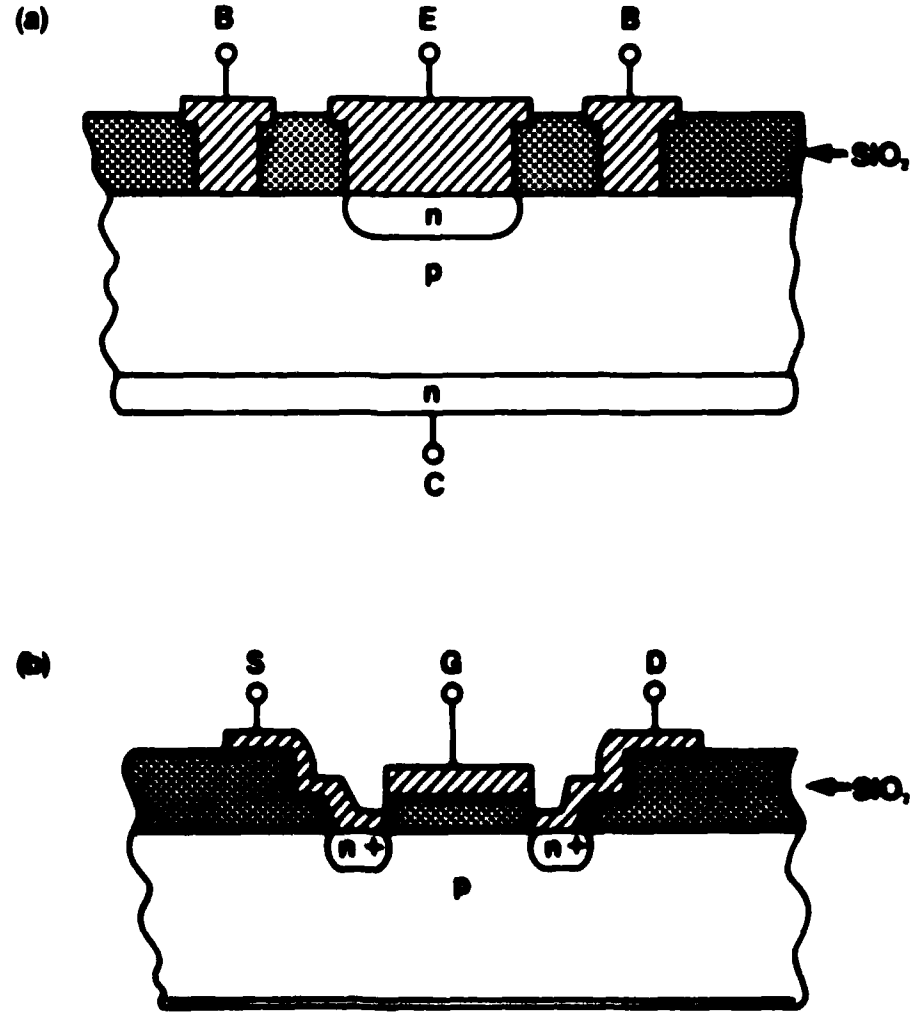

Fig 2 Inv

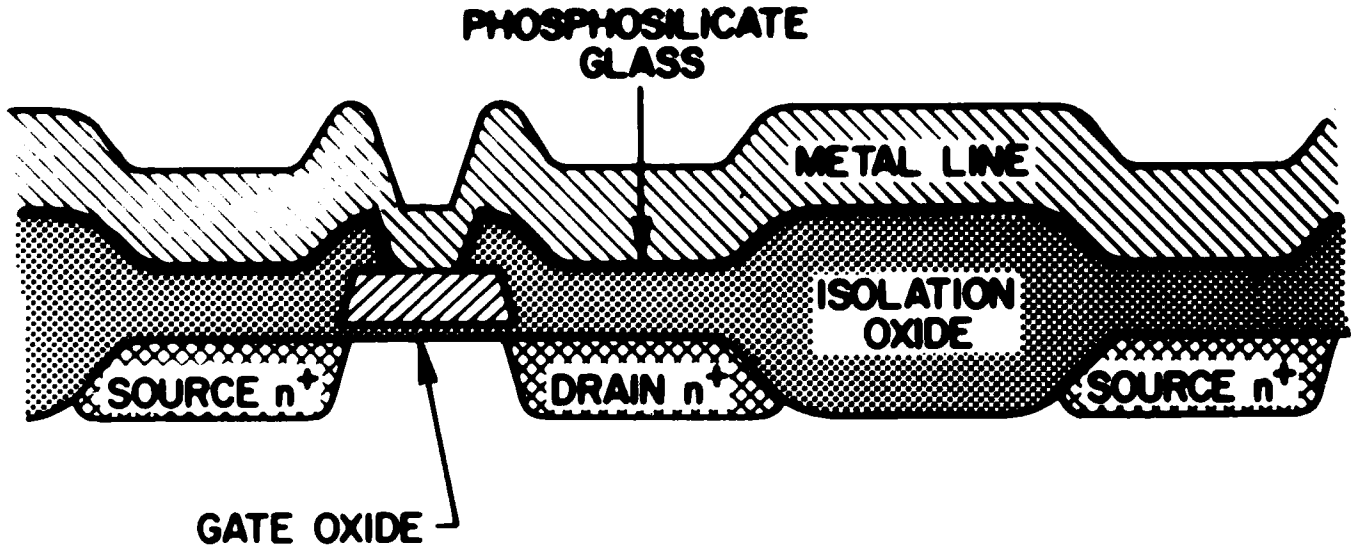
PHOSPHOSILICATE
GLASS
METAL LINE
ISOLATION
OXIDE
SOURCE n+
DRAIN n+
SOURCE n+
GATE OXIDE
p-TYPE SILICON

Fig 3 Irene

Silicon Oxidation System

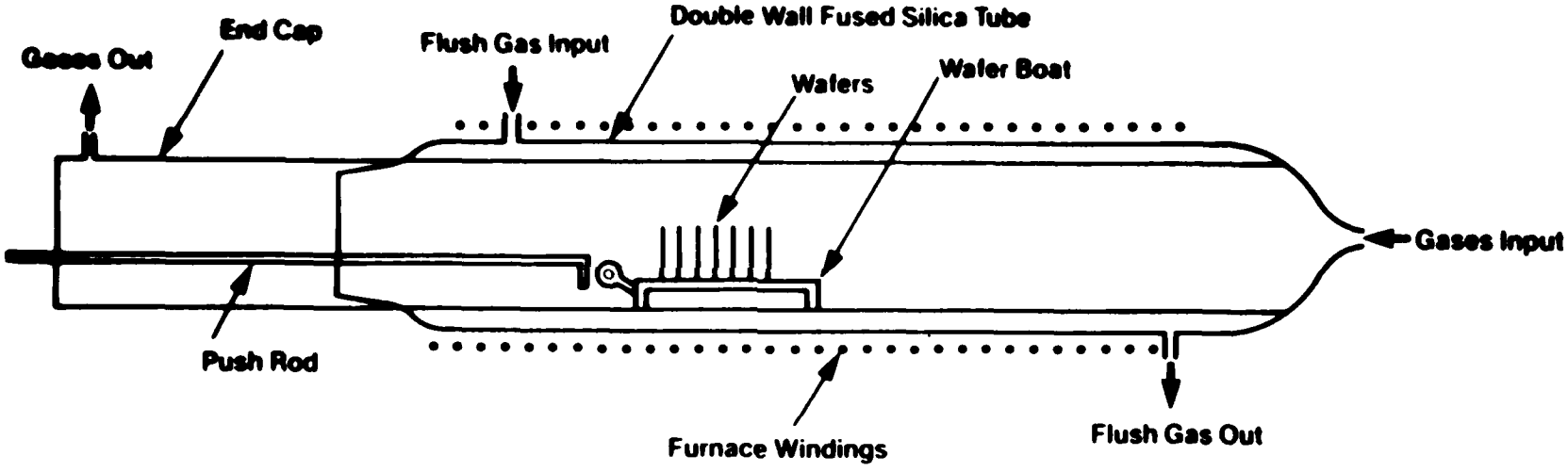

Fig 4 Irene

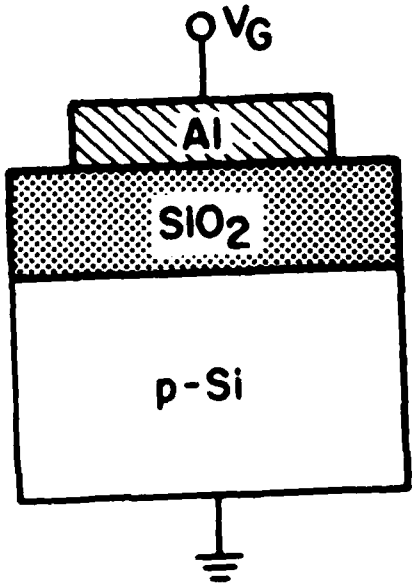

a) MOS CAPACITOR

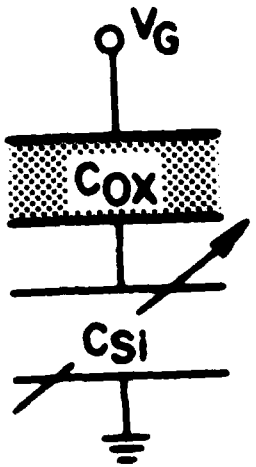

b) EQUIVALENT SERIES COMBINATION

Fig 5 Inv

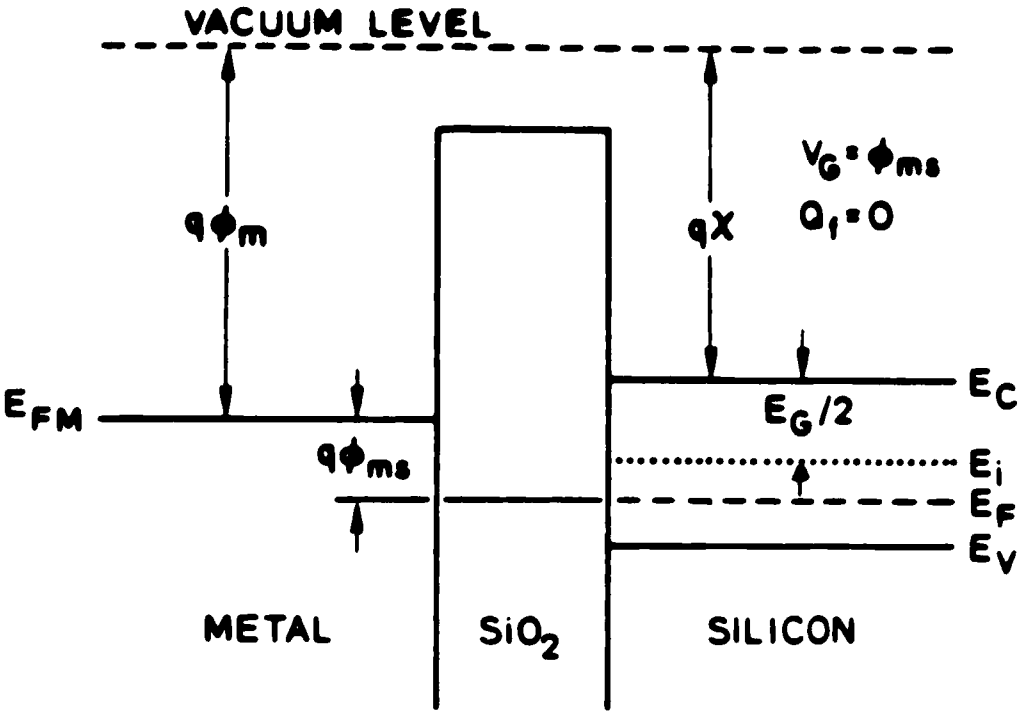
VACUUM LEVEL
$V_G = \phi_{ms}$
$Q_i = 0$
$q\phi_m$
$q\chi$
E_{FM}
E_C
$E_G/2$
$q\phi_{ms}$
E_i
E_F
E_V
METAL
SiO_2
SILICON

Fig 6 Irene

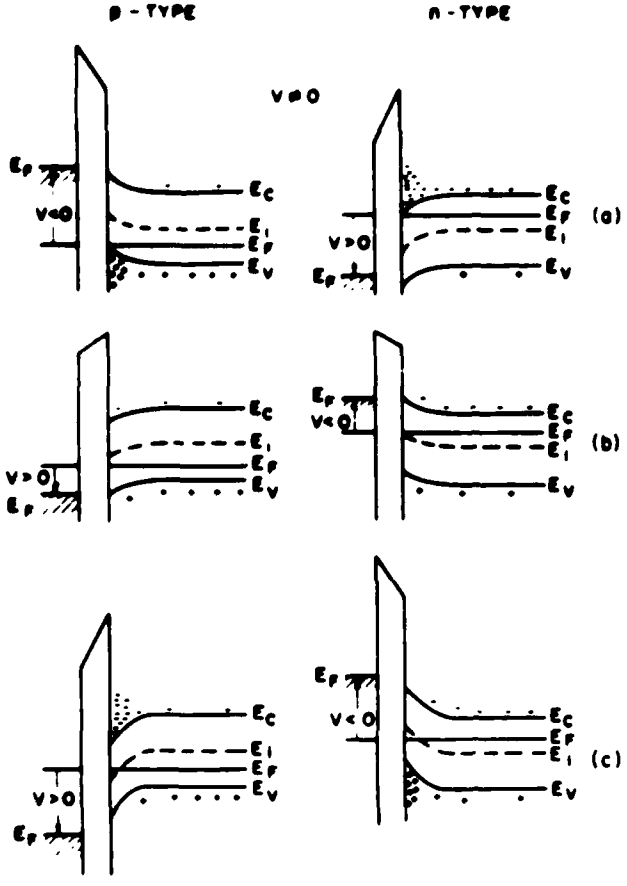
P - TYPE
n - TYPE
V = 0
E_F
E_C
V<0
E_i
E_F
E_V
V>0
E_F
E_C
E_F
E_i
E_V
(a)
V>0
E_F
E_C
E_i
E_F
E_V
E_F
V<0
E_C
E_F
E_i
E_V
(b)
V>0
E_F
E_C
E_i
E_F
E_V
E_F
V<0
E_C
E_F
E_i
E_V
(c)

Fig 7 Irene

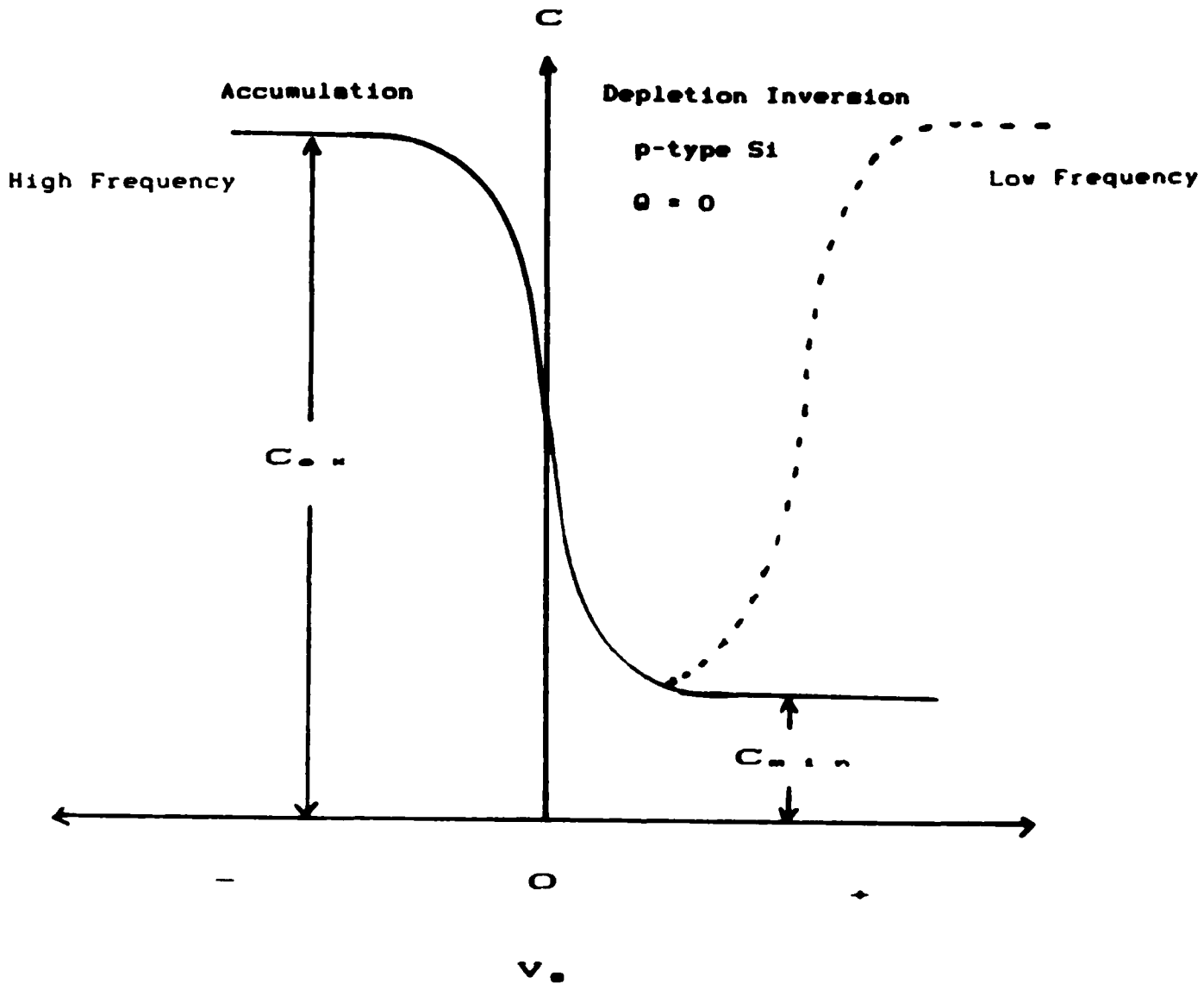
C
Accumulation
Depletion Inversion
p-type Si
Q = 0
High Frequency
Low Frequency
C_ox
C_min
−
0
+
V_G

Fig 8 Irene

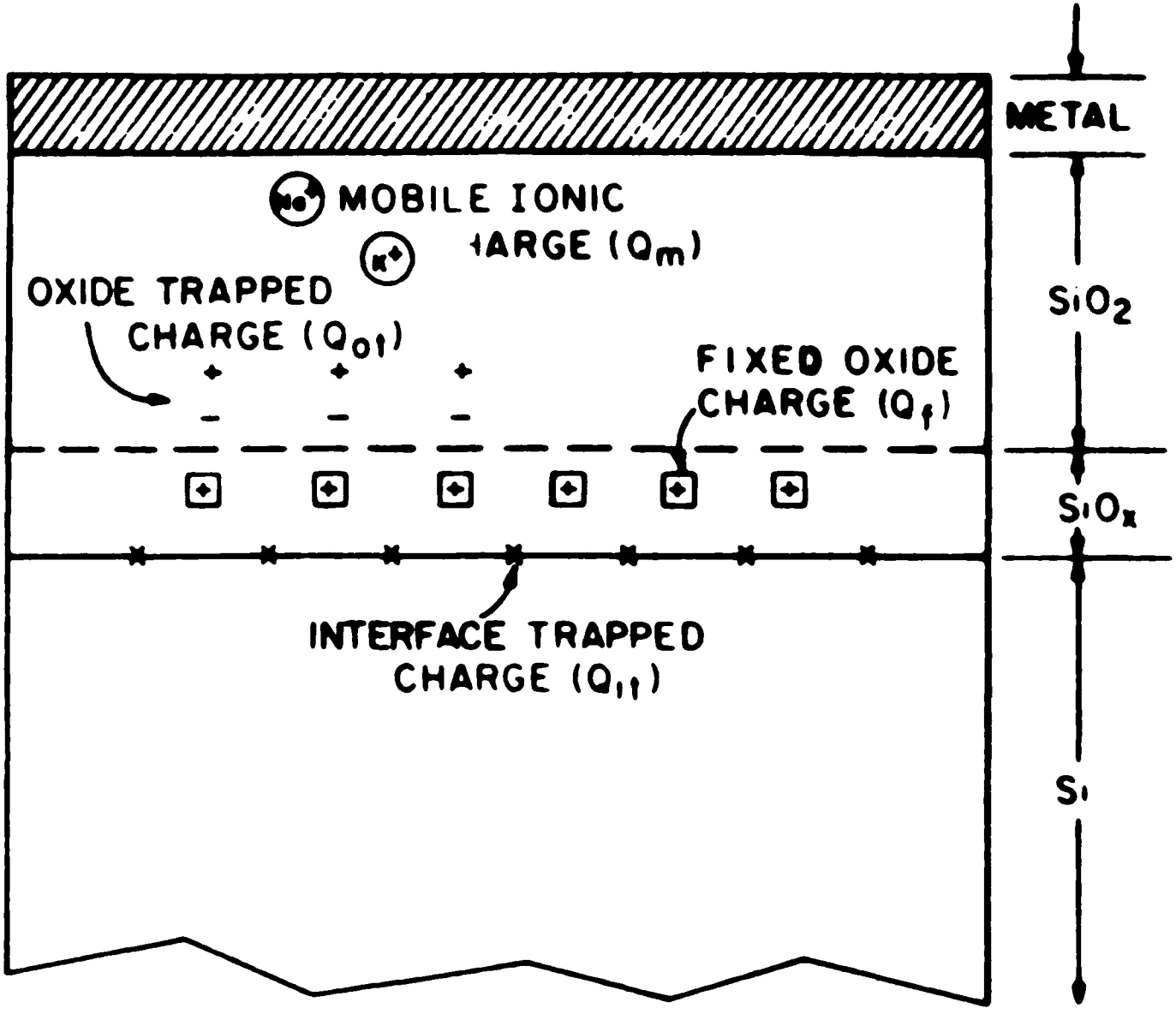
METAL
MOBILE IONIC
CHARGE (Q_m)
OXIDE TRAPPED
CHARGE (Q_{ot})
FIXED OXIDE
CHARGE (Q_f)
INTERFACE TRAPPED
CHARGE (Q_{it})
SiO_2
SiO_x
Si

Fig 1 Insu

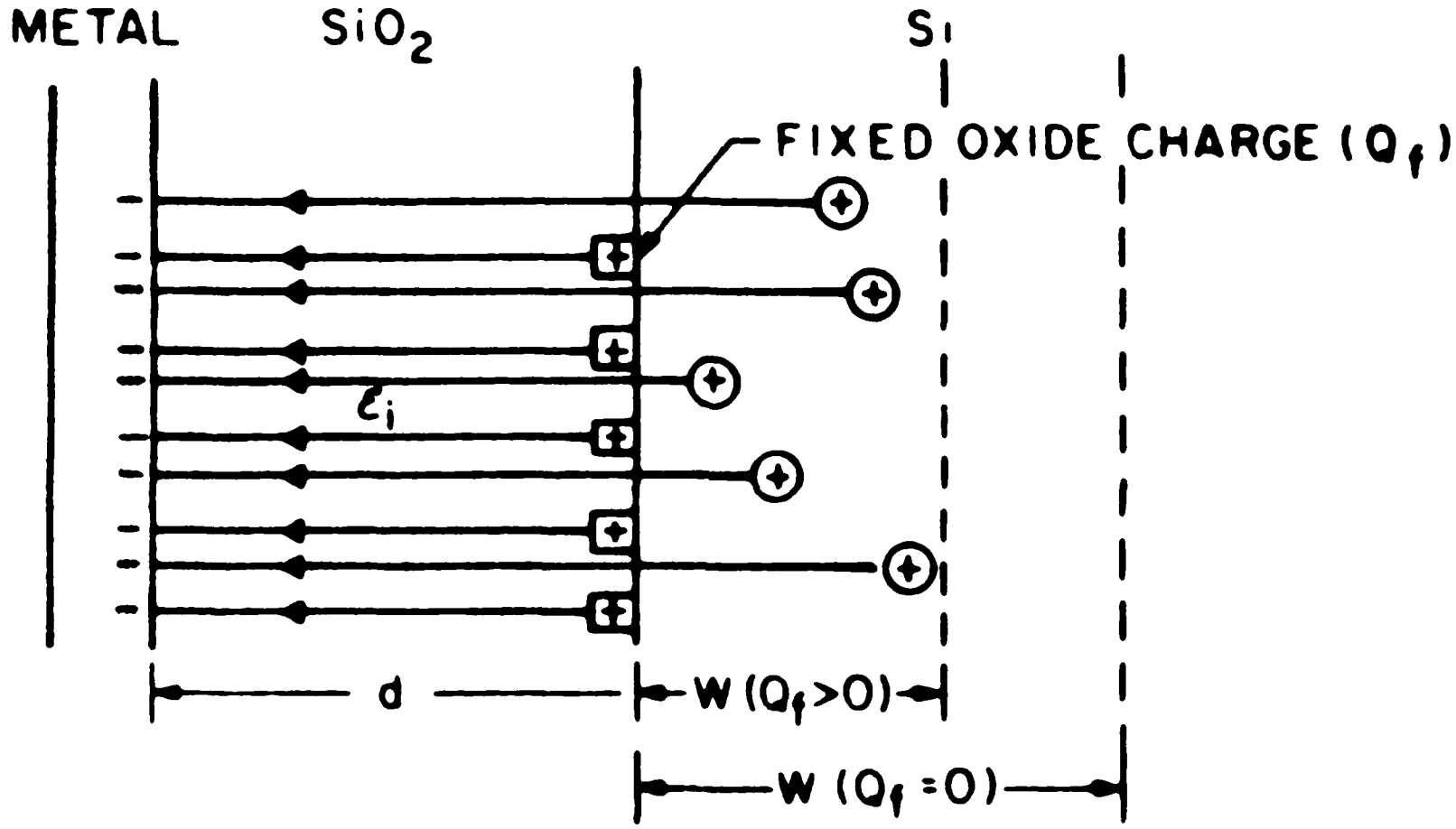

Fig 10 Irene

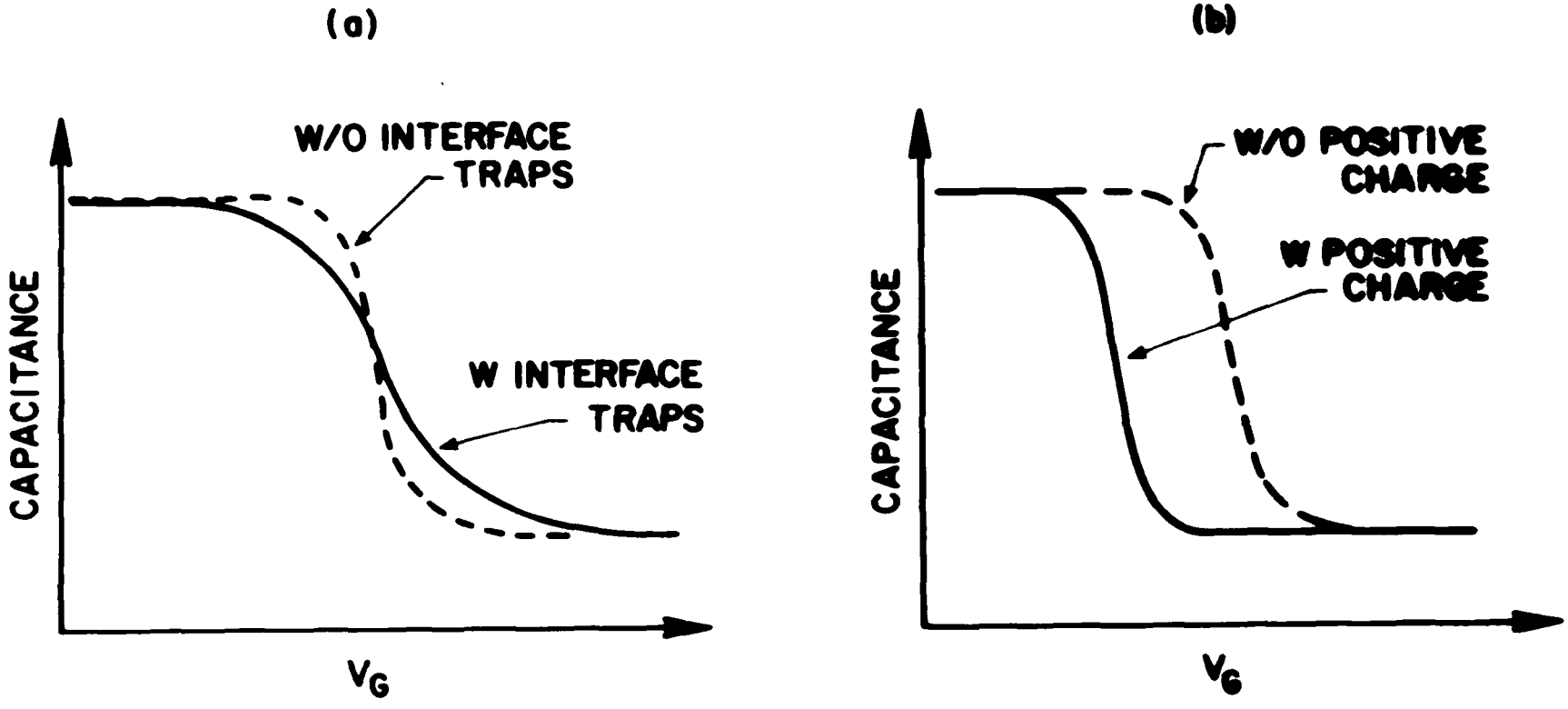
(a)
W/O INTERFACE TRAPS
W INTERFACE TRAPS
CAPACITANCE
V_G
(b)
W/O POSITIVE CHARGE
W POSITIVE CHARGE
CAPACITANCE
V_G

Fig 11 Irene

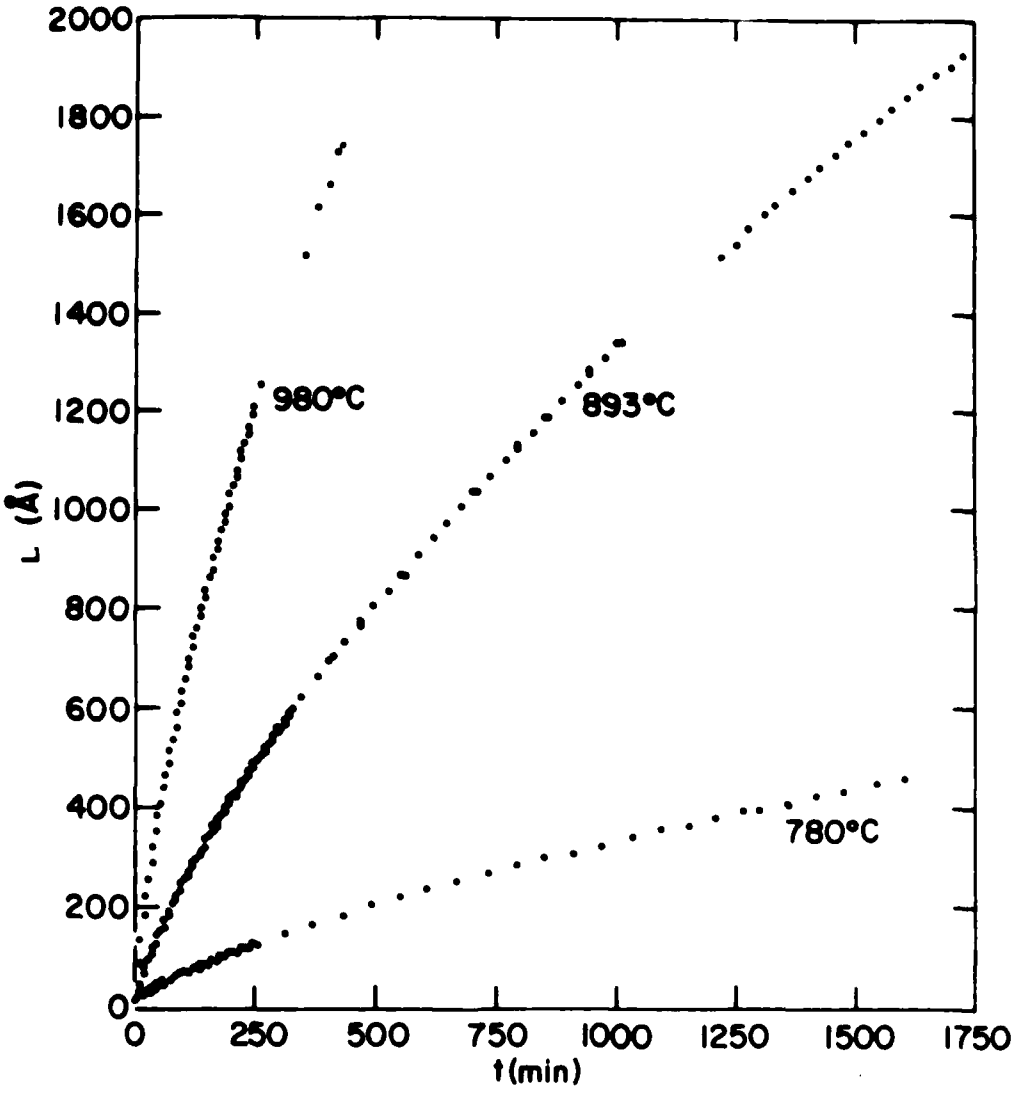
2000
1800
1600
1400
1200
1000
800
600
400
200
0
L (Å)
980°C
893°C
780°C
0
250
500
750
1000
1250
1500
1750
t(min)

Fig 12 Irene

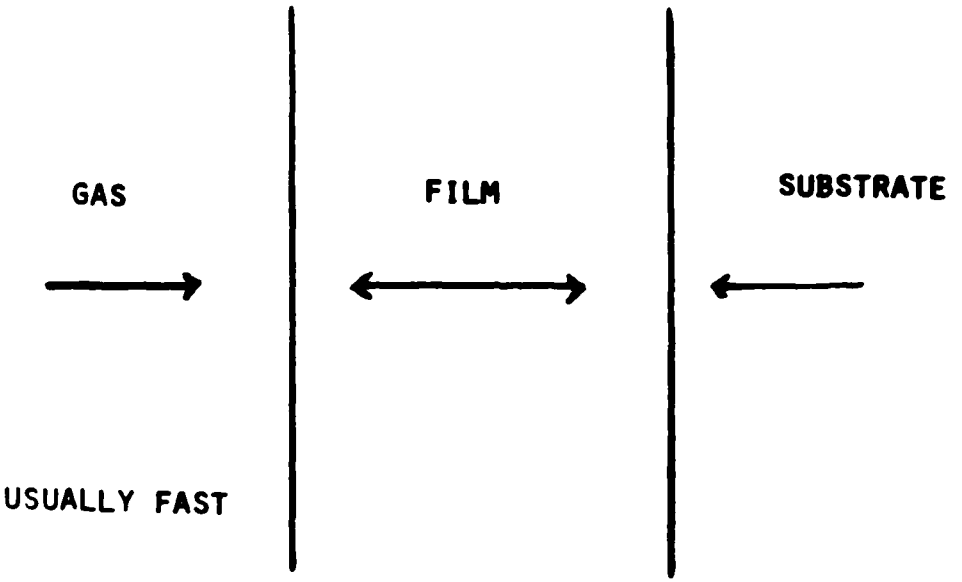

Fig 13 Irene

Linear - Parabolic Model

Fig 14 Irem

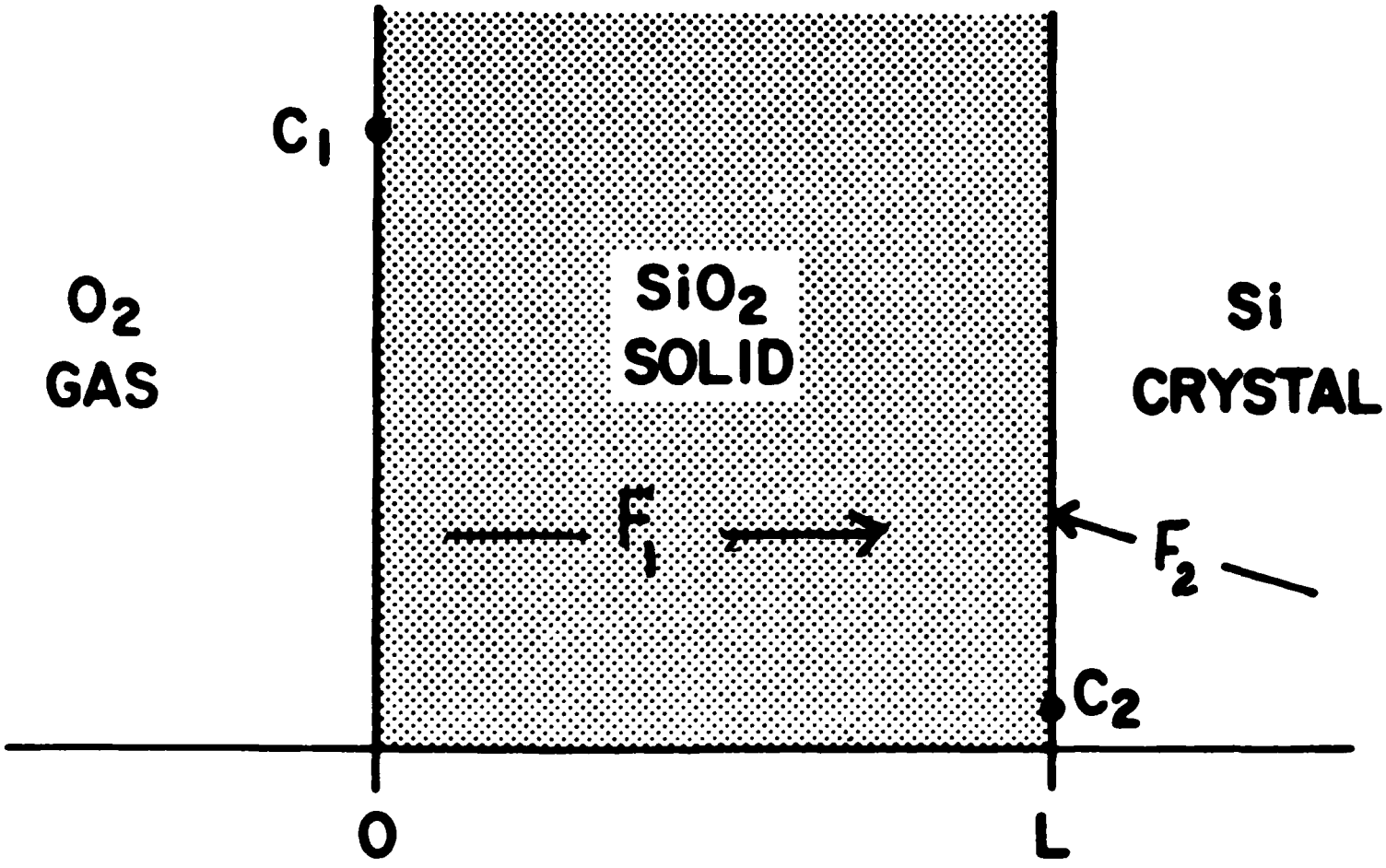

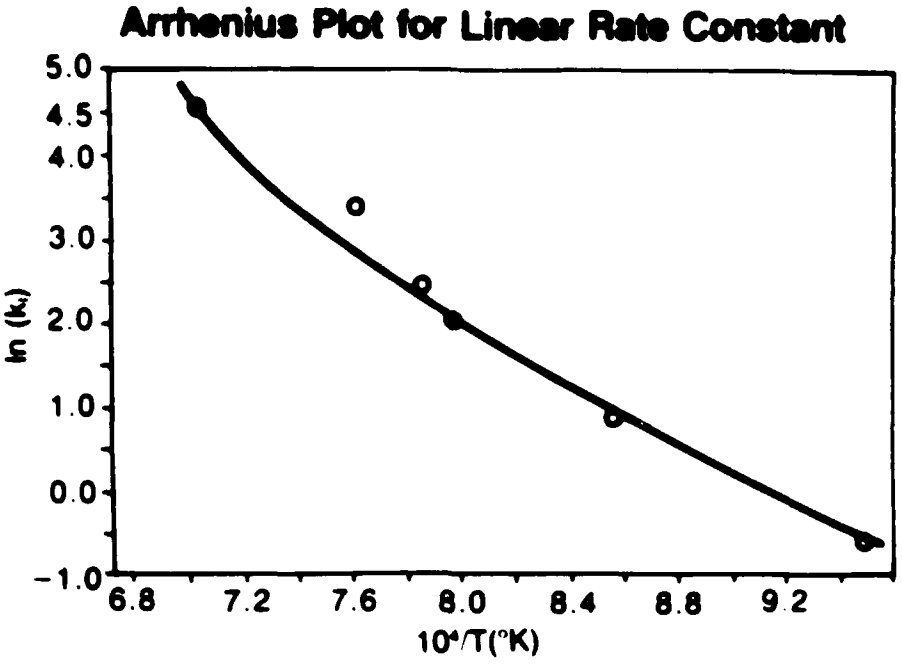
Arrhenius Plot for Linear Rate Constant
5.0
4.5
4.0
3.0
2.0
1.0
0.0
−1.0
ln (k_l)
6.8
7.2
7.6
8.0
8.4
8.8
9.2
10⁴/T(°K)

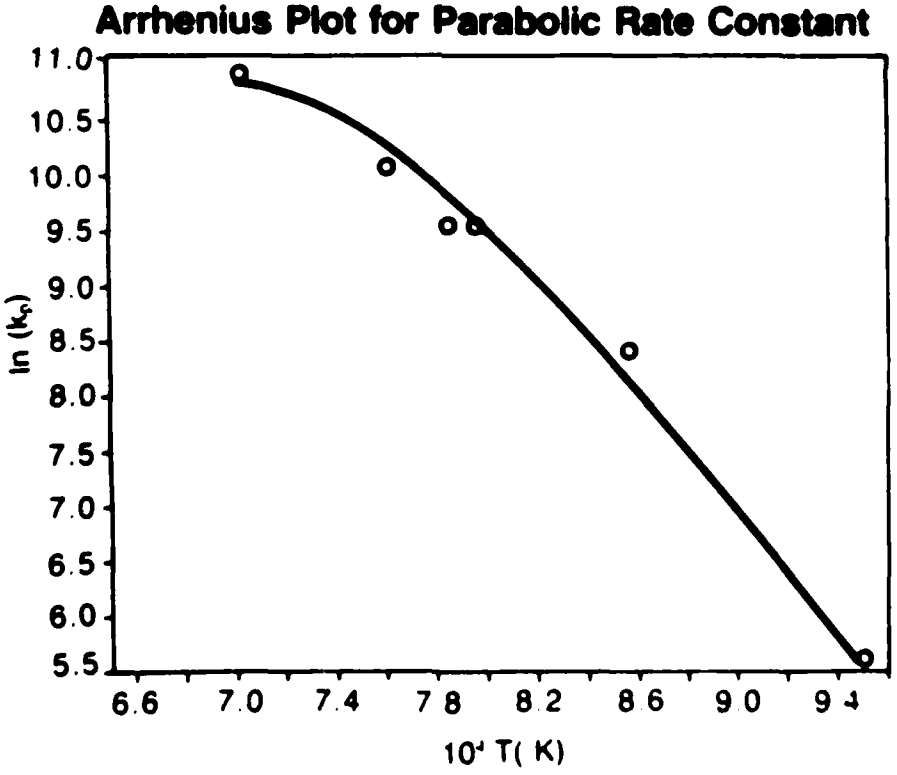
Arrhenius Plot for Parabolic Rate Constant
11.0
10.5
10.0
9.5
9.0
8.5
8.0
7.5
7.0
6.5
6.0
5.5
ln (k_p)
6.6
7.0
7.4
7.8
8.2
8.6
9.0
10⁴ T(K)

Fig 15 Inset

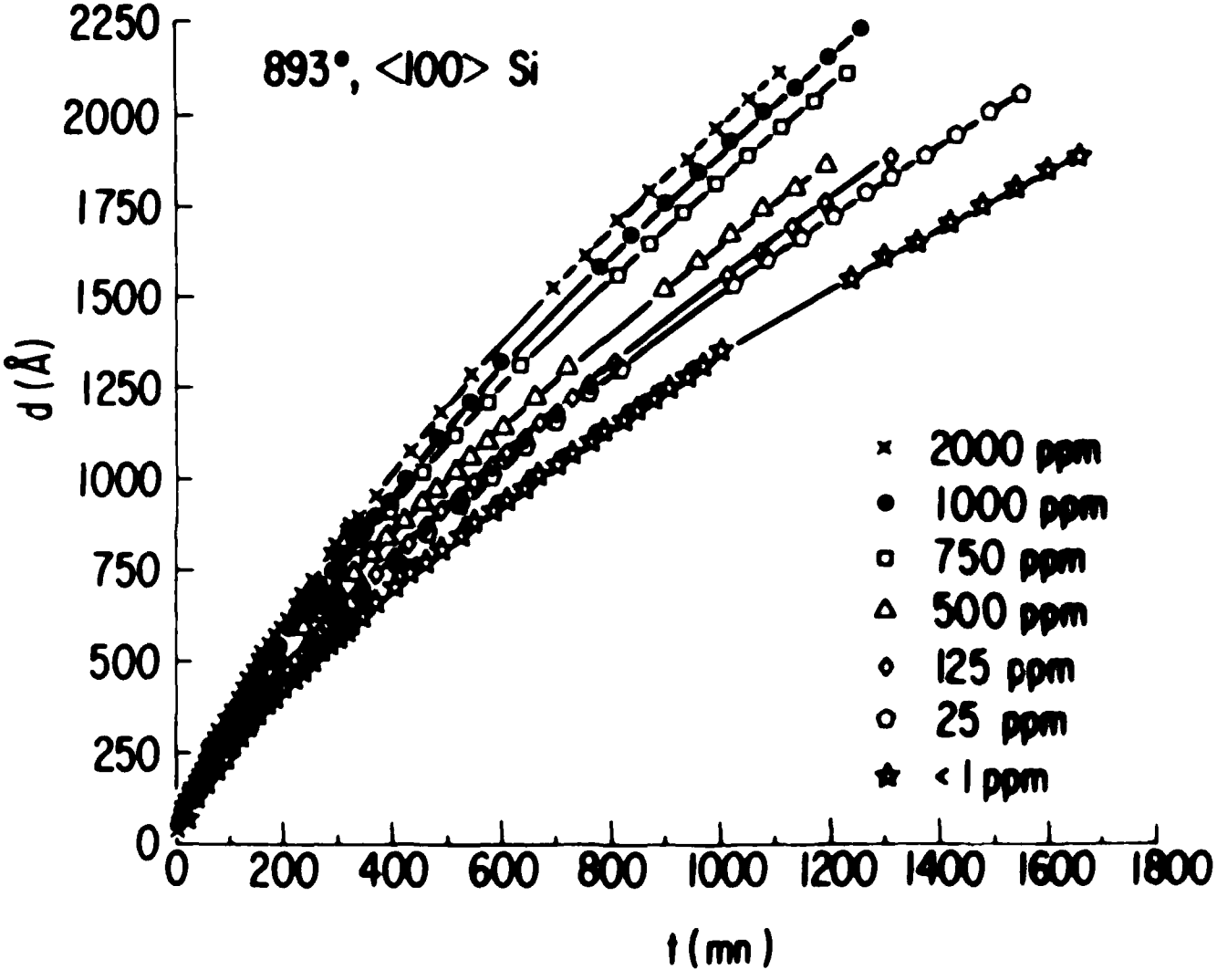
893°, <100> Si
d (Å)
t (mn)
2250
2000
1750
1500
1250
1000
750
500
250
0
0
200
400
600
800
1000
1200
1400
1600
1800
2000 ppm
1000 ppm
750 ppm
500 ppm
125 ppm
25 ppm
< 1 ppm

Fig 16 Irene

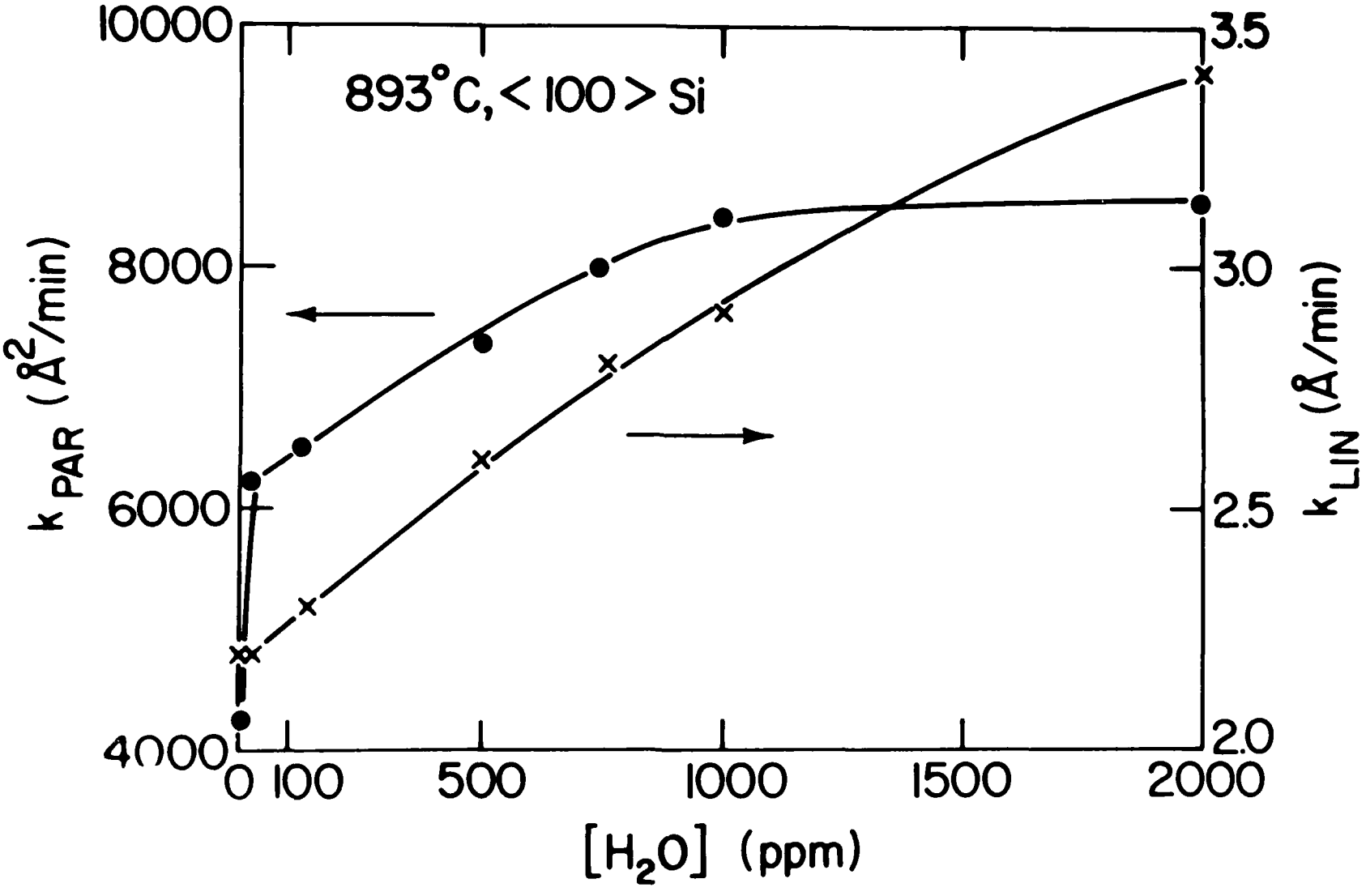
893°C, <100> Si
10000
8000
6000
4000
3.5
3.0
2.5
2.0
0
100
500
1000
1500
2000
k_{PAR} (Å²/min)
k_{LIN} (Å/min)
[H_2O] (ppm)

Fig 17 Irene

AD-A181 329 MODELS FOR THE OXIDATION OF SILICON(U) NORTH CAROLINA 2/2
UNIV AT CHAPEL HILL DEPT OF CHEMISTRY E A IRENE
03 JUN 87 TR-16 N00014-86-K-0305

UNCLASSIFIED F/G 20/12 NL

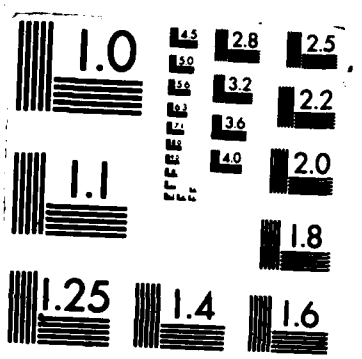
1.0
1.1
1.25
1.4
1.6
1.8
2.0
2.2
2.5
2.8
3.2
3.6
4.0
4.5
5.0
5.6
6.3
7.1
8.0
9.0
10.0

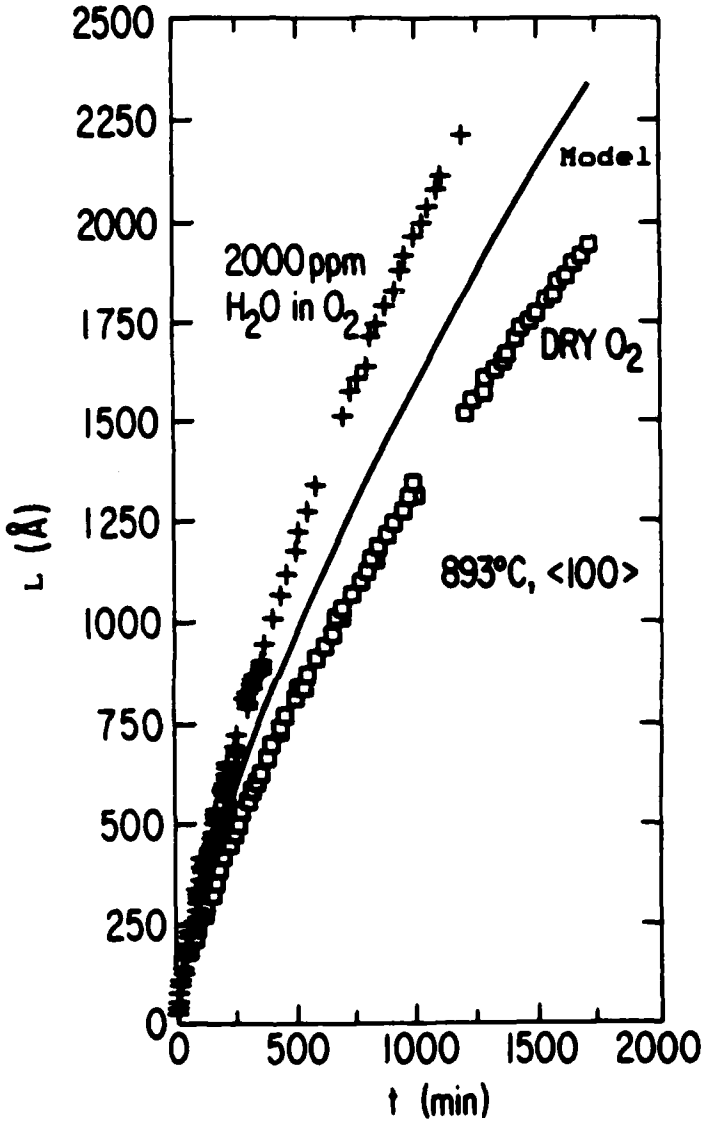
2500
2250
2000
1750
1500
1250
1000
750
500
250
0
L (Å)
0
500
1000
1500
2000
t (min)
Model
2000 ppm
H_2O in O_2
DRY O_2
893°C, <100>

Fig 18 Irene

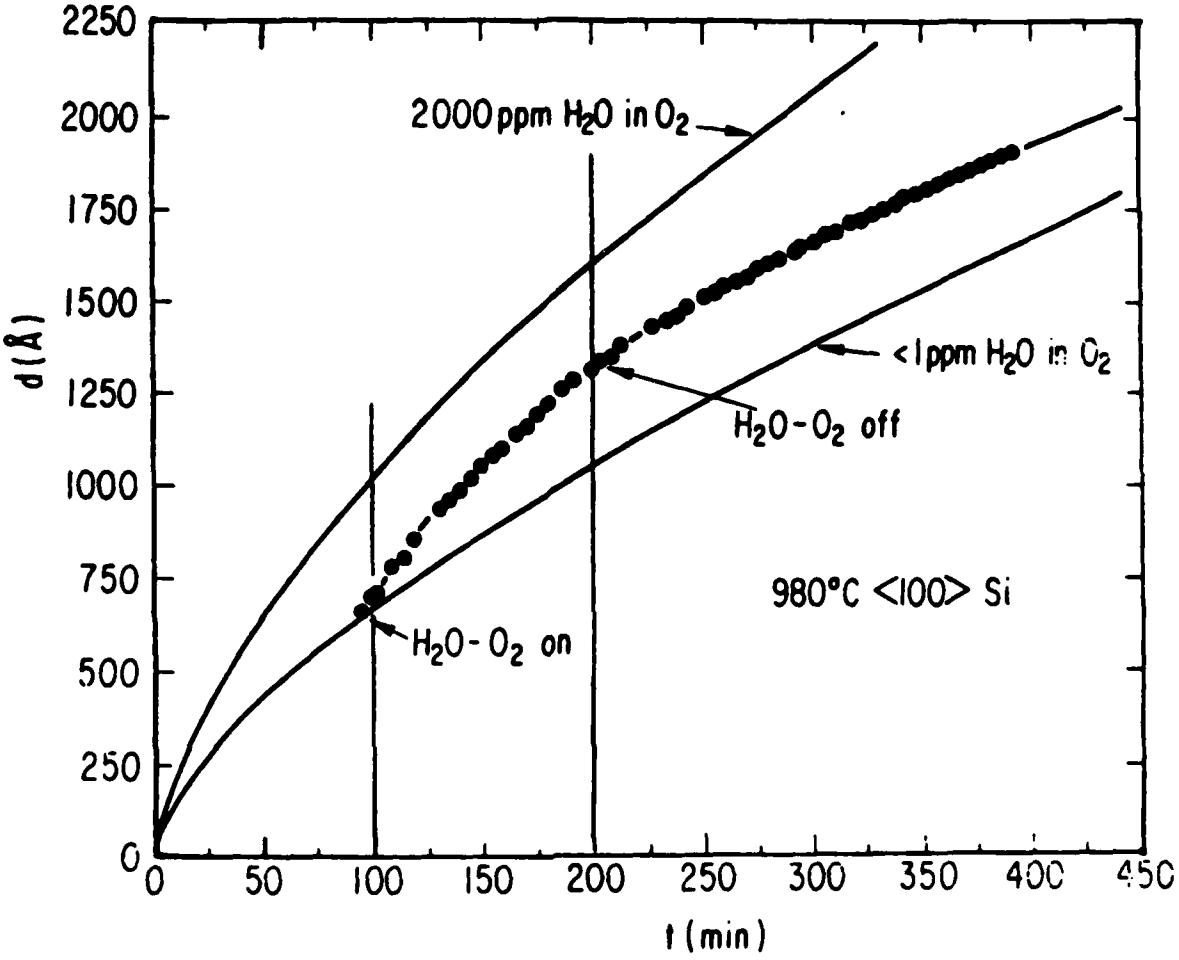
2250
2000
1750
1500
1250
1000
750
500
250
0
d(Å)
2000 ppm H_2O in O_2
< 1 ppm H_2O in O_2
H_2O-O_2 off
H_2O-O_2 on
980°C <100> Si
0
50
100
150
200
250
300
350
400
450
t (min)

Fig 19 Irene

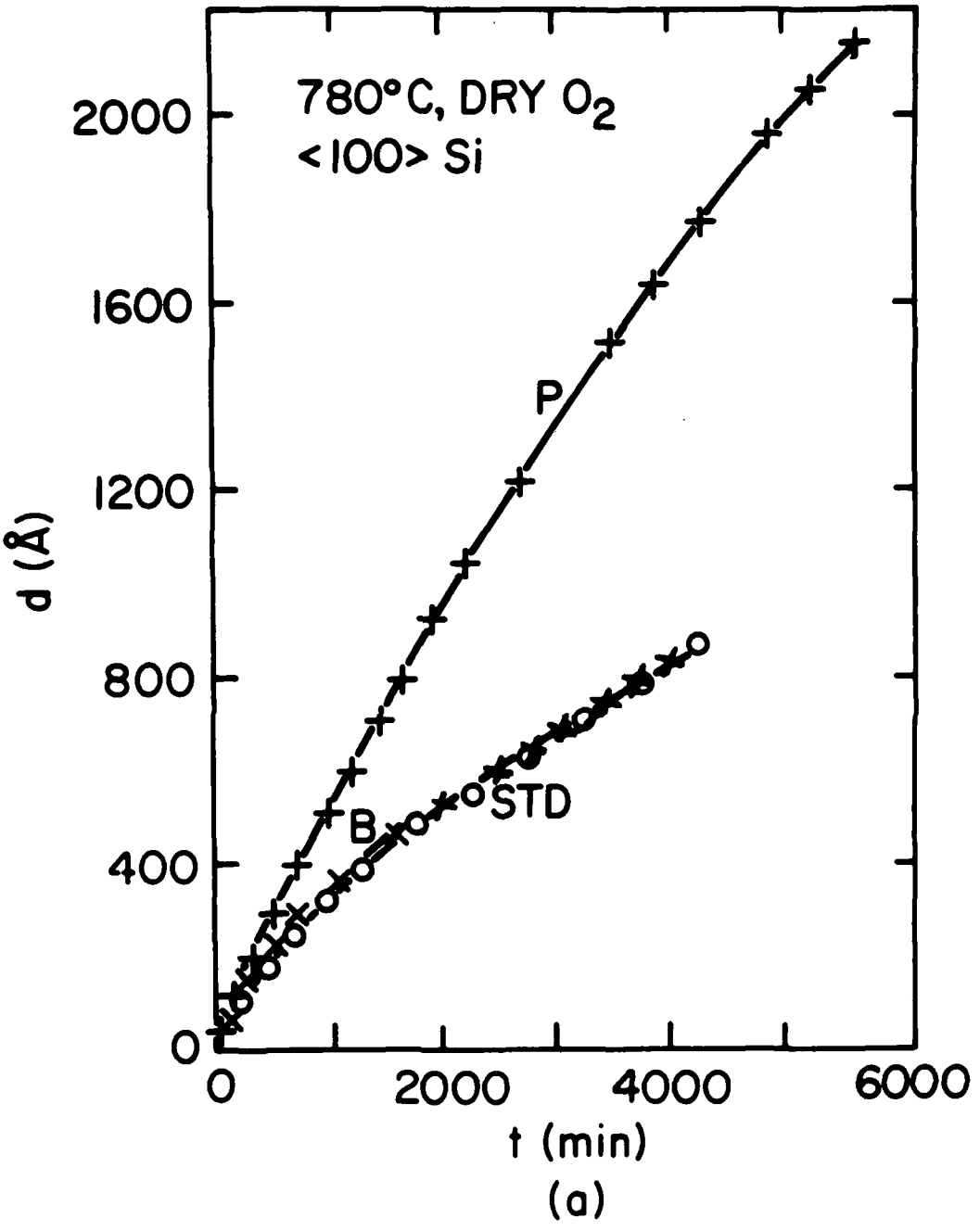
780°C, DRY O_2
<100> Si
2000
1600
1200
800
400
0
d (Å)
P
B
STD
0
2000
4000
6000
t (min)
(a)

Fig 20 Irene

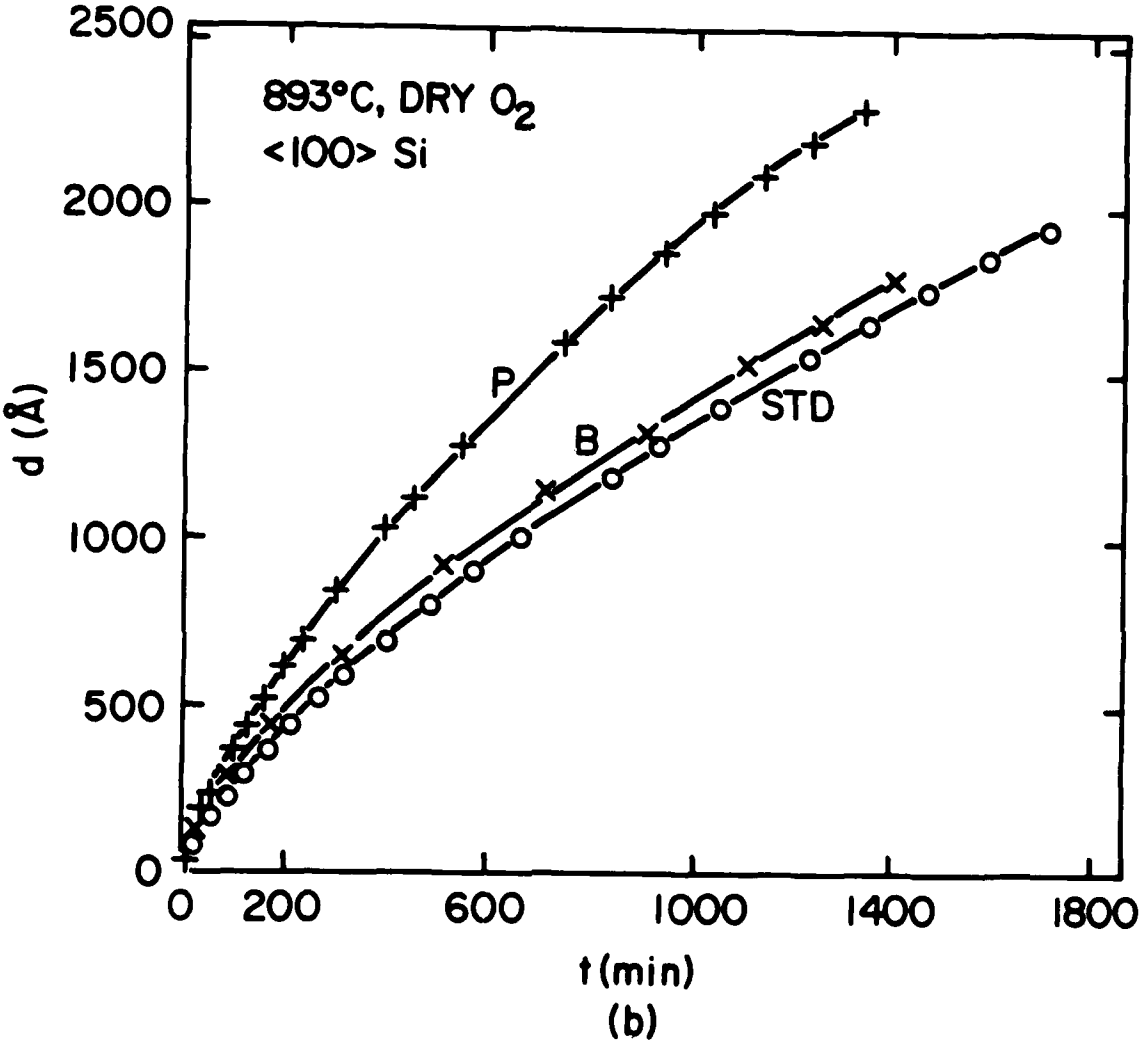

(b)

Fig 20 Irene

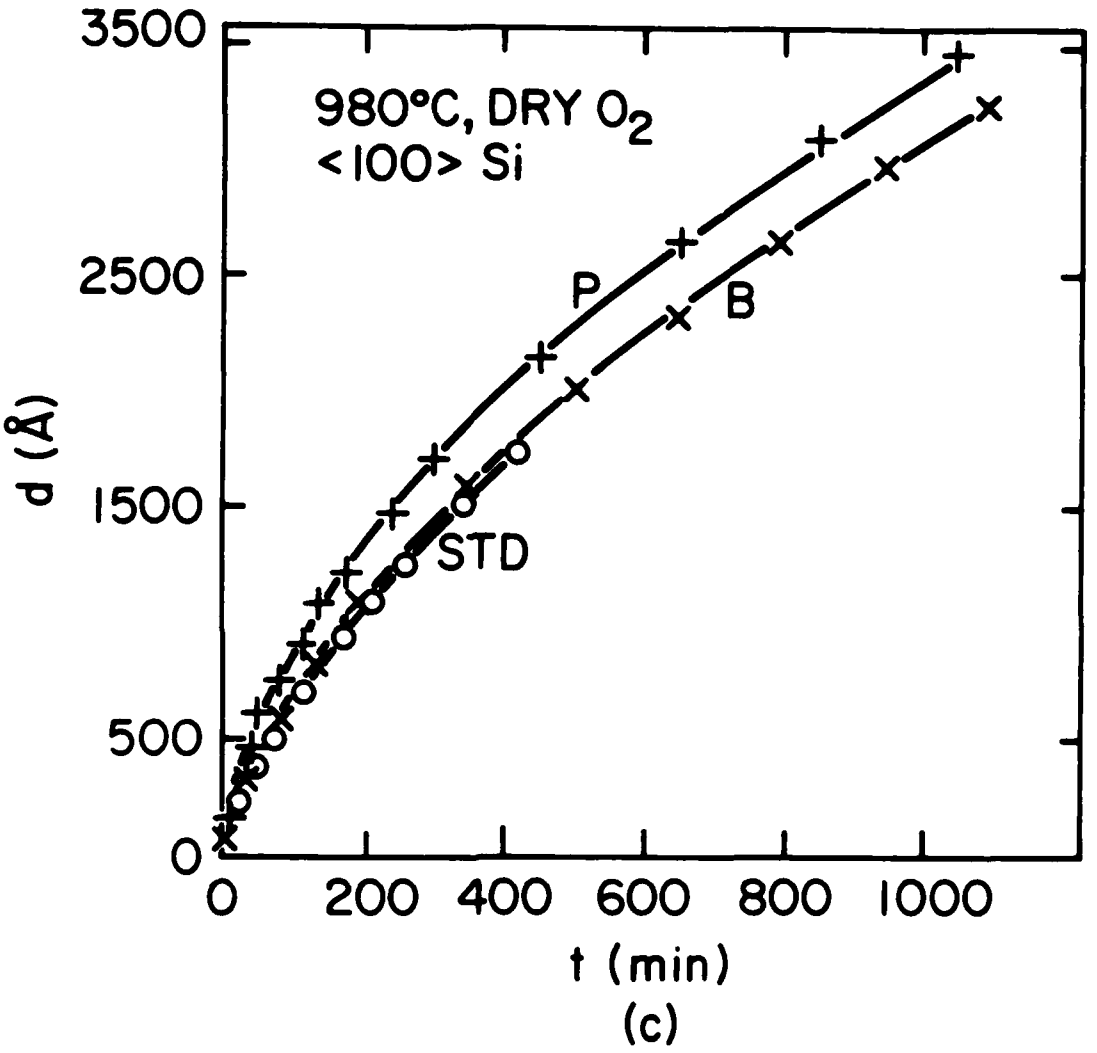

(c)

Fig 20 Irene

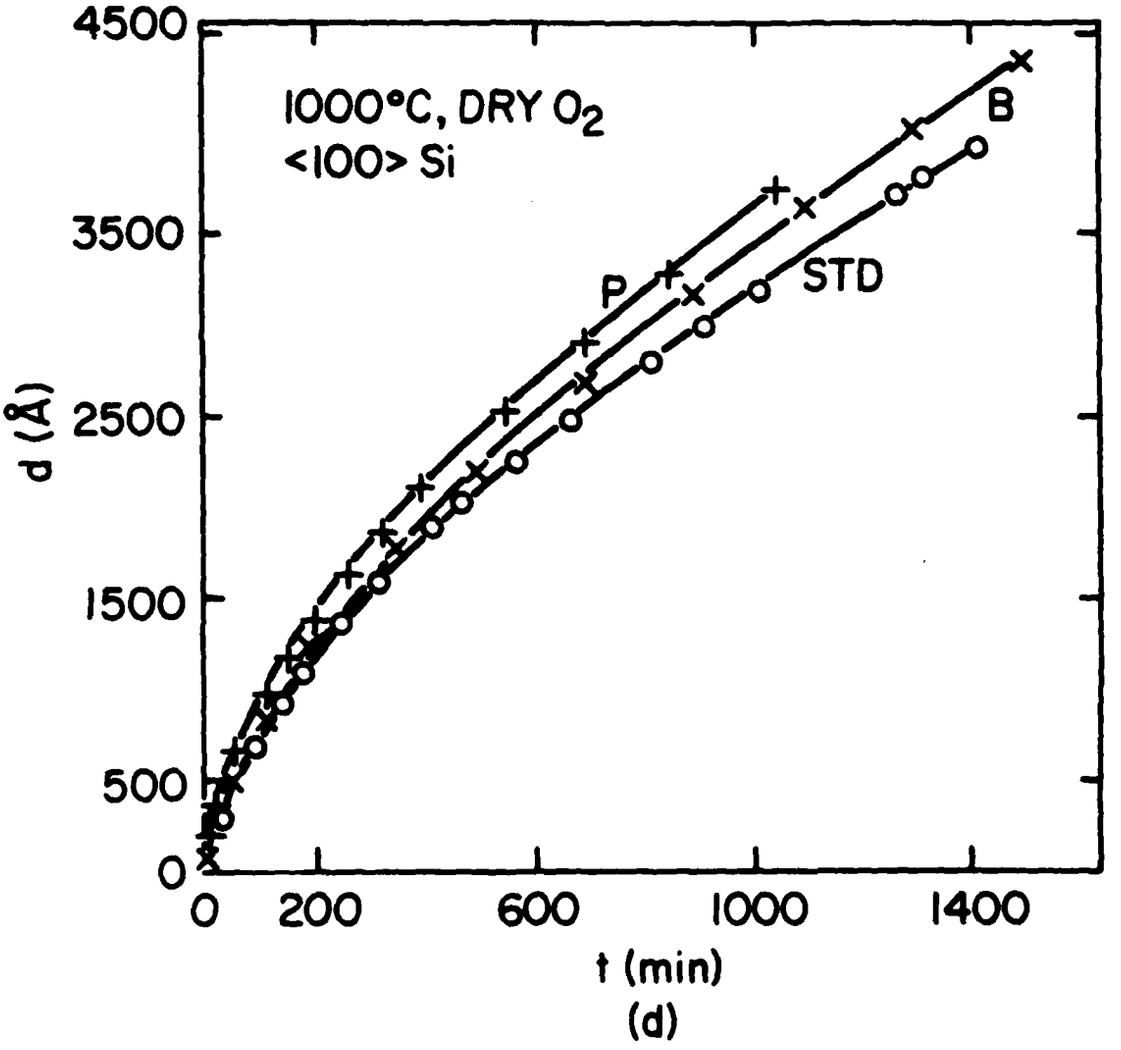
4500
3500
2500
1500
500
0
d (Å)
1000°C, DRY O_2
<100> Si
B
P
STD
0
200
600
1000
1400
t (min)
(d)

Fig 20 Irene

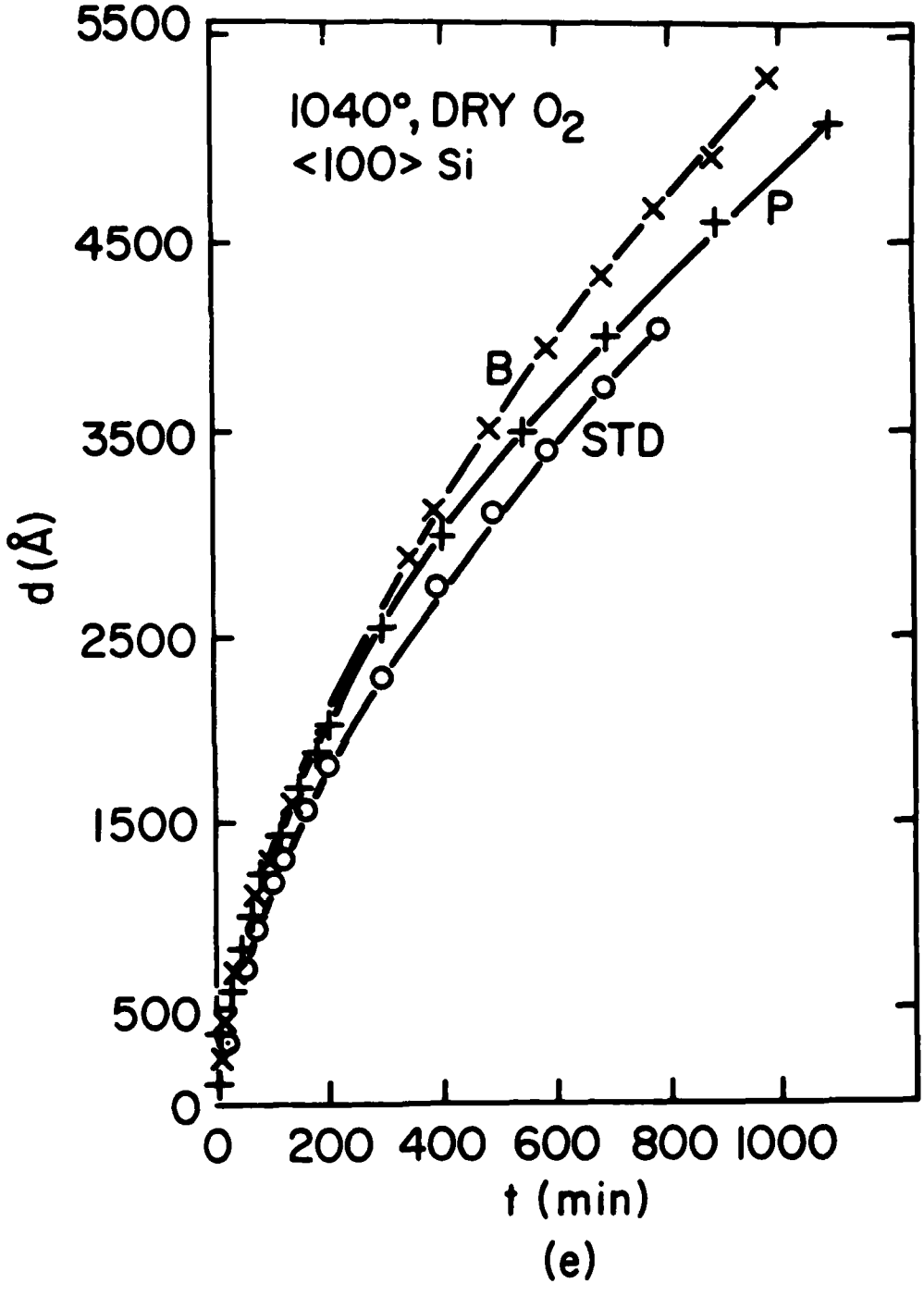
5500
4500
3500
2500
1500
500
0
d (Å)
1040°, DRY O_2
<100> Si
B
P
STD
0
200
400
600
800
1000
t (min)
(e)

Fig 20 Irene

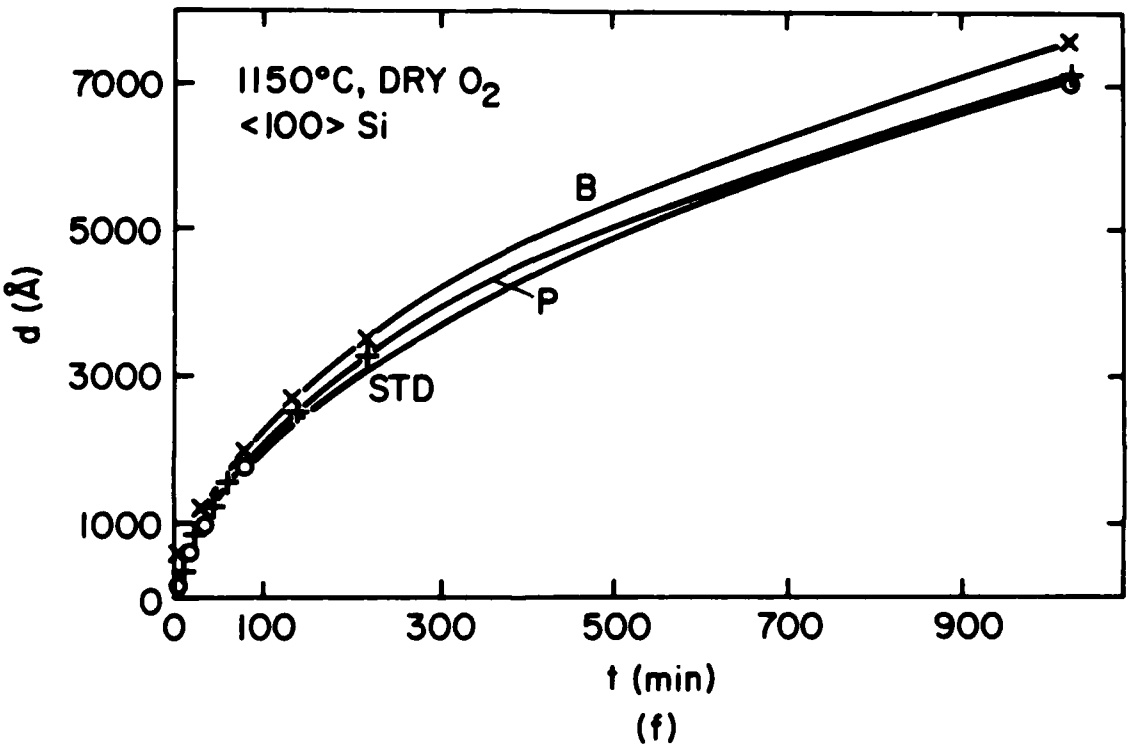
1150°C, DRY O_2
<100> Si
B
P
STD
d (Å)
7000
5000
3000
1000
0
0
100
300
500
700
900
t (min)
(f)

Fig 20 Irene

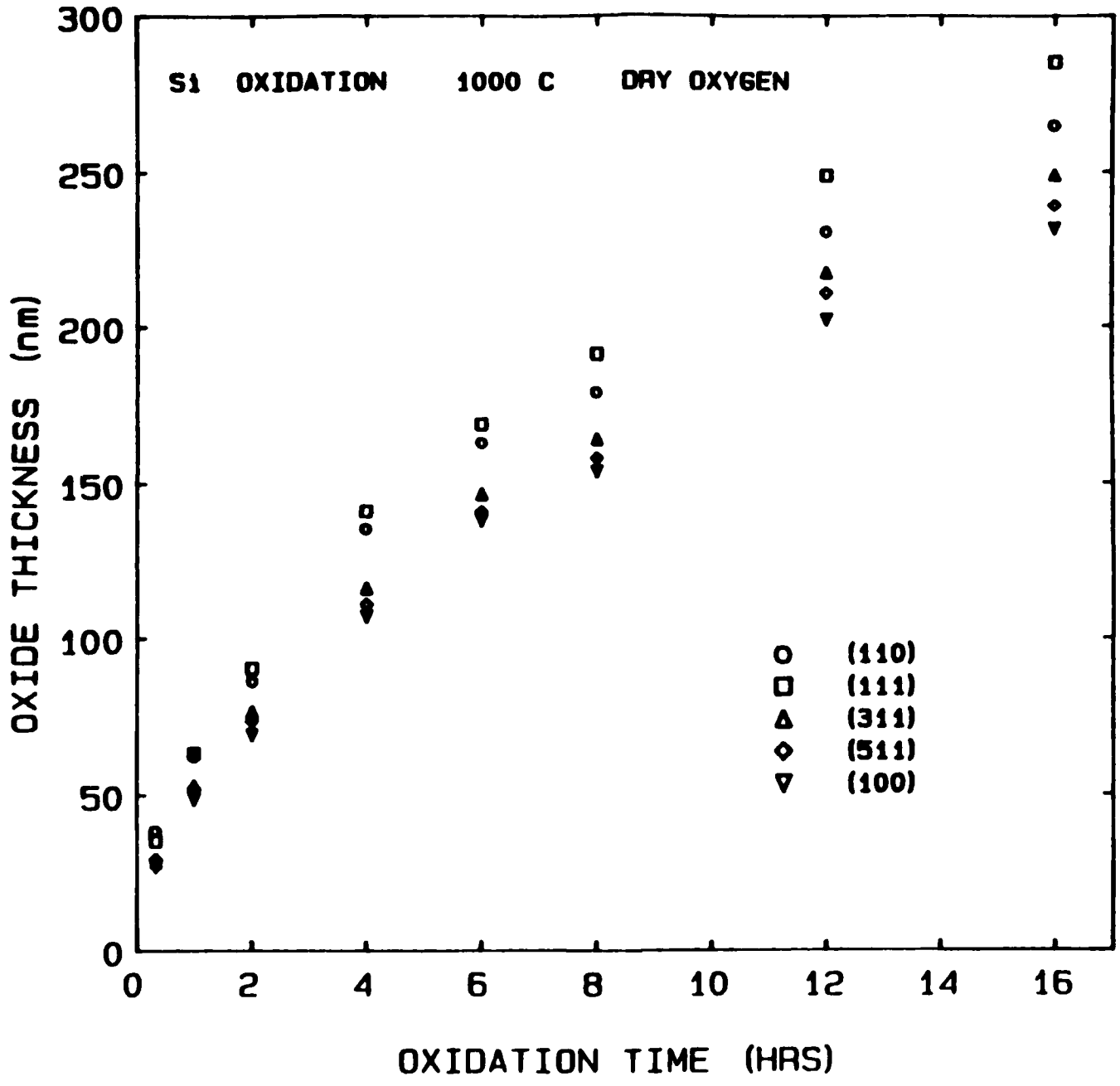
Si OXIDATION 1000 C DRY OXYGEN
OXIDE THICKNESS (nm)
OXIDATION TIME (HRS)
0
50
100
150
200
250
300
0
2
4
6
8
10
12
14
16
(110)
(111)
(311)
(511)
(100)

Fig 21 Irene

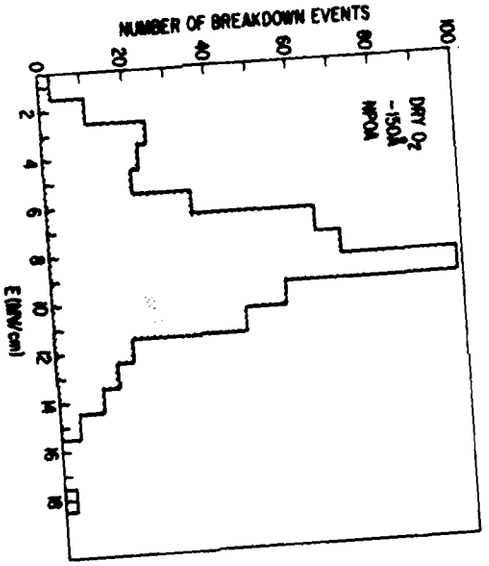

Fig 22 a Irene

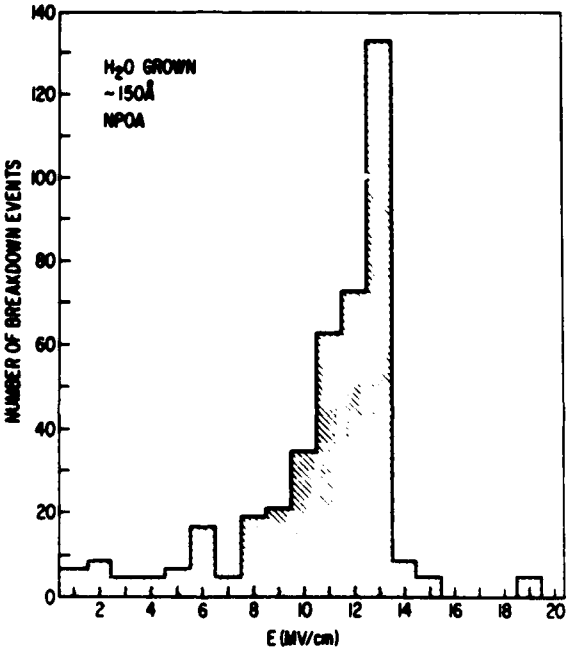

Fig 22 b Irene

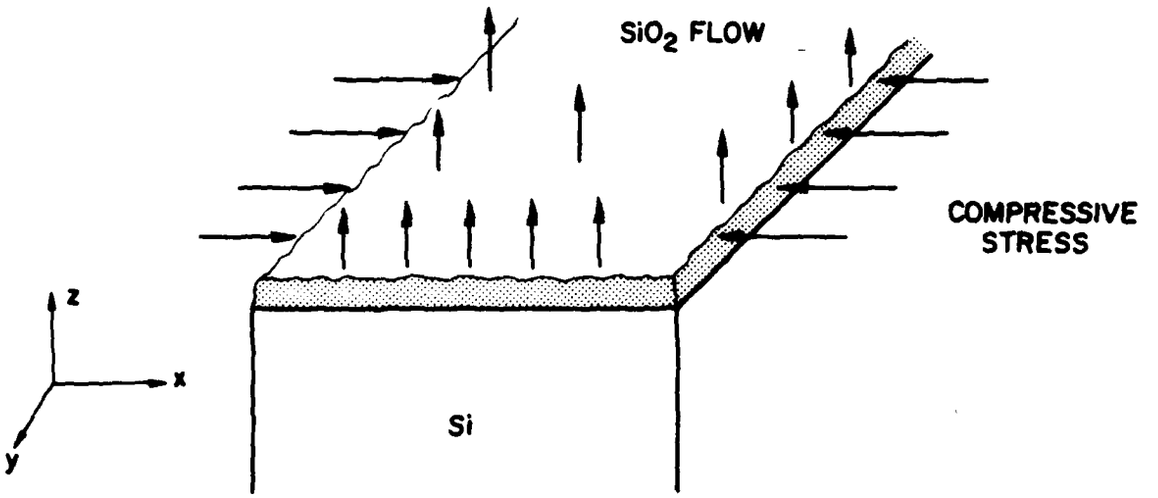

Fig 23 Irene

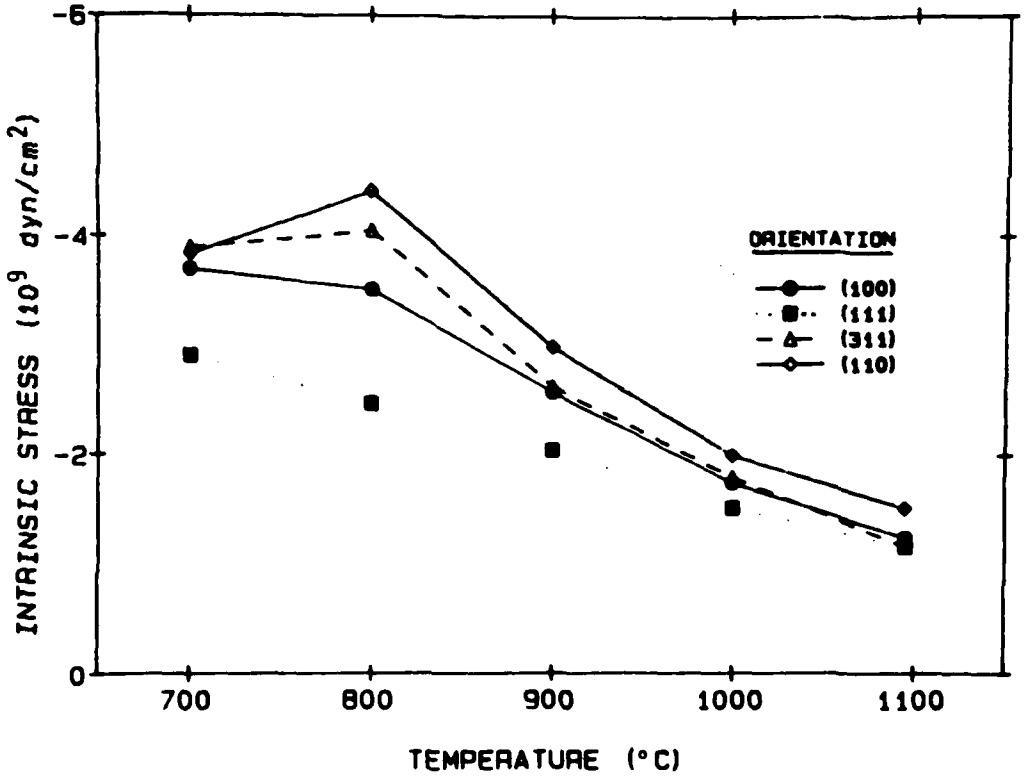

- Fig 24a Irene

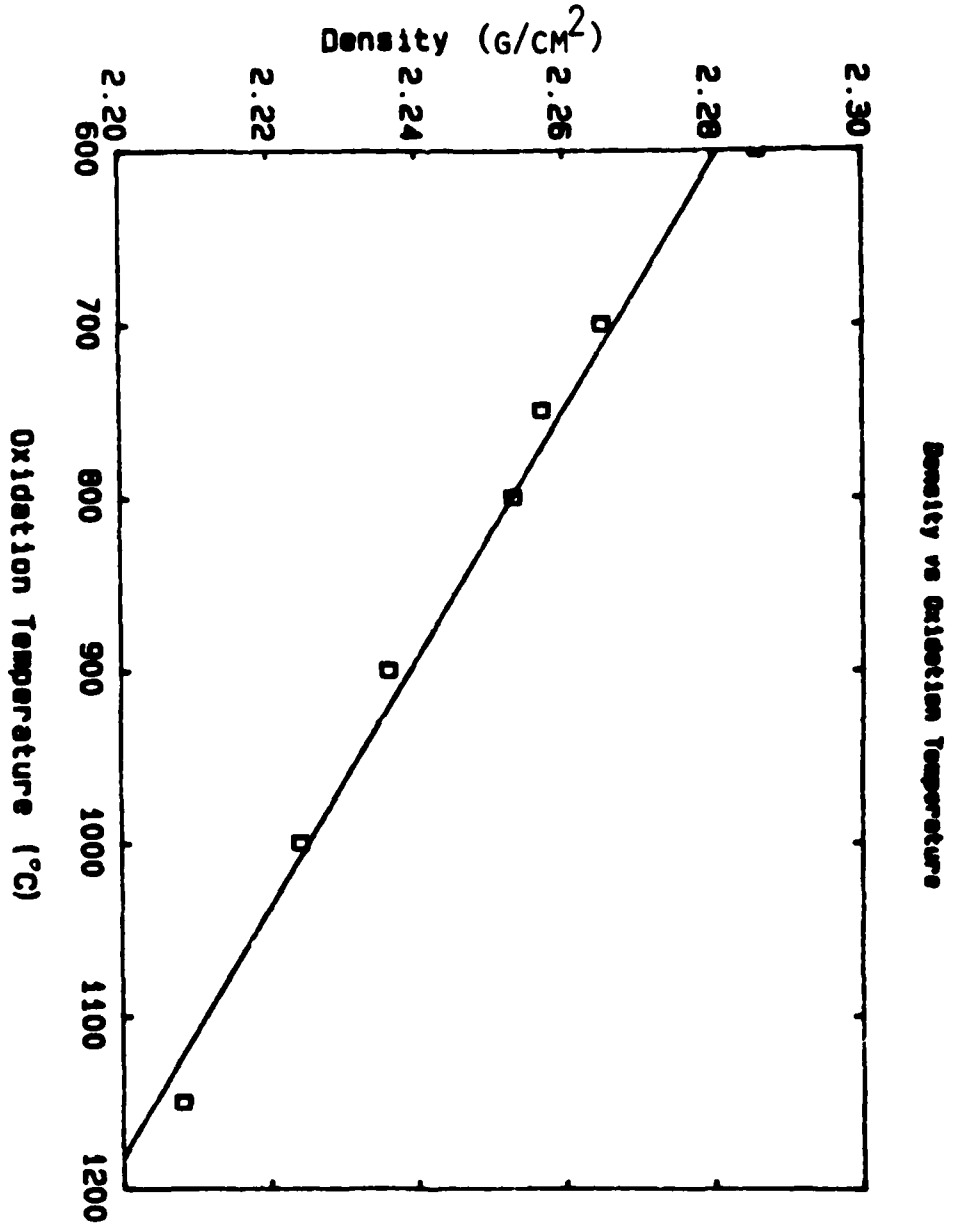

Fig 24 b Irene

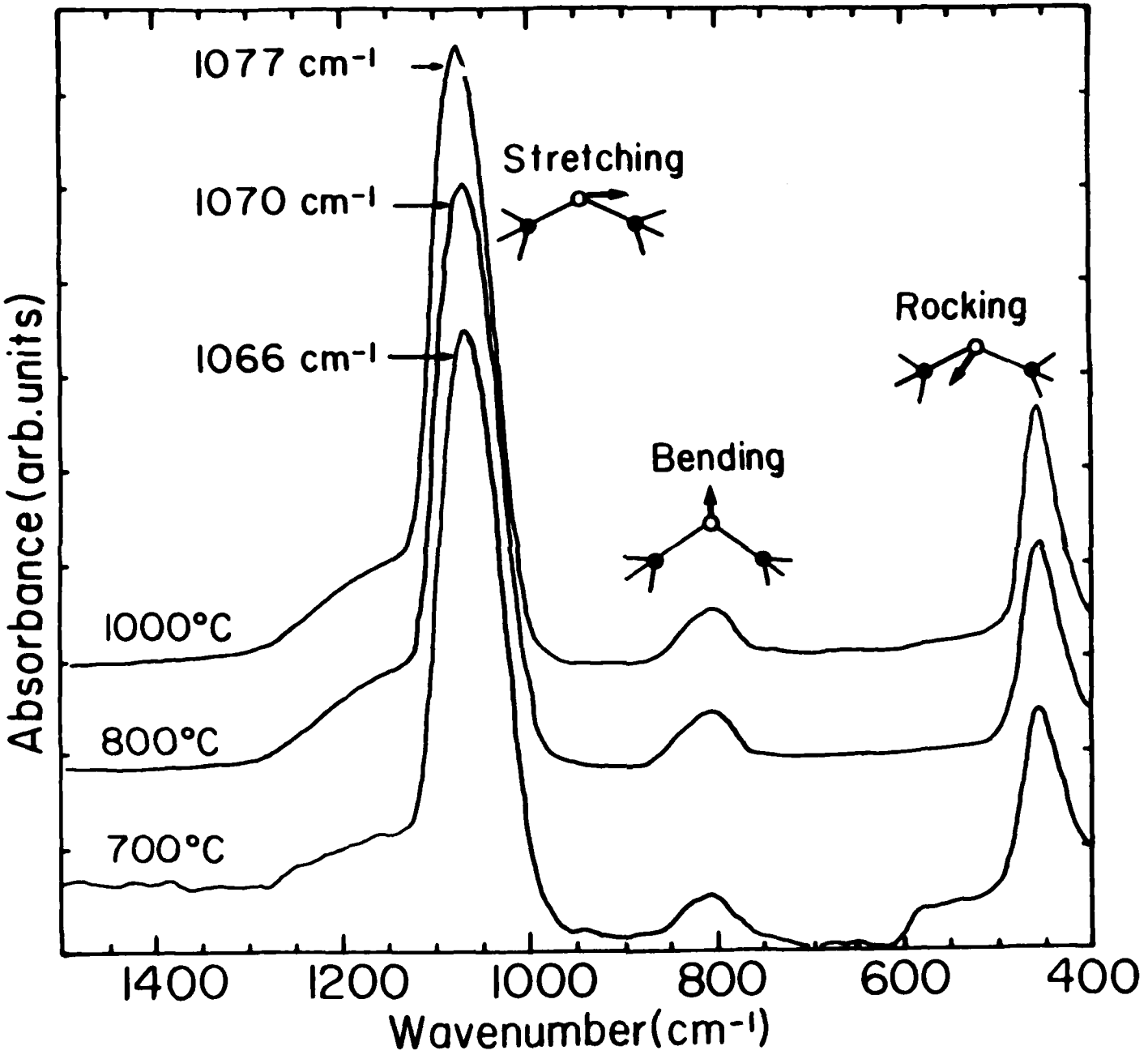
1077 cm⁻¹
1070 cm⁻¹
1066 cm⁻¹
Stretching
Rocking
Bending
1000°C
800°C
700°C
Absorbance (arb.units)
1400
1200
1000
800
600
400
Wavenumber (cm⁻¹)

- Fig 25 Inset

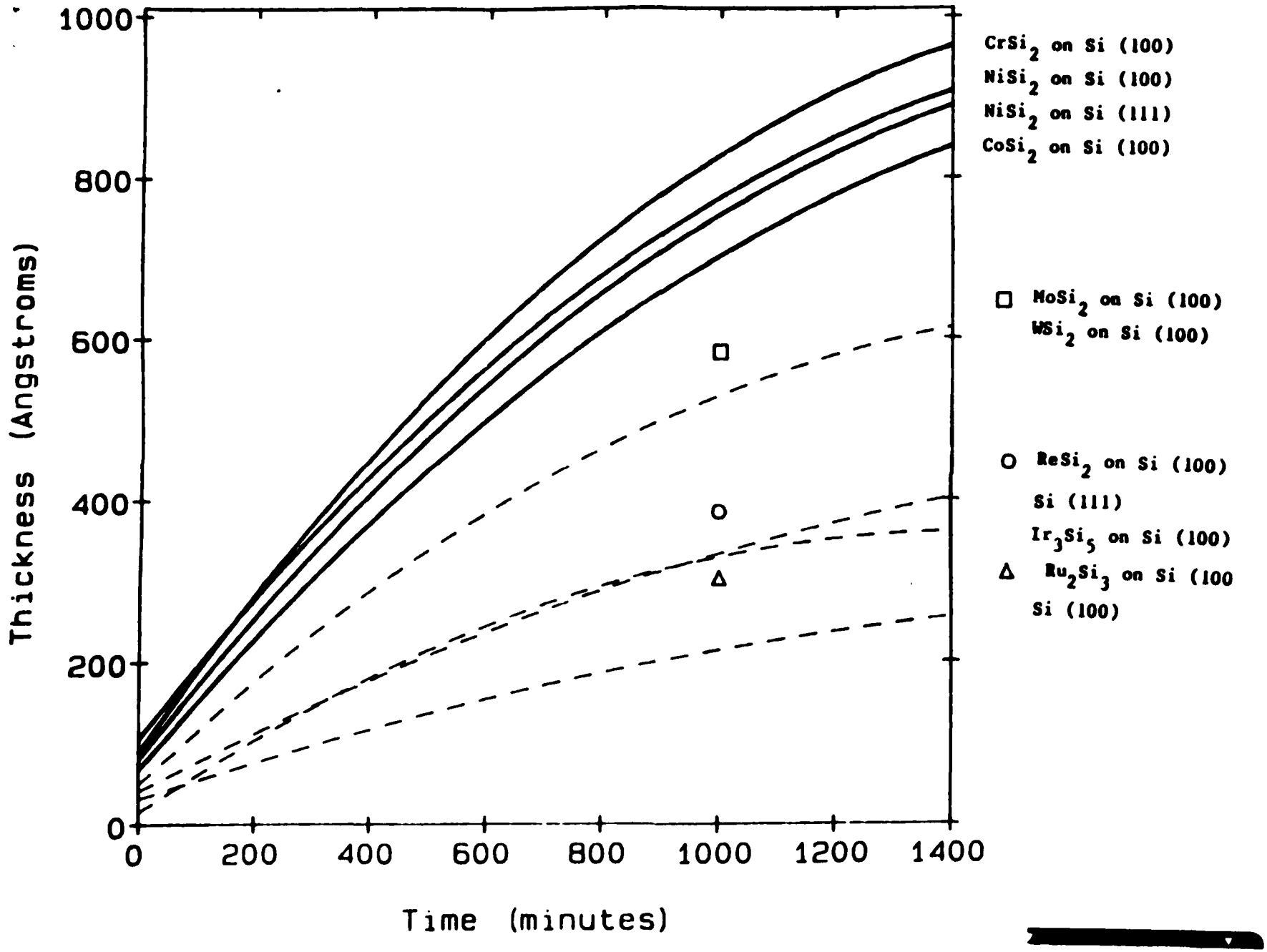
1000
800
600
400
200
0
0
200
400
600
800
1000
1200
1400
Thickness (Angstroms)
Time (minutes)
CrSi2 on Si (100)
NiSi2 on Si (100)
NiSi2 on Si (111)
CoSi2 on Si (100)
MoSi2 on Si (100)
WSi2 on Si (100)
ReSi2 on Si (100)
Si (111)
Ir3Si5 on Si (100)
Ru2Si3 on Si (100
Si (100)

Fig 26 Irene

END

7-87

DTIC